Surface Electromyography Driven Hand Motion Recognition for Long-term Rehabilitation Use

Dalin Zhou

School of Computing
University of Portsmouth

The thesis is submitted in partial fulfilment of the requirements
for the award of the degree of
Doctor of Philosophy

June 2019

This thesis is dedicated to my parents, Libiao Zhou and Hui Liang.

Declaration

Whilst registered as a candidate for the above degree, I have not been registered for any other research award. The results and conclusions embodied in this thesis are the work of the named candidate and have not been submitted for any other academic award. The final thesis comprises 30352 words.

Dalin Zhou
June 2019

Acknowledgements

First I would like to acknowledge the contribution of my supervisor, Prof Honghai Liu, who has continuously supported me in both academic research and career development. Significant attention has been paid by Prof Liu to my research that has broadened my view in the field of rehabilitation and inspired me motivationally to explore the feasibility of this study. His encouragement and our discussion have contributed to the ideas and the completion of this thesis.

The acknowledgement is also given to Prof Haibo Ji, Prof Yu Kang, Prof Naoyuki Kubota, Dr Janos Botzheim and Miss Daxin Wang, who have helped me during my stay in their research groups. A plenty of ideas and approaches have been inspired under their guidance.

And I would also like to thank my colleagues and friends in the Intelligent Systems & Biomedical Robotics Group who have helped me during my course of study including Dr. Zhaojie Ju, Dr Yinfeng Fang, Dr Nalinda Hettiarachchi, Dr Haibin Cai, Dr Dongxu Gao, Dr Kairu Li, Mr Peter Boyd and Mr Wei Zeng. Special thanks go to Dr Yinfeng Fang, who has been guiding my experiments and data analysis throughout my course of study, providing selfless encouragement to me and sharing his knowledge and expertise in muscular sensing.

I am also thankful to Dr Kate Dingley, who has provided me with important advice on my course progress during my study. The help from Hobbs Rehabilitation and ProActive Prosthetics in related clinical experiments is also sincerely acknowledged here.

Last but not least, I want to express my sincere gratitude to my family. My studies could not be possible without their unconditional love and support.

Abstract

The control of prosthetic hands and other upper-limb assistive device for rehabilitation relies on the premise that users' hand motion intention is accurately recognised. Among all the feasible modalities, surface electromyography (sEMG) based hand motion recognition has been most widely adopted for its intuitiveness and effectiveness. However, the reported promising recognition accuracy is mostly confined to intra-day scenarios, which ignores the performance degradation of inter-day application for long-term use. To address the challenging inter-day hand motion recognition for long-term use, current sEMG driven solutions are further developed with an improved performance verified by experiments in this thesis. The contributions are recognised in terms of improved pattern recognition based classification, additional sEMG feature extraction and selection, novel multimodal fusion based hand motion recognition, and new long-term sEMG benchmark building.

First, both conventional pattern recognition and deep learning approaches are developed to accommodate the long-term use with inadequate and adequate training data respectively. Based on the feasibility of a force driven subclass division in our preliminary work, subclass division based linear discriminant analysis (LDA) frameworks using solely sEMG signals are proposed. Both explicit and implicit subclass division strategies are explored including the K-nearest neighbour based LDA (KNN-LDA) and subclass discriminant analysis (SDA) with a verified improvement of long-term hand motion recognition accuracy for inadequate training data. A convolutional neural network (CNN) architecture is adopted using raw sEMG as the input without preprocessing, whose significant improvement of long-term recognition accuracy has been seen with adequate and pooled training data across multiple days and subjects. Then the feasibility of merging handcrafted features and non-handcrafted features is proved in combination with a diversity of classification algorithms for the long-term hand motion recognition. And a novel multi-threshold based handcrafted feature vector is proposed and achieves an improved recognition accuracy. The feature selection is conducted with the bacterial memetic algorithm for achieving different targets including a compromised yet comparable recognition result at a largely reduced computational cost with selected subsets of existing features, and an improved recognition accuracy with selected features from enriched sub-segments of multiple lengths. To further remedy the lack of deep

muscle activity sensing in myoelectric sensing, the ultrasonic sensing is investigated as a complementary modality and integrated with the myoelectric sensing, which contributes to an improved accuracy of hand motion recognition. Finally, the lack of long-term constraints and low-density representations in existing public databases is addressed by building a new dataset comprising the long-term sEMG signals of 13 hand motions captured from 10 subjects in consecutive 10 days under a standardised protocol as a public benchmark for the research community.

Table of Contents

List of Figures

List of Tables

Nomenclature

Acronyms / Abbreviations

ACMC Assessment for Capacity of Myoelectric Control

ApEn Approximate Entropy

AR Autoregressive Coefficients

BMA Bacterial Memetic Algorithm

CNN Convolutional Neural Network

DoF Degree of Freedom

DWT Discrete Wavelet Transform

ECoG Electrocorticogram

EEG Electroencephalography

EMG Electromyography

ENG Electronystagmography

EOG Electrooculography

FD Frequency Domain

FES Functional Electrical Stimulation

FMG Force Myography

FSR Force Sensitive Resistor

GMM Gaussian Mixture Model

GNG Growing Neural Gas

HMI Human Machine Interface

HMM Hidden Markov Model

iEMG Intramuscular Electromyography

IMU Inertial Measurement Unit

KNN K Nearest Neighbours

LDA Linear Discriminant Analysis

LFC Linear Fitting Coefficients

MAV Mean Absolute Value

MDF Median Frequency

MMG Mechanomyography

MNF Mean Frequency

MUAP Motor Unit Action Potential

MU Motor Unit

NIRS Near-infrared Spectroscopy

QDA Quadratic Discriminant Analysis

ReLU Rectified Linear Units

RQA Recurrence Qualification Analysis

SampEn Sample Entropy

SDA Subclass Discriminant Analysis

sEMG Surface Electromyography

SMG Sonomyography

SSC Slope Sign Changes

SVM Support Vector Machine

TAC Target Achievement Control

TDARM Multi-threshold TDAR

TDAR Time Domain and Autoregressive Coefficients Features

TD Time Domain

TMR Targeted Muscle Reinnervation

WL Waveform Length

WPT Wavelet Packet Transform

ZC Zero Crossings

Chapter 1

Introduction

1.1 Background and Motivation

Fine hand motor function plays a critical role in daily life activities and is essential for performing dexterous and accurate gesture-based interaction and object manipulation. Upper limb impairment and amputation are common causes that deprive the patients of their normal hand movement, which in turn hinders their quality of life. The loss of hand functionality significantly affects the autonomy of human subjects and their capability of performing complex and useful tasks in daily living, working and social activities. Patients who have their hands amputated usually demand the bionic replacement such as prosthetic hands and upper-limb assistive devices to remedy the loss of hand motor function. According to NHS England D00/P/a and D01/S/d [7, 8], the prevalence of upper limb amputation is likely to be 10000 of 250000 per year with an estimated 55000 - 60000 of amputees attending specialist rehabilitation service centres in the UK. The rapidly growing need of upper limb motor function replacement forms one of the primary concerns in the healthcare community. As a result, extensive research has been conducted to develop life-like prostheses and improve their functionality. The desired properties of an ideal prosthetic hand are studied and identified by Cordella et al. [9] in terms of the accurate execution of daily life tasks including grasping and manipulation with an increased number of motion types, the integration of tactile sensory feedback into prosthetic hands to enable contact, sliding and force detection instead of solely relying on the visual feedback, the better control system comprising both position and force control of the fingers on the objects, and the improved dexterity of prosthetic hands with more degrees of freedom (DoFs). In summary, the potential improvement can be arbitrarily categorised into the development of prosthetic hardware design and the enhanced reliability of human machine interfaces (HMIs) grounded on the current motion intention recognition solutions.

Within our knowledge, to meet the growing need of amputees to replace their lost upper extremity, the development of prosthetic solutions has been continuously reported in the rehabilitation field for decades [10–12]. Besides the cosmetic appearance, execution of clinically viable and dexterous hand motion through prostheses is vitally desired by patients who suffer from upper limb impairments and attracts great attention from researchers. In the attempt to conduct fluid life-like hand motions clinically, both physical features of prosthetic hardware design, and sensing techniques and control strategies of HMIs should be well designed. Physical features like functionality and wearability are determined by the mechanical design of prosthetic hands [13]. With the emphasis on the integration of mechanisms, sensors and actuators [14], a large variety of dexterous robotic hands with multiple DoFs have been developed in recent years. The progress in the hardware design of assistive devices such as prostheses and exoskeletons has been propelled in both academia and industry by the growing need of upper limb motor function restoration [15, 16]. However, the types of executed hand motions in applications are still limited despite the improved prosthesis dexterity [17] and the HMIs adopted in commercial devices hardly differ from decades ago [18, 19]. The discrepancy is mainly attributed to the circumscribed development of the adopted HMIs for prosthetic hand control, which facilitates sensing physiological signals related to forearm muscle movement and decoding the intention of hand motion into executable commands to prosthetic devices. Fully exploiting the dexterous prostheses with multiple DoFs and other assistive devices for active upper-limb rehabilitation relies on the premise that users' motion intention is accurately recognised from their voluntary efforts [20, 21]. Thus to accommodate the increasing dexterity of bionic device and bridge the gap between prosthetic hardware design and HMIs for hand motion recognition, it is essential to overcome the limitations of existing HMIs by accounting for the sensing and recognition respectively.

Currently most HMIs for prosthetic control are noninvasive myoelectric sensing based ones, where the recognition of hand motion intention is based on the analysis of the surface electromyography (sEMG) over forearm muscles. And a typical flowchart of sEMG based prosthetic hand control can be seen in Fig. 1.1. Research has been frequently published on multiple stages including myoelectric signal capturing device development [22], preprocessing of captured physiological signals [23], the sEMG based hand motion recognition [2], the postprocessing of the decision stream generated by the recognition approach [24], and the evaluation criteria of real-time performance [5], whose effort is mostly targeted at improving the recognition accuracy. Though a promising recognition accuracy has been achieved in various publications [25–27], the gap between academic progress and clinical application keeps expanding in the absence of an ideal HMI. The myoelectric HMIs dated back to the

1950s and 1960s are still equipped by the vast majority of commercially available powered prostheses at present [28]. A possible cause of this situation is that the long-term usability is not guaranteed in current control strategies. Due to the natural characteristics of sEMG signals, inevitable physiological changes and electrode displacement in long-term use will result in the variation of signal manifestation, which hinders the accurate motion recognition in a clinical environment [29]. And the long-term usability is less concerned and remains to be addressed in multiple stages as depicted in Fig. 1.1.

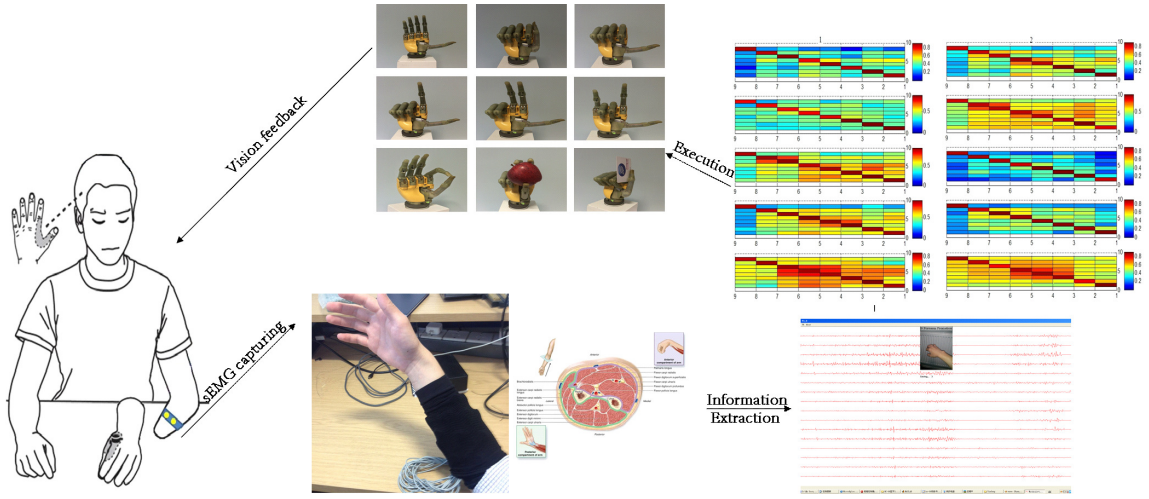

Fig. 1.1 A typical loop of prosthetic hand control with sEMG based HMI

Based on the background and the necessity of an improved HMI for long-term use, this thesis aims to develop a set of methodologies and techniques for hand motion recognition to deal with the problems and challenges described in Section 1.2.

1.2 Problems and Challenges

For prosthesis users, good intuitiveness, high success rate, low latency and limited adaptation cost of the devices are the prior properties to be fulfilled [2]. In details, the premise of an ideal control is crafted by the accurate recognition of users' intention, the imperceptible delay between the execution of the mechanical extremity and the employment of users' residual limb, and their consistent feasibility for long-term use. Among various feasible approaches, sEMG based pattern recognition for prosthetic hand control has been the most widely investigated one for its most promising performance [30]. The aim of such methodology is to distinguish users' intention of hand movement through classifying the patterns extracted from sEMG signals captured during forearm muscle contractions. Increasingly high accuracy and improved robustness have been frequently published within the framework of pattern

recognition in academia [31, 32] in terms of development of classifiers [33] and features [34]. And the superiority of pattern recognition based solutions in clinical scenarios has been stated in various recent research [35–37]. However, the intrinsic randomness of the sEMG signals contributes to a degraded performance in long-term use, which has been addressed by researchers [38–40] yet not fully accommodated. From the users' perspective, it is a time consuming burden for them to conduct the re-training for every day. Thus it is meaningful to improve the existing methods without re-training or reduce the training burden. To develop an sEMG driven solution to the inter-day hand motion recognition for long-term use, the following challenges need to be addressed:

1.2.1 Pattern Recognition Approaches Lacking Robustness to Inter-day Changes

Reports have shown that long-term use will deteriorate the hand motion recognition accuracy across multiple days. Various factors that affect the consistency of long-term sEMG signals have been taken into account like fatigue and electrode shift. The deterioration of inter-day performance leads to the requirement of everyday training effort from the users to adjust the applied recognition algorithm. The burden of re-training and re-calibration prevents the current research prototypes from being applied in clinical settings. Less or no re-training depends on a better priori knowledge of the potential invariance and inter-day relation of sEMG during long-term use. The inter-day performance of sEMG based hand motion recognition is improvable under the assumption that invariance and inter-day relation could be extracted from sEMG, which in turn is governed by jointly improved feature selection and classifier design. Mature classification approaches like linear discriminant analysis (LDA) have been widely applied in sEMG based hand motion recognition in combination with the classic Hudgins' time domain features together with autoregressive coefficients (TDAR), yet not able to fully exploit the invariant part and transfer it to inter-day use. It is challenging to propose suitable pattern recognition approaches for long-term use which can be identified in the development of both consistent features and robust classifiers.

1.2.2 Inherent Limitations of Noninvasive Unimodal Myoelectric Sensing

The intrinsic randomness and inevitable crosstalk of sEMG heavily prevent its feasibility of dexterous applications in the inter-day and inter-subject scenarios. The sensitivity to electrode shift and physiological changes like muscle fatigue and sweat also hinders sEMG

based solutions' long-term usability in clinical scenarios. Besides, the recognition accuracy and motion candidates are constrained by the intrinsic property of a noninvasive myoelectric sensing modality. SEMG only detects the electrical manifestation comprising the weighted contributions mainly from superficial muscles while dexterous limb motions are naturally regulated by deep muscles like flexor digitorum profundus, which hardly leads to a satisfactory recognition of finger movement. It is challenging to incorporate a suitable sensing modality that is complementary to myoelectric sensing, and form the basis of improved sEMG driven and multimodal fusion based solutions.

1.3 Overview of Approaches and Contributions

Taking into account the aforementioned challenges, this thesis proposes the improved pattern recognition frameworks in terms of developing both classifiers and features, together with the myoelectric and ultrasonic multimodal sensing. To mitigate the limited robustness to inter-day changes, subclass division is incorporated into the state-of-the-art patttern recognition methods for the scenario of inadequate training data while the deep learning approaches are considered to better exploit the adequate training data. Meanwhile, the classic feature extraction and selection strategies are further developed to enhance the robustness of the adopted pattern recognition framework which is reflected by the improved inter-day hand motion recognition accuracy. To remedy the constraint of unimodal myoelectric sensing, the sensing modality of wearable ultrasound is utilised to provide complementary information of muscular morphology to the bio-electrical manifestation of sEMG signals. The proposed approaches and main contributions of this thesis are presented as follows.

1.3.1 Subclass Division Based Discriminant Analysis for Hand Motion Recognition

Firstly, this thesis contributes to the hand motion recognition in conventional pattern recognition based classifier design to accommodate the training process with inadequate inter-day samples. This setting comprises the sEMG data of 1 or 2 days for training and the rest unseen days' data for testing. The discriminant analysis frameworks, taking into account the subclass division and invariant patterns that reside in sEMG signals, are proposed to improve the recognition performance in scenarios with less or no re-training. The subclass division is incorporated in the LDA in both explicit and implicit schemes. Similar to the fining and coarsening process in granular computing, the explicit subclass division leads to more class labels and the classification results of subclasses will be subsequently mapped into the

original classes. The subclass division based discriminant analysis is adopted to provide an improved recognition accuracy with limited training data, which reflects the potential benefits to the reduction of burden of training. The subclass division is first conducted in an explicit way through the totally unconstrained and unsupervised learning without a strict constraint of the subclass number across all the pooled data and followed by the LDA classification. Then the constrained and explicit subclass division utilising the relative distances between samples with the priori knowledge of class labels is conducted within each class and proposed as K-nearest neighbours based LDA (KNN-LDA). The subclass division analysis (SDA) combining the implicit subclass division strategy with a modified discriminant analysis algorithm is finally adopted for the inter-day hand motion recognition when inadequate training data is provided. And both the explicit subclass division and implicit invariance extraction strategies based discriminant analysis frameworks contribute to an improved hand motion recognition for long-term use.

1.3.2 Convolutional Neural Network for Low-density sEMG Based Hand Motion Recognition

Secondly, this thesis contributes to the low-density sEMG based hand motion recognition with deep learning approaches to utilise the adequate data across multiple subjects which comprises 7 days' data from 6 subjects for training and the rest for testing. A convolutional neural network (CNN) architecture with 2 convolution layers and 2 fully connected layers is adopted to fit the concatenated sEMG signals of multiple channels for inter-day hand motion recognition. A two-stage training approach comprising the pre-training and fine-tuning stages is employed to automatically extracts features of sEMG signals from multiple days across multiple subjects instead of using handcrafted features to gain the insight of their inter-day relation to address the long-term usability. The pooled adequate training data across multiple days and subjects are fed to the CNN to further address the feasibility of both inter-day and inter-subject knowledge transfer. A significantly improved long-term recognition accuracy is achieved by the CNN with adequate training data in comparison with the conventional pattern recognition approaches, which contributes to a potential baseline for the future research. The CNN is also modified to incorporate the classic handcrafted feature extraction to further improve the recognition accuracy.

1.3.3 Feature Extraction and Selection for Hand Motion

Thirdly, this thesis contributes to the hand motion recognition in feature extraction and selection. In the context of sEMG feature extraction, both handcrafted features and non-

handcrafted features are proposed in this thesis, in comparison with the most adopted TDAR features. The handcrafted TDARM features are proposed in the form of time domain (TD) descriptors with enumeration of conventional features in combination with multiple thresholds. The non-handcrafted features are extracted from the concatenated raw sEMG signals using the CNN with its first fully connected layer. The fusion of classic TDAR features and CNN features is validated for contributing to a better recognition accuracy in combination with multiple classification algorithms including both the conventional pattern recognition approaches and the deep learning architecture of CNN. Besides the feature extraction, feature selection is conducted to seek optimal and quasi-optimal feature subsets, targeting at reduced computational cost and better distinguishable performance respectively. The bacterial memetic algorithm (BMA) is utilised for its capability of simultaneous global and local search. The results indicate that selected subsets of TDAR feature candidates can achieve a compromised yet comparable performance at a largely reduced computational cost. Moreover, the features selected from TDAR candidates of multi-length windowed segments are beneficial for improving the recognition accuracy in comparison with the conventional single-length segmentation.

1.3.4 Myoelectric and Ultrasonic Fusion Based Hand Motion Recognition

Another contribution of this thesis is the incorporation of wearable ultrasonic sensing into the current singly myoelectric sensing based solutions. The feasibility of ultrasonic sensing based dexterous hand motion recognition is first validated among able-bodied subjects. And the drawback of significant sensitivity to probe shift is also identified in the wearable ultrasonic sensing. Along this line, the multimodal fusion based hand motion recognition is investigated using synchronously captured ultrasound and sEMG signals to exploit both the consistency of ultrasound based morphological representation and the relatively better robustness of sEMG to electrode distribution. In particular, the multimodal fusion based pattern recognition approaches are proposed by conducting the feature extraction on both sEMG and ultrasound signals and the subsequent classification of the concatenated feature vectors comprising the myoelectric TDAR features and the ultrasonic linear fitting coefficients (LFC), thereby improving the recognition accuracy with fused sensing modalities. And the evaluation on an amputated subject is provided as a case study on the targeted group of subjects to verify the superiority of multimodal sensing fusion.

1.3.5 Benchmark for sEMG Based Long-term Hand Motion Recognition

Last but not least, this thesis contributes to the research community of prosthetic control and hand motor function rehabilitation with a benchmark built for long-term evaluation of sEMG based hand motion recognition. The sEMG signals in inclusion are captured from 10 subjects performing 13 hand motions in consecutive 10 days under a standardised training and data acquisition protocol. Because of the standardised signal capturing protocol of the benchmark, it is straightforward to incorporate new subjects and new samples in the future, which allows the mitigation of current limitation of data size. Specifically, the dataset is made up of low-density sEMG signals captured in a prolonged inter-day scenario, which has not been simultaneously addressed by any other public datasets yet.

1.4 Thesis Organisation

The remaining chapters of this thesis are organised as follows.

Chapter 2 reviews the state-of-the-art work on muscular sensing based hand motion recognition with an emphasis on sEMG driven solutions. A comprehensive understanding of the wearable muscular activity sensing techniques and corresponding hand motion recognition algorithms is provided to the readers. The classic and prominent works and the most recent research perspectives are introduced in details. The concluding section finally summarises the progress and the limitations so far, and outlines the future research directions as well.

Chapter 3 first considers the development of conventional pattern recognition approaches of LDA. Discriminant analysis in combination with the subclass division strategy is adopted for long-term sEMG based hand motion recognition across multiple days with the inadequate training data provided. The conventional discriminant analysis is modified by subclass division strategies of unconstrained unsupervised clustering, constrained nearest neighbour based subclass division and implicit subclass division optimisation respectively. Different from the conventional discriminant analysis, subclasses of motion types of multiple days are generated either explicitly or implicitly to accommodate the varying sEMG patterns, which are attributed to physiological changes in long-term use. Explicit subclass division through K-nearest neighbours (KNN) is adopted to generate new labels of the training data by addressing the subclass division and the invariance within sEMG signals of multiple days in multiple subclasses within each motion type. The SDA utilises the subclass division implicitly and seeks the invariance within to reduce or eliminate the burden of re-training. This chapter further demonstrates the feasibility of deep learning approaches in the sEMG based

hand motion recognition, with an emphasis on the low-density electrode distribution based capturing system instead of the commonly used high-density ones. The data segmentation, network structure, pre-training and fine-tuning are routinely introduced in our applications. Specifically, the raw multi-channel sEMG signals are fed to the network for training and classification to further verify the practicality of the deep learning approaches in dealing with both inter-day and inter-subject knowledge transfer for long-term use, which is not considered in the conventional sEMG based hand motion recognition.

Chapter 4 addresses the importance of features from the perspectives of extraction and selection respectively. Both conventional priori knowledge based handcrafted features and deep learning based non-handcrafted features are discussed about and fused into the feature set to achieve a better classification result. A novel feature vector TDARM comprising conventional TDAR features and the TD descriptor enumeration with multiple threshold is proposed and tested for its feasibility. And the evolutionary algorithm BMA is adopted for the feature selection from both classic TDAR features and the ones extracted from multi-length windowed segments to address the need of computational cost reduction and the improvement of recognition accuracy respectively.

Chapter 5 incorporates the ultrasonic sensing modality into the current singly myoelectric modality based muscle activity sensing and hand motion recognition, following the verification of its feasibility in dexterous hand motion recognition across able-bodied subjects. The LDA classifier in combination with the TDAR features of myoelectric signals and the LFC features of ultrasonic signals is adopted to facilitate the multimodal sensing. The merits of myoelectric and ultrasonic fusion based hand motion recognition are validated with a case study on an amputated subject.

Chapter 6 provides the experiment setup and data acquisition details to form a new sEMG dataset with more subjects and prolonged scenarios involved for long-term use evaluation as a potential benchmark, followed by the experiments and thorough discussion.

Chapter 7 finally summarises the contributions of this thesis and discusses the future research directions.

Chapter 2

Literature Review

2.1 Muscle Activity Sensing

The taxonomy of sensing techniques for prosthetic hand control and active motor function rehabilitation is generally described in perspectives of their invasiveness and intuitiveness. Conservative noninvasive modules whose detecting sites are distributed over the skin surface are naturally preferred by prosthetic hand users. Among all the feasible sensing mechanisms, sEMG based myoelectric control has been the most adopted control strategy for decades in both academia and industry. Other noninvasive manifestations like sonomyography (SMG), inertial measurement units (IMU), electrooculography (EOG), electroencephalography (EEG), mechanomyography (MMG), force myography (FMG) and near-infrared spectroscopy (NIRS) have been utilised independently or in combination with sEMG signals in a multimodal scheme [30, 41, 42]. An invasive sensing modality typically requires surgery process like the electrode implantation or needle insertion for acquisition of intramuscular electromyography (iEMG) [43], the craniotomy and electrode implantation to retrieve electrocorticogram (ECoG) [44] and the grafting residual nerves that exert EMG signals to spare muscles through targeted muscle reinnervation (TMR) surgery [45]. Though invasive sensing approaches are rarely exploited as the sensing techniques in a commercial prosthetic hand control system, strategies like TMR surgery are clearly more suitable for proximal amputees, whose muscular structure of arms is no more accessible [6].

To date, let alone the numerous manifestations that represent muscle activity, sEMG remains the main equipped sensing modality for muscular activity sensing in the active control of almost every commercial upper limb prosthesis and exoskeleton for active limb motor function restoration. A main reason is that the EMG signals are directly related to the muscle contraction and provide an intuitive physiological perspective of the motion intention generation. Furthermore, the EMG allows the recognition of motion intention through the

muscle contraction within residual limbs and does not rely on the actual limb movement because of its bio-electric nature. In this thesis, the main focus is attached to the noninvasive sensing techniques with an emphasis on the sEMG driven solutions. This section primarily reviews the myoelectric sensing technique and address the alternative modalities suitable for multimodal fusion based sensing as a complement.

2.1.1 Myoelectric Sensing

Myoelectric signals are the electrical manifestation of active motor units (MUs) during muscle contractions, where the information of neural control signals and muscular physiological changes resides in [46]. MUs are the basic components involved in body movement, each of which consists of a motor neuron and its corresponding muscle fibres, following the all-or-none law to be recruited. When the stimulus on an MU induces a potential exceeding the threshold voltage during muscle contractions, the MU is recruited to undergo the cycle of depolarization and repolarization. The motor unit action potential (MUAP) occurs as a response to the flow of ions, whose magnitude and shape depend on intrinsic properties of muscle anatomy [47]. The MUAP intuitively depicts the electrochemical process of an MU during muscle contractions. It is reasonable to postulate that the muscle activity can be subtly interpreted through the potential variation of all the recruited MUs. However, the distinct detection of MUAP for every MU is impractical in a clinical application. Detected myoelectric signal is the weighted sum of MUAP contribution and normally illustrated by EMG in practice. The machinery of EMG provides a mildly compromised but fully practical approach to inspecting the MUAP with a relatively macroscopic perspective. EMG signal processing methods have been developed to extract the information on muscle activity dynamics and muscular physiological properties [12, 31], thus providing a natural source to decode the forearm movement for prosthetic control and motor function rehabilitation.

EMG is generally categorised into sEMG and iEMG according to the location of detection sites. Electrodes for sEMG detection are attached to the skin surface while iEMG requires invasive electrode implantation. As a result, sEMG only detects the compound electrical manifestation mostly from superficial muscles while iEMG allows selective recording from individual superficial and deep muscles. The research conducted by Kamavuako et al. [43] demonstrated a higher correlation between iEMG and force in comparison with sEMG, allowing representation of the applied grasping force with a selective EMG recording. A follow-up evaluation of iEMG based force estimation in 2 DoFs was reported with high accuracy on 3 able-bodied subjects [39]. Further research by Smith et al. [48, 49] demonstrated the feasibility of iEMG based simultaneous control of multiple DoFs in real-time application. Meanwhile, the crosstalk is inevitable for sEMG but absent for iEMG. In

another published comparison [50], strong correlation between sEMG captured from different channels has been seen while barely no correlation was found for iEMG among detection sites. A preliminary conclusion has been drawn that the independence of iEMG would provide superior local information of targeted muscles which permits intuitive, simultaneous and proportional control of multiple DoFs.

Despite the mentioned merits of iEMG, sEMG is more exploited in practice for prosthetic hand control mainly for its noninvasiveness and easy access, which is the prior concern for common users. SEMG signals are most commonly collected using one or more electrodes placed on the skin surface either with reference to particular muscles or equidistantly over an area of interest [51]. And sEMG can be captured by both wet and dry electrodes in either a passive or active mode without complicated setup and chronic adverse effect, which contributes to a better acceptance rate from the users [52]. A customised multi-channel sEMG capturing system with low-density electrode distribution is shown in Fig. 2.1 and a sample of the high-density sensing grid is shown in Fig. 2.2. In addition to the better acceptance by users, it has been validated on 6 able-bodied subjects that iEMG does not outperform sEMG in pattern recognition based myoelectric control [53]. And intensive research has highlighted the attempts in improving sEMG and pattern recognition based HMIs for prosthetic hand control. Besides the direct use of EMG in clinical applications, further exploitation of the information that resides within EMG from the perspective of single MUs have been revealed by extensive coherent research led by Farina et al. [54–59]. The generation and decomposition of electrical manifestation have been explored to derive the direct neural drive to muscles from the indirect description of neural activation based on sEMG.

Though sEMG sensing enjoys the merits of noninvasiveness, easy access and high temporal resolution, it still suffers from its intrinsic characteristics as will be shown in Section 2.2.5. To remedy the limitations, a plausible way is to incorporate other sensing modalities such as EEG, SMG, MMG, FMG and NIRS [60–62].

2.1.2 Multimodal Sensing

Besides sEMG, various noninvasive sensing modalities have been used for hand motion recognition in prosthetic control. A brief categorisation of the sensing modalities for hand motion recognition is given in Table 2.1.

SMG is the interpretation of morphological changes of forearm muscles such as thickness variance during the contraction in various motions which can be applied in prosthesis control and has attracted great attention from researchers. Fukumoto et al. [70] revealed the capability of ultrasonic signals in the identification of muscle volume changes and estimate

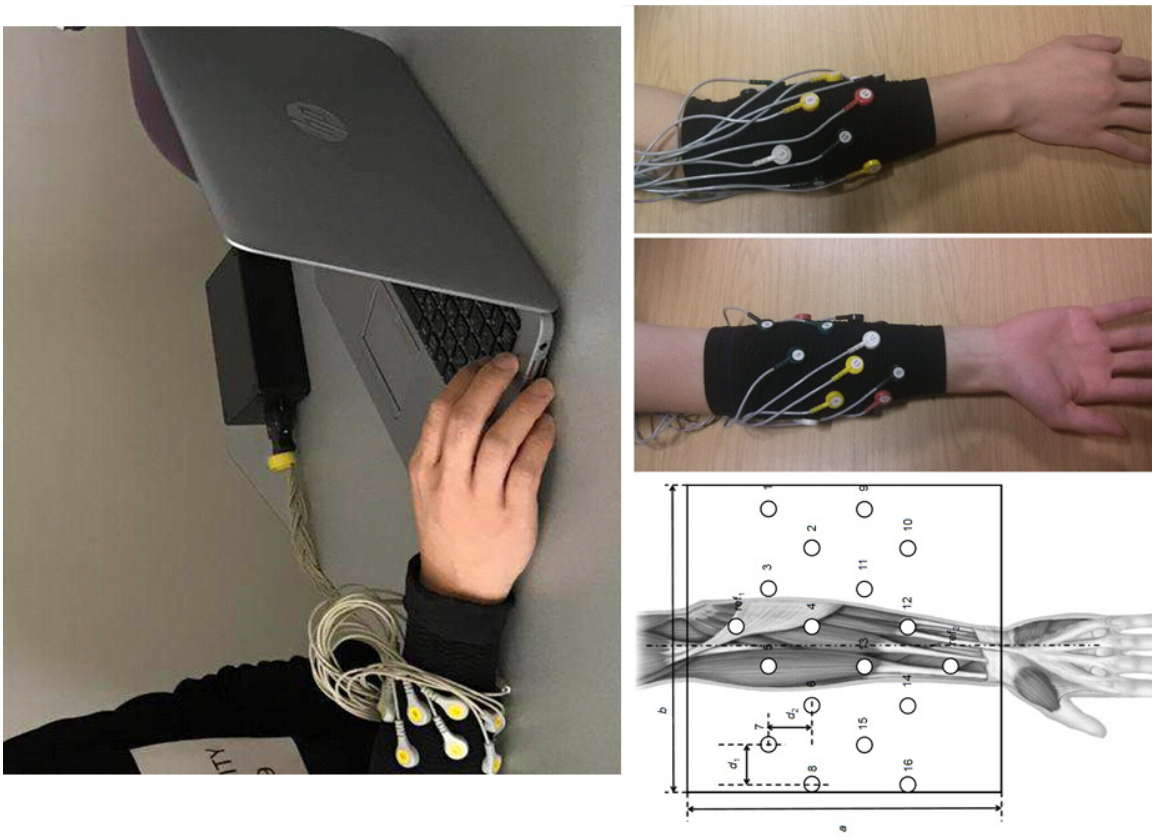

Fig. 2.1 A customised multi-channel sEMG capturing system with sleeve embedded low-density electrode distribution

Table 2.1 Categorisation of the sensing modalities for hand motion recognition

Category	Modality	Physiological Type	Physical Property
Muscular sensing	EMG [22]	Muscle action potential	Electric
	SMG [63]	Muscle morphology	Ultrasonic
	MMG [64]	Muscle oscillation	Acoustic
	NIRS [65]	Blood oxygen	Infrared
	FMG [66]	Resistance	Mechanical
Neurological sensing	ENG [67]	Peripheral neuronal activation	Electric
Brain sensing	EEG [68]	Brain neuronal activation	Electric
	ECoG [69]	Brain neuronal activation	Electric

muscular strength. Castellini et al. [71] stated in their research that there exists a clear linear relationship between the features extracted from ultrasound images and finger positions. Zheng et al. [72] first used the terminology of SMG and demonstrated that the relationship between wrist extension angle and the percentage of muscle deformation can be extracted by the selected echo features of ultrasound images. Furthermore, SMG has been used as

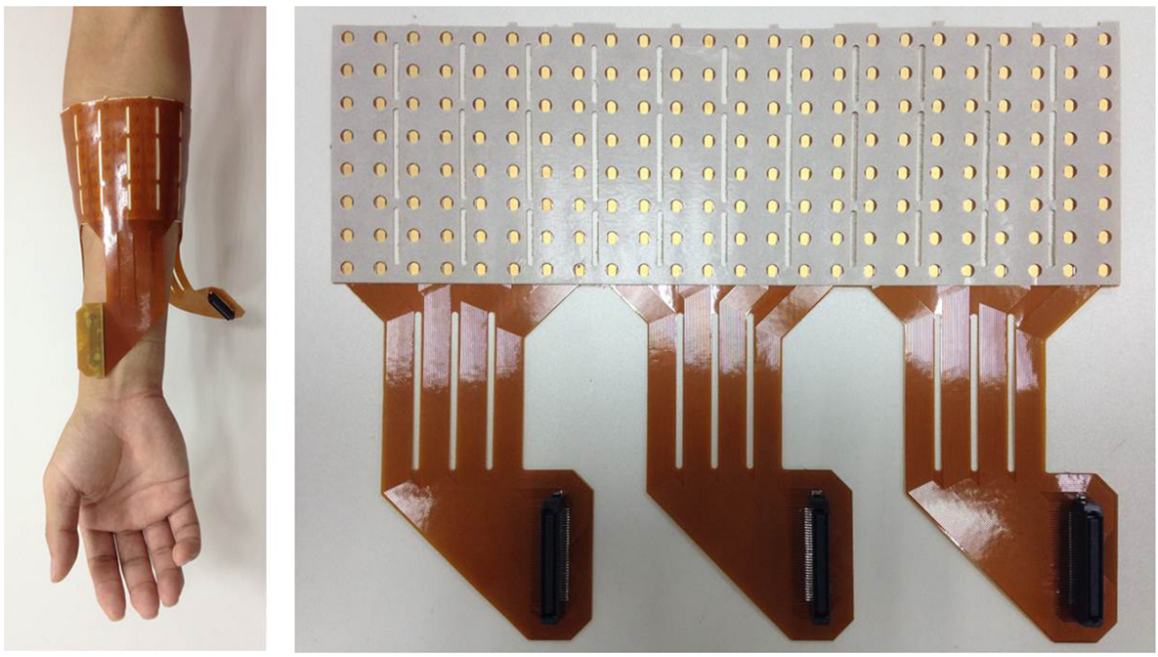

Fig. 2.2 An example of the high-density forearm sEMG sensing grid [1]

the sensing modality in various research on hand motion recognition especially dexterous finger movements. The estimation of wrist joint angles has been realised through tracking features in a window of ultrasound images in [73]. Shi et al. [74] adopted the Horn-Schunk optical flow algorithm to identify finger flexions from ultrasound images. Sikdar et al. [75] showed the capability of SMG to recognise individual finger movement with a significantly promising classification accuracy at 98%. And the feasibility of wearable SMG has been further demonstrated by various publications [76, 77].

IMU is the electronic device that measures the specific force and angular rate of human body, which can be used to extract limb positions for prosthetic control. A single sensing modality of EMG deteriorates the performance when taking into account numerous factors such as limb positions [78] and prosthesis weights [79]. The usability of sEMG signals tends to be adversely influenced under inevitable shift and mismatch between the arm postures and prostheses, while IMUs could compensate the lack of known geometric information. As a result, IMUs like accelerometers have been incorporated for tracking the changes of arm positions and applied as complement to EMG signals. Experiments have demonstrated that the inclusion of IMU signals can improve the hand motion recognition accuracy [80, 81] instead of adding more EMG detecting channels. In addition, IMU signals have also been used in a multimodal mechanism to detect muscle contraction by a dynamic threshold with MMG signals [82].

NIRS is a spectroscopic method that uses the near-infrared region of the electromagnetic spectrum and has been applied in the blood flow sensing over the skin surface of forearm muscles [62]. It is well accepted that EMG signals are sensitive to muscle fatigue, which results in faulty classification of hand motions [83]. NIRS is capable of measuring muscle fatigue [84], and has been utilised to compensate the negative effects of muscle fatigue in the sEMG driven multimodal fusion. Herrmann et al. [65, 85] proposed a feature named NIRSRMS that combines the weighted NIRS with the root mean squared values of EMG, and demonstrated that the combination of EMG and NIRS contributes to a better hand motion recognition accuracy.

EEG is an electrophysiological monitoring method that records electrical activity of the brain, where the recording of the nerve motor output could function as a natural HMI for prosthetic control. Rossini et al. [86] showed that EEG signals significantly improve the classification performance based only on electronystagmography (ENG) signal analysis, which coincides with the idea that hand-related activities can be decoded by the combined analysis of motor-related signals simultaneously gathered via intraneural electrodes implanted into the peripheral nerve system and EEG signals recorded from scalp to control a dexterous prosthesis. Tombini et al. [68] also demonstrated the improvement of recognition accuracy through focusing ENG in an EEG driven time window. Li et al. [60] further analysed the hand motion recognition based on the combination of sEMG and EEG signal with its feasibility validated.

MMG is also known as vibromyography and acousticmyogram that captures the lateral oscillations generated by dimensional changes in active muscle fibres [87], and is detected by microphones or low-mass accelerometers. MMG has been studied for monitoring of muscle pain, tracking of muscle fatigue, measurement of muscle contractility in myopathic diseases, and bi-functional prosthetic upper-limb control. It is worth noting that MMG has the potential to detect weaker muscle contractions than EMG [88] and is suitable for prosthetic control as either the main sensing modality or the complement to EMG. A study conducted by Zeng et al. [89] showed that an acceptable classification result can be achieved in hand motion recognition with extracted novel features of MMG in combination with the quadratic discriminant analysis (QDA). And Silva et al. [82] has conducted and validated the MMG based multisensory data fusion for prosthesis control.

FMG is developed on polymer thick film technology of FSR, which externally resembles a membrane switch but has a resistance that varies continuously with applied force [90]. FMR enjoys the robustness to external electrical interference and sweating compared to EMG in hand motion recognition at a low cost. Additionally, FMG is capable of detecting movements at a low speed in comparison with commercially available accelerometer based

devices [91]. A detailed comparison among FMG, SMG and EMG sensing based hand motion recognition [92] demonstrated that FMG yields a comparable recognition accuracy with sEMG as opposed to SMG while enjoys a much better stability than sEMG. Within the same article, though the typical nonlinear behaviour of the FSR sensor guarantees no repeatability across sensors, yet can be remedied by incorporation of additional sites. Jiang et al. [93] showed a promising result in classifying 48 hand gestures with only 8 FSR sensors equipped in the customised sensing band. What's more, by using all 16 FSRs on the band, the developed device achieved a significantly higher accuracy in the same scenario. Particularly, the multimodal sensing with the combination of the wrist FMG and forearm sEMG contributes to accommodating potential clinical constraints in a hierarchical scheme.

Based on the fact that the singly myoelectric sensing based hand motion recognition suffers from the intrinsic sEMG characteristics as a single modality, the significance of multimodal fusion sensing based hand motion recognition for prosthetic control has been addressed by various researchers and reviewed in [30]. Multimodal sensing provides a feasible strategy to improve the overall consistency of captured signals, which promisingly leads to a better hand motion recognition accuracy for targeted applications. In terms of the fusion of sensing modalities, there are two approaches commonly adopted. One is the hierarchical approach utilising a dual-stage or multi-stage scheme, which first identifies the predefined hierarchy or indices using one single modality, and then recognises targeted hand motions through analysis of the rest modalities. The other approach simply extends the feature vectors of the original modality by additional features of the fused ones [78, 94]. A more detailed examination of the multimodal fusion based sensing and analysis will be presented in Chapter 5 with an emphasis on the pattern recognition based methods applied to myoelectric and ultrasonic sensing modalities.

2.2 Myoelectric Hand Motion Recognition

A feasible HMI for prosthetic control relies on the premise that the hand motion intention is accurately recognised. Due to the absence of observable canonical hand movements and the various degree of amputation across subjects, a coherent combination of sensing modalities and corresponding recognition algorithms is desired. Conventional sEMG based hand motion recognition strategies are generally categorised into direct recognition and pattern recognition based recognition, both coping with the classification of users' motion intention. This section will introduce the recognition approaches with a specific emphasis on the pattern recognition based solutions through a detailed review on all the involved stages.

2.2.1 Direct Recognition

Though the pattern recognition based myoelectric hand motion recognition has reached a promising accuracy of 90% in a laboratory environment in numerous publications, there still exist a wide choice of direct control. This is mostly attributed to the fact that pattern recognition control enables the recognition of more sophisticated predefined motions yet confined to a sequential and non-proportional mechanism. In this thesis, the sEMG based direct hand motion recognition is defined as the mapping of sEMG signals into control commands of individual DoFs without the reference to any predefined motion templates. Amplitude based direct control allows robust and proportional control of employed DoFs [95], which is similar to natural movement. However, it has been revealed that the usability of direct control is seriously affected by the crosstalk of sEMG [58]. Simultaneous activation of multiple DoFs using direct control is only clinically feasible in individuals who have undergone the surgery of TMR [96], which severely restricts the complexity of distinguishable motions, and leads to a low acceptance rate because of the invasiveness.

Despite the restriction of an invasive surgery that may occurs, a most recent research focus has been seen in the muscle synergy based control or simultaneous and proportional control. This approach is also categorised into the direct control in this thesis because of its direct control of multiple DoFs instead of using the predefined motion templates. Muscle synergy is defined as the coordinated activation of grouped muscles. The feasibility of sEMG synergies in characterising hand grasps has been proved, which is largely invariant among different subjects [97]. And the simultaneous and proportional force and kinematics estimation has been realised in a similar mechanism through mirrored bilateral training in [98] and [99] respectively. Principal component analysis (PCA) and non-negative matrix factorisation (NMF) have been frequently used to denote the synergistic sEMG activity of hand grasping [100]. However, no solid proof of the anatomical relevance has been revealed [101] since sEMG does not retrieve the morphological changes of muscles. Despite the simultaneous and proportional control of multiple DoFs robust to the electrode shift [102], the performance is with limited dexterity in the involved DoFs. Besides the anatomical relevance, the cross-subject similarity, repeatability and stability are also disregarded in most existing research on sEMG based hand motion recognition. To date, the DoFs controlled by muscle synergies are mostly confined to wrist movement [103, 104], which is far from dexterity. It is worth noting that the direct control is further developed to a large extent in a recently published work, where Farina et al. [59] identified the motor-neuron behaviour through deconvolution of the electrical activity of muscles and mapped the series of motor-neuron discharges into control commands across multiple DoFs.

Regardless of the significant scientific progress in direct control, pattern recognition based myoelectric hand motion recognition remains essential to be further enhanced in its clinical usability and long-term performance based on its outstanding accuracy in selected dexterous motion templates, before the maturity of control of multiple DoFs simultaneously and proportionally with an extended number of the available DoFs in practical applications, which possibly relies on the incorporation of more robust sensing modalities.

2.2.2 Conventional Machine Learning Based Recognition

Pattern recognition based myoelectric control has been investigated and exploited as the mainstream HMI in academia for the last two decades for its feasibility of multiclass classification among dexterous predefined motion templates which contributes to the sequantial but fluid movement changing between different dexterous motions in a seamless manner without an explicitly manual switching. A typical conventional pattern recognition flowchart for sEMG based hand motion recognition is illustrated in Fig. 2.3. Raw sEMG signals are first captured by either dry or wet electrodes attached on the skin surface of forearms. After the preprocessing by filters to remove common mode noises, power line noises and irrelevant components, the stream is segmented by windows with either overlapping or non-overlapping increments. For each segment, its features are extracted and dimensionally reduced, then fed to the classifier and categorised into predefined motion types, which forms the sequence of recognition results and will be concatenated to generate the decision stream. Finally the postprocessing techniques such as majority vote are used to transfer the decision stream into executable commands to the prosthetic hands.

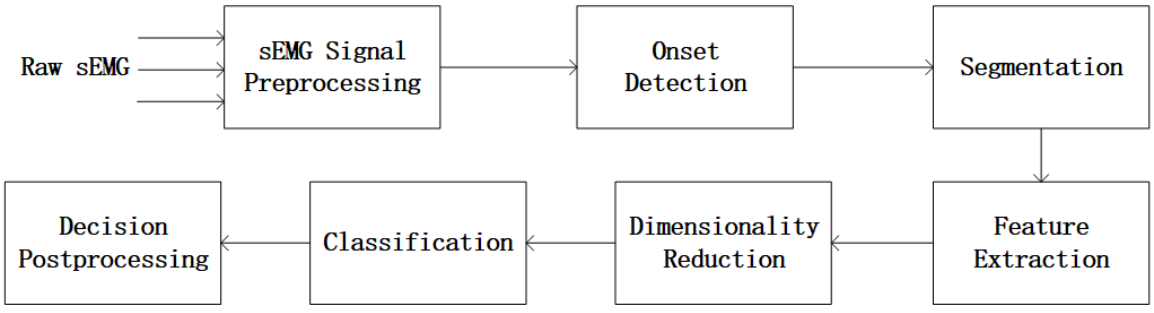

Fig. 2.3 A typical flowchart of pattern recognition based myoelectric control

Notwithstanding the high recognition accuracy in differentiating multiple complex motions, most of current commercial devices are equipped with amplitude based direct control. A most recent study conducted by Kuiken et al. [35] has reached a preliminary conclusion that the efficiency and efficacy of pattern recognition would enable a successful control

to complete the functional tasks. Different from previous publications, the evaluation was conducted in a home environment through usability tests on three amputee subjects. Better intuitiveness and improved customised response measurements such as cognitive load, performance and learnability have been seen in pattern recognition based control in comparison with direct control for clothespin relocation tasks [36]. Hargrove et al. [37] demonstrated the effectiveness of the combination of TMR surgery and pattern recognition approaches on transhumeral amputees equipped with commercial prostheses, while different findings have been reported by Resnik et al. [105] to support the direct control. Though it is still inconclusive whether pattern recognition based control strategies outweigh the direct ones in clinical settings, the conventional stages of pattern recognition are worth further investigation to improve the accuracy in inter-day scenarios for long-term use, which has not been fully accommodated and keeps attracting intensive research interest.

Besides the validation of the clinical viability of pattern recognition based myoelectric control, various combinations of feature extraction and classification strategies, from the most classic TDAR features with LDA and support vector machine (SVM) [25] to nonlinear recurrence qualification analysis (RQA) with fuzzy Gaussian mixture models (FGMM) [26], have been continuously reported with a promising intra-day recognition accuracy above 90% as a baseline in laboratory conditions [28, 106]. Let alone the emphasis on the combination of features and classifiers, progress on other topics like the preprocessing of captured myoelectric signals [23, 107], the onset detection of muscle activity [108, 109], the postprocessing of decision stream generated by the classifier [24, 110], and the evaluation paradigm for real-time performance [5, 111] have also been frequently published. Adverse factors including electrode shift and muscle fatigue during long-term use, inherent cross-day and cross-subject variation of sEMG signals all lead to the heavy burden of classifier re-training that impedes the widespread use of pattern recognition based control [40], which has been addressed by various research to overcome as well. Direct usage of the previously trained sEMG based model on a new subject naturally provides a negative result [112], to solve which multiple compromised solutions have been proposed. Modified classifiers within various machine learning frameworks from adaptive learning [113] to domain adaptation [33] have been explored to reduce the size of required data for re-training. There also have been attempts in pooling of data captured in multiple electrode displacement conditions [114], dynamic contraction conditions [115] and from multiple days [116] to achieve a more robust performance.

In the last two decades, research on myoelectric sensing based pattern recognition for hand motion recognition has been particularly marked by fragmented development, which is introduced in details as follows.

Preprocessing

When raw sEMG signals are captured, the bandpass Butterworth filter and the notch filter are first applied to the signals to exclude the power line noise and preserve the signals between desired frequencies. Then the preprocessing is conducted to polish the sEMG data to better accommodate the subsequent analysis. Normalisation is the most trivial and frequently used preprocessing strategy to alleviate the adverse effects brought by the varying sEMG amplitudes of the same motion types, which is routinely done based on the amplitude of sEMG during a preliminary training phase. Hargrove et al. [117] compared various PCA based preprocessing techniques like motion-class-specific PCA and universal PCA across all motion classes, whose results favoured the classwise PCA in combination with a sequential forward selection scheme. Liu et al. [23] used the signal whitening for preprocessing to reduce the random error of the processed sEMG. The whitening process temporally decorrelates the sEMG signals, increasing the effective number of signal samples and reducing the variance in the amplitude estimation, which leads to an improved classification accuracy. A group of preprocessing techniques including sEMG whitening, spatial filtering and PCA are examined in [110] to enhance the performance of their self-correction based pattern recognition system.

Onset Detection

The suppression of unintentional prosthetic movement is important in both direct recognition and pattern recognition based prosthetic control to achieve a reliable practical application. Onset detection is commonly adopted to distinguish the active and inactive status at the very first stage for suspension of erroneous activation. The research on onset detection has been conducted for over 20 years [118] to improve the clinical performance of prosthetic control. It has been stated that consistent onset patterns exist for each motion of the same subject, however differs across subjects. Most onset detection methods adopted in real scenarios are threshold based for the computational efficiency to meet the real-time requirement. Merlo et al. [119] utilised the continuous wavelet transform based descriptor to detect muscle activity. The Teager-Kaiser energy operator which highlights both amplitude and instantaneous frequency on muscle activity has been employed for onset detection with a threshold based avenue [120]. The experiments on 8 able-bodied subjects reported by Lorrain et al. [115] showed the pattern recognition in combination with a threshold based onset detection would lead to a better performance. Sample entropy (SampEn) has also been employed with an optimised threshold for the onset detection by [108] with an improved performance against spurious background spikes. A most recent detection method proposed

by Yang et al. [109] applied the Teager-Kaiser energy operator to amplify the signal variance change and used the morphological open/close operators to filter the artefacts for suppression of sEMG outliers.

Data Segmentation

Signal segmentation is performed after the motion onset is detected. The filtered myoelectric signals are partitioned into segments through either disjoint or overlapped windowing depicted in Fig. 2.4 and Fig. 2.5. The feature extraction and classification will be conducted on the myoelectric signals within each segment to generate a recognised motion type for the time interval. A preliminary test on the relation between hand motion recognition accuracy and the segment length is seen in Fig. 2.6. It is visually observable that the classification results monotonically improve with the increasing length of sEMG segments for the 2 subjects, which favours a selection of longer windows to segment the signals. However, it has been widely accepted that a delay of more than 300 ms is perceivable to prosthetic hand users and leads to a low acceptance rate of the device [32]. A research based on 13 able-bodied subjects has indicated an optimal interval of window length between 150 ms and 250 ms [121] while Farrell et al. [122] suggested an optimal optimal delay between 100 ms and 125 ms for most people without a large variation in motor functionality. And the choice of segmentation length does not always comply with the suggested interval. For example, a window length of 128 ms with an increment of 50 ms was adopted for the recognition of static parts of the signals for long-term evaluation in [123], a 300 ms window length with 75 ms increment was effective in the research on motion recognition against EMG degradation in [124], and a window length of 100 ms with 60 ms overlapping was employed for the prediction under varying arm postures in [125]. As mentioned above, though the perceivable delay is well acknowledged as the segmentation is confined to a length of no more than 300 ms, yet a discrepancy remains on the optimal length of segmentation.

Feature Extraction and Classification

Similar to general pattern recognition problems, the accuracy of EMG based hand motion recognition heavily relies on the extraction of repeatable and distinguishable features. Features with maximum class separability, robustness and less computational complexity are naturally desired [29]. The feature extraction strategies of sEMG signals are generally categorised into time domain (TD), frequency domain (FD) and time-frequency domain (TFD). Despite the large amount of potential features [34], the Hudgins' TD features proposed in the cornerstone paper [12] and the autoregressive coefficients have been mostly exploited

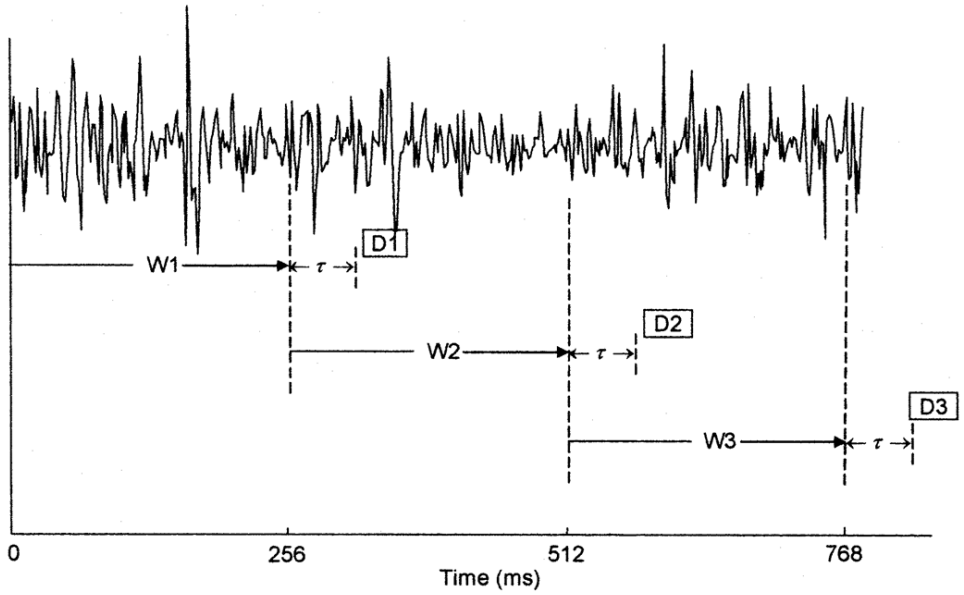

Fig. 2.4 Disjoint windowing for sEMG segmentation [2]

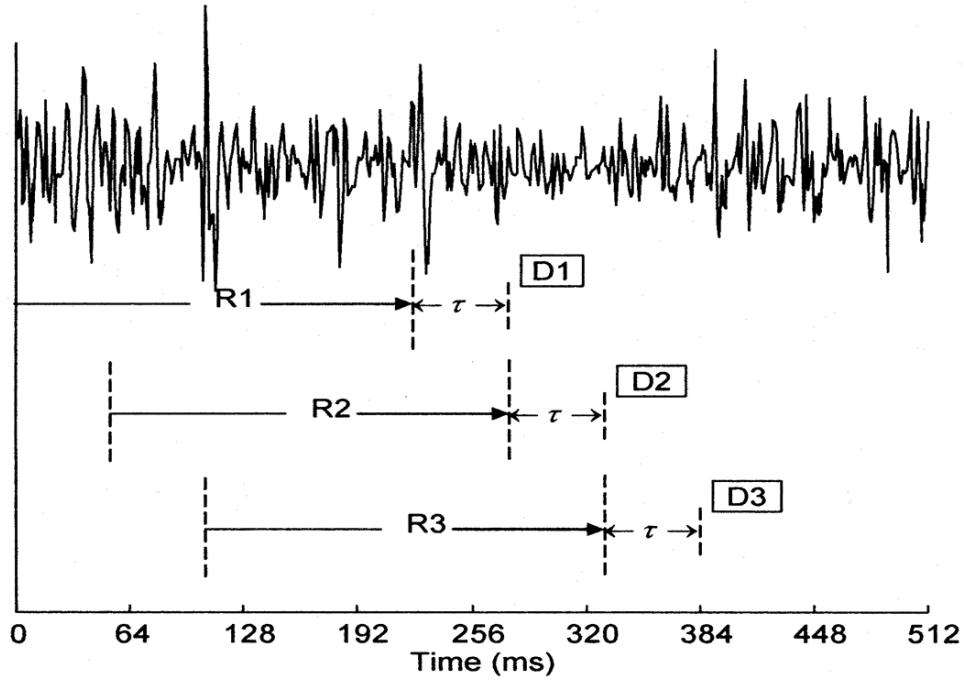

Fig. 2.5 Overlapped windowing for sEMG segmentation [2]

for their less time consumption and robust performance, and remained the state-of-the-art for years as TDAR features. The detailed extraction of the TDAR features including mean absolute value (MAV), waveform length (WL), zero crossings (ZC) and slope sign changes (SSC) together with autoregressive coefficients (AR) are listed as follows.

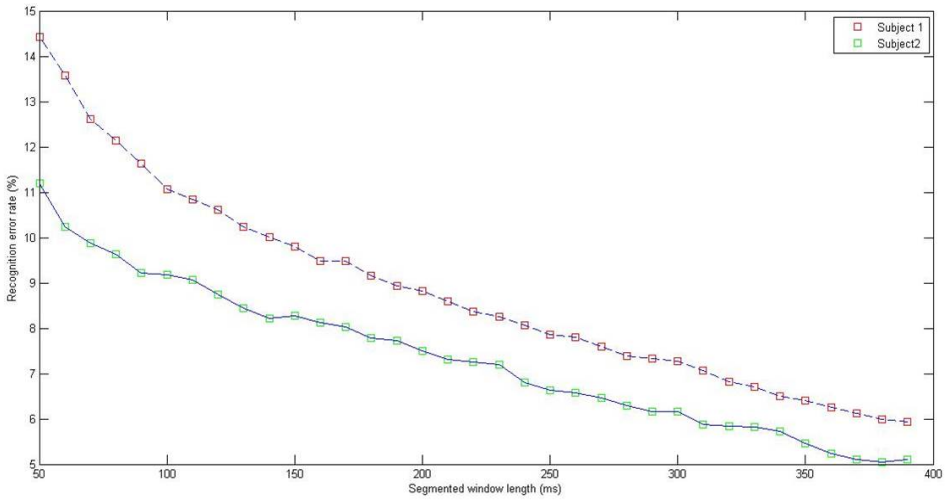

Fig. 2.6 A decreasing recognition error rate with increasing window lengths of segments

Mean absolute value provides estimation of the mean amplitude of the sEMG signal within segment i comprising N samples where x_k is the k-th sample in the i-th segment of sEMG signals.

$$MAV_i = \frac{1}{N}\sum_{k=1}^{N}|x_k| \tag{2.1}$$

Waveform length provides the information of waveform complexity in the i-th sEMG segment, which is the cumulative length of the waveform over the segment that measures the waveform amplitude, frequency, and duration all within a certain feature.

$$WL_i = \sum_{k=1}^{N-1}|x_{k+1} - x_k| \tag{2.2}$$

Zero crossings provide the counting of times when the waveform crosses zero. x_k and x_{k+1} are two adjacent samples within the i-th sEMG segment, and the threshold ε must be well designed to reduce the noise induced zero crossings.

$$ZC_i = \sum_{k=1}^{N-1}[sgn(x_{k+1}\cdot x_k)\cdot\delta(|x_{k+1}-x_k|)] \tag{2.3}$$

$$\delta(x) = \begin{cases} 1, & x > \varepsilon \\ 0, & x \leqslant \varepsilon \end{cases}$$

Slope sign changes provide another counting of times when the slope sign of the waveform changes. x_{k-1}, x_k and x_{k+1} are three adjacent samples within the i-th sEMG segment, and the threshold ε should also be properly picked to avoid the noise induced counting number.

$$SSC_i = \sum_{k=2}^{N-1} \delta[(x_k - x_{k+1}) \cdot (x_k - x_{k-1})]$$
$$\delta(x) = \begin{cases} 1, & x > \varepsilon \\ 0, & x \leqslant \varepsilon \end{cases} \tag{2.4}$$

Autoregressive coefficients provide the autoregressive model representation of the sEMG segment i with order p, and x_t is the t-th sample within.

$$x_t = c + \sum_{i=1}^{p} \varphi_i x_{t-i} + \varepsilon_t \tag{2.5}$$

where c is a constant, φ_1 ... φ_p are the parameters of the model that will be concatenated to shape the p-dimensional AR features, and ε_t is the white noise.

Research that addresses the feature evaluation for myoelectric prosthetic hand motion recognition has been continuously seen for decades [126]. Besides the recognition accuracy or error rate, multiple criteria have been utilised for feature evaluation such as mutual information that possesses better robustness than the error rate [127], and the correlation based feature selection that efficiently determines a separability index using the Mahalanobis distance between classes [128]. A thorough evaluation of 50 features that covers the extraction strategies in TD, FD and TFD can be tracked in [34]. As indicated in the review paper, FD features such as mean frequency (MNF) and median frequency (MDF) are good indicators for muscle fatigue. And the entropy based indices such as sample entropy (SampEn) and approximate entropy (ApEn) perform robustly under circumstances where small contractions and noises are included. The TFD features such as discrete wavelet transform (DWT) and wavelet packet transform (WPT) contribute to a better recognition performance in combination with nonlinear classifiers like SVM. A brief test of individual features in combination with conventional classifiers like LDA, QDA and SVM is conducted on our captured sEMG signals presented in Table 2.2. It can be seen that the extent of recognition accuracy remains relatively consistent for a single feature type across different classifiers. Features like RMS, MAV and the two modified versions of MAV show a similar average recognition accuracy because they all aim at extracting the accumulated amplitude within each segment. Besides, the performance of an individual feature or classifier is not consistent, which supports the necessity in considering combinations of features instead of solely

investigating single features for all classifiers. A more systematic evaluation of the enlarged candidate sets of feature types can be referred to in [34].

Table 2.2 Test of single feature types in combination with conventional classifiers

Feature	**LDA**		**SVM**		**QDA**	
	Accuracy %	σ	**Accuracy %**	σ	**Accuracy %**	σ
AR	79.96	7.73	73.29	9.89	69.47	7.31
HG	58.44	6.84	56.76	6.08	50.09	9.22
KATZ	69.16	6.84	70.49	8.83	55.56	10.06
RMS	55.13	19.79	58.04	15.85	61.25	11.66
MAV	55.89	19.82	58.16	15.32	59.68	13.36
MMAV1	55.99	19.71	57.52	14.53	58.81	12.46
MMAV2	55.69	18.09	59.66	11.31	59.30	10.70
WL	53.45	21.99	62.16	20.39	58.68	11.66
ZC	56.61	7.69	52.05	6.68	49.87	7.55
SSC	69.29	6.09	62.34	8.24	63.60	6.75
VCF	70.46	10.66	70.96	7.79	64.77	8.53
MFL	73.50	8.67	69.39	12.90	70.78	10.07
MYOP	57.51	14.72	56.07	15.54	60.34	14.67
WAMP	57.98	13.78	60.76	18.20	59.23	16.77
MNF	68.92	9.82	64.49	8.10	57.56	8.47
MDF	60.52	6.84	58.55	6.74	58.70	4.31
APEN	47.01	7.67	46.47	9.05	48.94	9.21
SAMPEN	42.97	5.98	41.16	5.36	40.63	5.79

With a growing emphasis on the usability in research community, novel features have been continuously proposed to accommodate clinical confounding factors. Khushaba et al. [129] proposed a robust feature set for hand motion recognition under various limb positions. He et al. [130] derived two features from sub-band power to achieve a robust performance under varying muscle contraction levels. Similarly, Al-Timemy et al. [131] proposed a feature vector based on power spectrum moments of 3 orders and validated its robustness to force variation on 9 amputees. After the feature extraction, a step of dimensionality reduction is usually taken to remove the components that contribute less to the targeted application. Dimensionality reduction can be realised by either feature selection or feature projection. Feature selection is conducted in an offline scheme while feature projection tends to take place in an online way. PCA and its modified versions [117] are the most utilised feature dimensionality reduction scheme to decorrelate the measured data to achieve a robust performance.

Despite the feasibility of PCA in the dimensionality reduction, it still requires the calculation of all named features to exploit the most of the information. However, with the

increase in the number of detection sites, the increasing computational cost would heavily hinder the real-time performance in clinical use. An alternative is to use the feature selection strategy instead of the feature projection, which could be done in an offline scheme. Feature selection methods such as genetic algorithm [132] and particle swarm optimisation [133] have been previously utilised in the sEMG based hand motion recognition. The best trade-off is to achieve a comparable recognition accuracy with the computation complexity reduced to a certain extent. Intuitively, training the classifier with pooled samples of multiple trials directly is plausible to utilise the redundancy to boost the across-trial performance. The endeavour to improve the hand motion recognition with supplementary data has been seen in many publications. Extra sEMG patterns under the displacement of detection sites are incorporated to enhance the robustness to electrode shift [114]. The inclusion of sEMG signals captured under various limb positions associated with normal use for training is suggested to mitigate the corresponding clinical degradation [80]. The idea is intuitive that a redundant dataset would cover most cases of sEMG signals exerted under various conditions, thus providing a robust assignment of membership to new samples in an unseen scenario. The hypothesis could be formulated by an adaptive distribution of sEMG patterns whose parameters like mean and covariance are updated according to additional data. The update of data distribution represents a simple but efficient trade-off between specialisation and generalisation. The distribution is expected to favour the robustness and precision at the same time, as long as the dataset is large and diverse enough. However, it is not always the case because of the diversity of sEMG for its nature of randomness. A further investigation into the feature selection and the evaluation of the feature redundancy and potential improvement will be introduced in Section 4.2.

Conventional classification strategies have been thoroughly investigated in sEMG based hand motion recognition, like LDA, SVM [25], QDA [27], K-nearest neighbors (KNN) [134], multilayer perceptron network (MLP) [135], artificial neural networks (ANN) [12], hidden Markov models (HMM) [136], Gaussian mixture models (GMM) [137], multiple-binary classifier (MBC) [138] adopted in sEMG based prosthetic control. Among diverse sEMG pattern classifiers, LDA and its modified versions remain the most popular techniques which guarantee the real-time online performance while preserving the robustness to abrupt changes. Clustering methods like fuzzy c-means have also been utilised in [139] to map EMG signals to different functions in real time. Clustering methods allow participants to freely select and label their own movements and require no pre-set contractions, where the HMI automatically determines the most discernible and repeatable muscle signals individually. And numerous modified control strategies based on classic classifiers have been continuously proposed like LDA with rejection (LDAR) [140], uncorrelated LDA (ULDA) [141] and FGMMs [26].

Among all the conventional classifiers, the robustness of LDA over other nonlinear classifiers has been demonstrated in [116]. And the TDAR features showed a better performance in the classification of both transient and stationary parts of sEMG signals using LDA. Thus in this thesis, the hand motion recognition accuracy achieved by the LDA classifier in combination with the TDAR features comprising MAV, WL, ZC and SSC together with AR of the same window length is adopted as the baseline for comparison.

Postprocessing

Regardless of the possibly high recognition accuracy for each sEMG segment, a fragment of the decision stream inevitably suffers from the artefacts and is sometimes unreliable. To remove the spurious and abrupt outliers, the postprocessing is necessary prior to the formation of final control commands. The majority vote is capable of eliminating the spurious error present in the unprocessed decision stream [2, 142, 143] and has been most adopted in a vast majority of myoelectric control applications for its simplicity. Intuitively, with a denser stream of decisions, the majority vote processing can utilise more decisions to generate a more robust output without abrupt changes. However, due to the strict constraint of perceivable delays, the number of errors increases with shorter segments in the decision stream. The majority vote is capable of averaging out these errors, thus a well balanced trade-off is required between the length of segmentation and the population of segments involved. Khushaba et al. [144] have proposed the Bayesian fusion based postprocessing which relies on the conditional probability of each windowed data belonging to a certain class. When the following window arrives, the probability of class assignment given the accumulated windowed segments is deducted by the Bayes' rule. Threshold based approaches are commonly adopted for postprocessing as well. Simon et al. [24] proposed a technique named velocity ramp attenuating the movement speed after a change in classifier decision, whose validation was conducted in the applications of both virtual prostheses and physical prostheses. Besides the offline recognition accuracy, the clinical criteria including completion rate, path efficiency and completion time were improved as well. Scheme et al. [140] cascaded the LDA classifier with a rejection module to calculate the confidence using a softmax function, which rejects the decisions with scores below a threshold to improve the pattern recognition performance. Amsuss et al. [110] utilised ANN to assign the confidence value according to the RMS values and maximum likelihood of the current point with previous 10 segments. The decision is rejected when its score is below the predefiend threshold following a similar routine.

2.2.3 Deep Learning Based Recognition

The prevalence of deep learning approaches in sEMG based hand motion recognition has been propelled by the cutting edges in the field of conventional pattern recognition applications like computer vision and natural language processing. The use of CNN for sEMG analysis started in the year of 2016 [145], inspired by the maturity of deep neural network frameworks and the enhanced computing capability. The following years have witnessed the preference towards CNN over other available deep learning frameworks like deep belief network (DBN) [146] and recurrent neural network (RNN) [147] in the research community of sEMG based hand motion recognition. Currently, most publications of deep learning solutions to sEMG based hand motion recognition have been focusing on the utilisation of deep learning algorithms instead of the development of architecture design and parameter tuning strategies, like the adopted architecture in Fig. 2.7. The enumeration of some most noticeable applications is listed in Table 2.3.

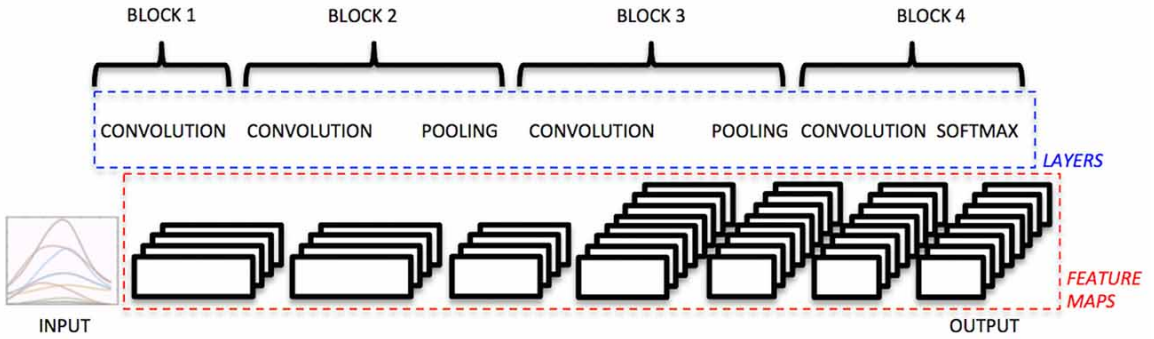

Fig. 2.7 First adopted architecture of CNN for detailed analysis of sEMG based hand motion recognition [3]

Table 2.3 Enumeration of deep learning applications for sEMG based hand motion recognition

	Model	Dataset	Input Type	Segment	Platform
[146]	DBN	Local data	4 TD features	166 ms	DeepLearnToolbox
[147]	RNN	Ninapro	Raw sEMG	200 ms	Microsoft Cognitive Toolkit
[145]	CNN	Ninapro	Raw sEMG	200 ms	N/A
[148]	CNN	CapgMyo	Raw sEMG	Single frame	MxNet
[149]	CNN	CapgMyo	Raw sEMG	Single frame	MxNet
[150]	CNN	Local data	Raw sEMG	260 ms	Theano
[151]	CNN	Local data	Raw sEMG	150 ms	Tensorflow

Besides the direct application of the existing deep learning algorithms, fragmented improvement has also been put forward for the sEMG based hand motion recognition. Zhai

et al. [152] proposed a self-calibration CNN model using the dimensionally reduced and realigned spectrogram that was computed by 256-point fast Fourier transform in a Hamming window as the input. They demonstrated that the CNN model could improve the intra-session classification accuracy on the public dataset of NinaPro DB2 by 1.15% in the comparison with the baseline classifier RBF-SVM without self-calibration. However, it is not yet clear if the model is suitable for inter-day scenario, because NinaPro database could not reflect the daily difference of sEMG patterns with only 1 day's data captured from all subjects. Allard et al. [150, 153] adopted the CNN in the control of JACO arm Kinova, in which the spectrograms were calculated on 8 EMG channels to form a spectrogram matrix as the input, and a robust control in real-time experimental scenarios was achieved. Atzori et al. [3] evaluated a CNN architecture with 4 convolution layers on intra-session gesture recognition tests, however not able to achieve a better performance than conventional pattern recognition based classification methods. Geng et al. [148] discovered that the hidden sEMG pattern in a high-density sEMG amplitude map at an instant could be exploited for gesture classification, which would allow a better responding speed for human machine interaction. Yu et al. [149] proposed a domain adaptation approach for inter-session gesture classification, and achieved significant improvement on inter-subject gesture recognition. A most recent work by Rehman et al. [154] focused on the performance over multiple days using sEMG signals captured by the commercially available MYO armband as input to deep networks in comparison with the classic approach utilising LDA and TDAR. Besides the single architecture based deep learning frameworks, the combination of CNN and RNN has been investigated as well [147].

A detailed discussion about the architecture of CNN and extracted non-handcrafted features will be further presented following the deep learning based hand motion recognition evaluation in Chapter 3 and 4 respectively, where low-density sEMG signals of multiple days and multiple subjects are concerned.

2.2.4 Evaluation Criteria and Benchmarks

Evaluation remains a critical part in hand motion recognition for prosthetic control, by providing both offline and online metrics for researchers to further improve their outputs. The offline recognition accuracy is the most trivial metric and chased after in most academic research of sEMG based hand motion recognition. As a result, various public datasets have been proposed for coherent comparisons of recognition approaches such as NinaPro, CSL-HDEMG and CapgMyo. NinaPro [155] built by Atzori et al. is a low-density sEMG database comprising a total of 52 hand motions performed by 67 subjects including both able-bodied subjects and amputees. The sEMG acquisition system comprised of 10 or 12 bi-polar electrodes that were evenly placed on the forearm. For each subject, signals of

only 1 session and 1 day were captured with each movement repeated for 6 times. The whole dataset is divided into 3 sub-datasets: DB1, DB2, and DB3. Although NinaPro is the most massive public dataset with the most number of both hand motions and recruited subjects, it is not suitable for the inter-day evaluation since the data was only captured for 1 day from each subject. CSL-HDEMG is a high-density sEMG database published by Amma el al. [156] which was captured with 192 densely distributed electrodes from the forearm muscles contributing to 27 hand motions. And a total of 5 subjects were employed for the data collection on 5 days in CSL-HDEMG. CapgMyo [149] is another high-density sEMG database comprising 128-dimensional sEMG signals acquired from 23 intact subjects through a customised device with an 8×16 electrode array. CapgMyo consists of 3 sub-datasets: DB-a, DB-b, and DB-c. Specifically, 8 hand motions obtained from 18 and 10 out of the 23 candidate subjects formed the DB-a and DB-b respectively. Besides, 12 basic movements of the fingers were obtained from 10 out of the 23 candidate subjects to form DB-c. The number of hand motion types, recruited subjects and the detecting channels are further introduced in Table 2.4, together with part of their performance in intra-session (intra-day), inter-day and inter-subject scenarios achieved so far. Currently the largest amount of motion types are included in the benchmark of NinaPro as shown in Fig. 2.8, which can be referred to for later establishment of datasets. Ortiz el al. [157] also established an online platform of benchmarks for comparison of pattern recognition based prosthetic control, and has been one of the mostly adopted platform with a compound analysis framework in research community.

Table 2.4 Publicly available datasets of sEMG based hand motion recognition

DataBase	NinaPro [155]			CSL-HDEMG [156]	CapgMyo [149]		
	DB1	DB2	DB3		DB-a	DB-b	DB-c
Motion Type No.	53	50	50	27	8	8	12
Subject No.	27	40	11	5	18	10	10
Channel No.	10	12	12	192	128	128	128
Intra-session (%)	75.32	75.27[155], 78.81[152]	46.27	90.4[156], 96.8[149]	99.5	98.6	99.2
Inter-day (%)	-	-	-	59[156], 62.7[149]	-	47.9	-
Inter-subject (%)	<20 [158]	-	-	-	-	39.0	26.3

Due to the clinical nature of the application and the fact that high recognition accuracy does not necessarily guarantee satisfactory usability [159], though numerous published benchmarks for offline evaluation are considering the metric of recognition accuracy, the online evaluation on performing certain tasks has been gradually proposed and adopted in clinical tests on subjects with amputation.

The target achievement control (TAC) was first proposed by Simon et al. [5] focusing on the controllability of prosthetic hands. The TAC test evaluates the users' control and positioning of a multifunctional prosthesis in a virtual environment shown in Fig. 2.9. During

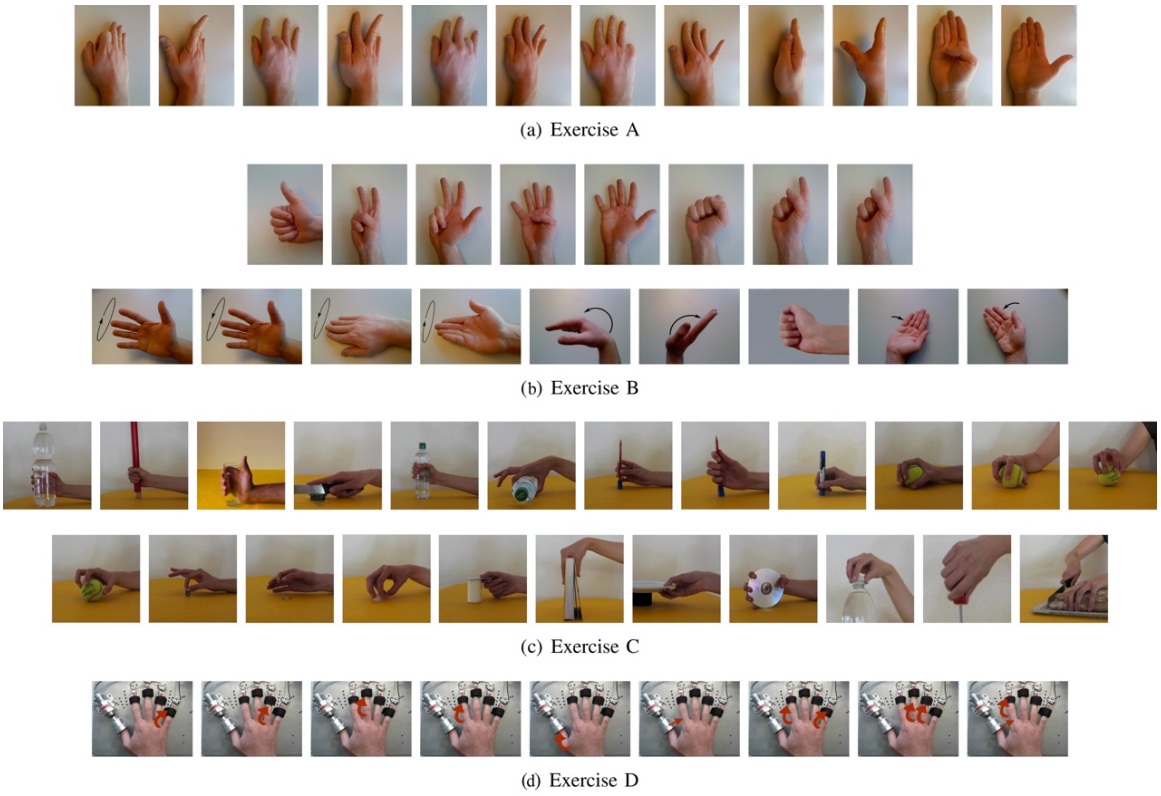

(a) Exercise A

(b) Exercise B

(c) Exercise C

(d) Exercise D

Fig. 2.8 Hand motions included in NinaPro [4]

the test, users are instructed to move a virtual prosthetic hand into the targeted posture and maintain the posture for a period of time lasting several seconds. The success of the task is determined by whether the user could finish reaching the target posture without unnecessary movements such as volitional control or motion misclassifications. The Motion Test proposed by Kuiken et al. [6] still focused on the accuracy related metrics including recognition motion selection time, motion completion time, and motion completion rate. These quantities measure how quickly EMG signals can be translated into correct motion recognition results. As a platform for the testing realisation, a virtual hand system in Fig. 2.10 was built for those who have undergone the TMR surgery. Both Motion Test and the TAC test were employed in [160] to verify the capability of classifiers arranged in a distributed topology to recognise simultaneous movement. Assessment for capacity of myoelectric control (ACMC) was proposde by Hermansson et al. [161] to provide scores on clinical observations of the gripping, holding and releasing daily life objects. A total of 30 items in daily life activities were included in the ACMC test and the interaction with each of them was assigned with a 4-point ordinal scale.

Besides the aforementioned tests, other assessment tools like the Southampton Hand Assessment Protocol, the Jebsen-Taylor Test of Hand Function, the Box and Blocks Test,

the Clothespin Relocation Task, and the Cubbies Task have been proposed and utilised to prove the effectiveness of recognition algorithms in combination with commercially available physical prostheses or implementations of virtual hands [35, 37].

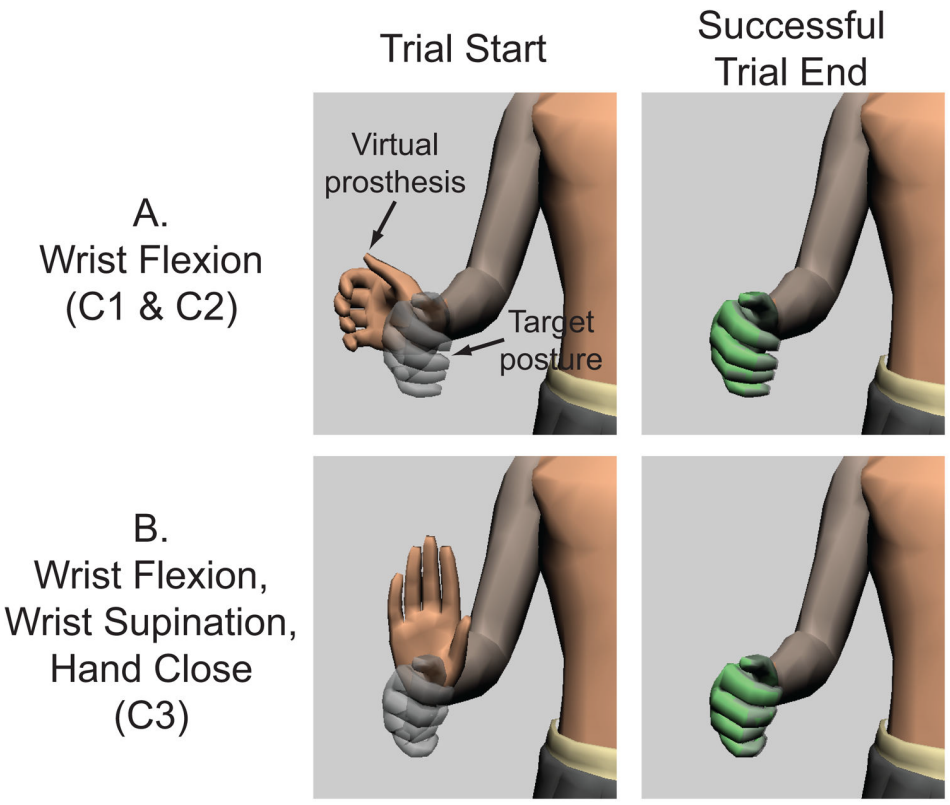

Fig. 2.9 TAC test environment and tasks [5]

2.2.5 Limitations

It has been emphasised in various publications that the gap between clinical use and academic research of myoelectric prosthetic control keeps expanding and results in a low acceptance rate of multi-functional prostheses from the users [28]. The vast majority of prosthetic hand users tend to choose simply aesthetically pleasing or amplitude based ones in the lack of an ideal control. An ideal prosthetic control is of intuitiveness, robustness, low computational complexity, real-time performance and limited burden of re-training [58]. Other desired properties of the HMI include a minimal number of electrodes, an easy user training process, a closed-loop control with sensory feedback and long-term usability. Efforts towards the ideal properties have been extensively seen in recent years [131, 162, 163]. Yet to date, there are still quite many limitations to be addressed in current myoelectric prosthetic control as follows.

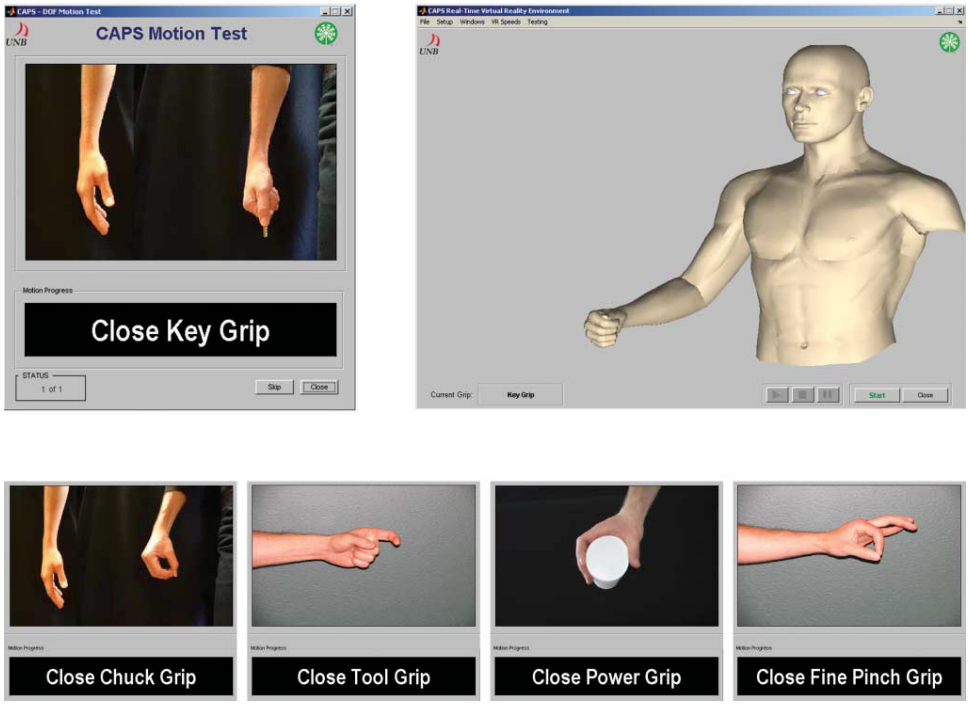

Fig. 2.10 Motion Test environment and tasks [6]

Failure in Deep Muscle Activity Sensing

Myoelectric signals can be acquired in either an invasive or noninvasive way, which leads to the iEMG and sEMG. The iEMG is capable of providing an insight into deep muscular structure and changes of targeted compartments. However, it suffers from the invasiveness while the noninvasiveness remains one of the most desired properties for prosthetic hand users. On the other hand, the sEMG can only detect activities mostly from superficial muscles and hardly capture the electrical manifestation of deep muscle contractions while some dexterous finger movements are naturally related to deep muscle contraction [76]. As a result, the failure in deep muscle activity sensing impedes the dexterous hand motion recognition especially in a long-term use, where the weak physiological signals from deep compartments become even more unstable for sEMG based detection.

Intrinsic Randomness and Sensitivity to Physiological Changes

Irrespective of the high recognition accuracy achieved in an offline scheme and short-term testing scenarios in a laboratory environment, the performance of hand motion recognition deteriorates severely for long-term clinical use [162]. The premise of accurate recognition of hand motions is crafted by the consistency of sEMG patterns. However the randomness of myoelectric signals in long-term use will result in the large variation of signal manifestation,

which hinders the accurate motion recognition in a clinical cross-day environment [29]. Typically, the inherent variability of myoelectric manifestation and inevitable day-to-day physiological changes contribute to a heavy burden of re-calibration and re-training [33]. Besides, physiological changes like fatigue and sweat remain some of the most severe factors that adversely impact the hand motion recognition accuracy. Muscle fatigue generally occurs after long-term muscle activity and results in a decline of the muscular ability to generate the desired force through contraction.

Electrode Shift and Crosstalk

Isotonic contraction of muscles tends to cause relative movement between targeted muscles and skin surface where the electrode is attached and negatively impacts the predefiend detection site distribution. The electrode shift has been pointed out as the most significant dynamic factor that adversely influences the performance of myoelectric pattern recognition based control [164]. Hargrove et al. [114] enriched the training dataset with samples captured from potential displacement locations to remedy the performance degradation caused by electrode shift. But the enlarged pooled samples are commonly captured at the price of a heavy burden of training which is undesirable for users. Intuitively, iEMG is less affected by muscular crosstalk than sEMG, which allows a more independent detection of targeted muscles. But it has been validated that iEMG does not outperform sEMG in pattern recognition based myoelectric control [53]. What's more, crosstalk has been identified as an influential factor on the performance of recognition [103], which can be mitigated by pattern recognition based control [53] yet whose performance heavily depends on the robustness of the adopted classification strategy.

Lack of Sensory Feedback

An ideal prosthetic control process is expected to be closed-loop with proper sensory feedback modules. However, a practical feedback is missing in most cases of prosthetic hand control and has been highlighted as the drawback of existing myoelectric control systems since last decade [20, 28]. Though functional electrical stimulation (FES) is a module that provides sensory feedback and has been utilised in various motor function rehabilitation targeted applications, the inherent properties of FES inevitably lead to electrical interference in combination with traditional myoelectric control. To date, limited clinically viable feedback approaches have been proposed for myoelectric prosthetic control. Thus a non-electrical manifestation is desired to support the feedback instead of using solely visual feedback.

Burden of User Training

Controversy remains whether adequate user training is desired in clinical applications to date. On the one hand, repeated re-training process is time-consuming and forms a heavy burden on the users. On the other hand, the user training intuitively improves the consistency of sEMG patterns exerted by users [165]. Inconsistencies between the academic and clinical applications partly reside in the user training phase. In a laboratory environment the subjects are normally seated in a comfortable position without surrounding disturbances while in clinical scenarios the amputated users are involved in interactions with multiple objects under various abrupt changes. Powell et al. [166] introduced a clinical protocol to train the users with pattern recognition related concept and a prosthesis-guided training process for classifier re-calibration. Despite the advantages of user training in improving the recognition performance, the training burden remains to be further reduced from the users' perspective [33].

2.3 Summary

This chapter systematically reviews the sEMG sensing driven prosthetic control in terms of the muscle activity sensing modalities and hand motion recognition approaches respectively, where the myoelectric sensing based pattern recognition solutions are addressed with extra emphasis.

First the most prevalent noninvasive and wearable muscular activity sensing techniques are introduced. On the one hand, sEMG remains the only available sensing modality equipped in commercial prosthetic hands with an active control, and has been extensively investigated in both academic and clinical scenarios. On the other hand, alternative sensing modalities have been widely considered in academia, based on which the hand motion recognition has been improved in various directions. For example, SMG is capable of deep muscle activity detection allowing the analysis of dexterous hand motions including finger movements. FMG is robust to external electrical interference and physiological changes, and suitable as the sensing modality with integration of electrical stimulus as the sensory feedback. IMUs provide the geometric information of limb movement which potentially contributes to a robust sensing under varying limb positions. NIRS measures the oxygen saturation and can be utilised to identify muscle fatigue with a quantitative index to shape the hierarchical application with various degree of fatigue. In summary, the single modalities of EMG, SMG and FMG are suitable for forearm muscle activity sensing and have been applied for unimodal sensing based hand motion recognition with reported promising results. Furthermore, other modalities like IMU, NIRS and MMG can be integrated with EMG for multimodal fusion

based sensing, which improves the integrity of pooled sensory data with supplementary physiological information and robustness under various external changes.

Then a thorough review of myoelectric hand motion recognition approaches is provided with an emphasis on pattern recognition based solutions. Some cornerstone works like [12] have been emphasised in terms of the contribution to the conventionally adopted baseline of using combined TDAR features and LDA classifier. The steps in a typical conventional pattern recognition based myoelectric hand motion recognition are introduced with corresponding fragmented development. The most recently trending deep learning approaches are introduced with enumeration of several architectures as the potential complement to conventional models. The review of recognition algorithms is followed by the evaluation criteria and some most prevalent benchmarks at last.

Finally the limitations of existing myoelectric prosthetic control are concluded in terms of intrinsic randomness of sEMG, sensitivity of sEMG to electrode shift, crosstalk, and physiological changes, lack of deep muscle activity sensing, burden of re-training and re-calibration for long-term use, and the absence of sensory feedback.

Based on the reviewed progress and limitations, potential future research directions for sEMG driven hand motion recognition are listed as follows. Current pattern recognition approaches for sEMG based hand motion recognition deteriorate under various factors including limb position variation, physiological changes and long-term use. Thus a specialised model is needed to accommodate these factors with essential development of steps within a pattern recognition scheme including preprocessing, feature extraction and selection, classification and postprocessing. In this thesis, the long-term use targeted development of discriminant analysis methods, CNN based deep learning, feature extraction and selection are studied respectively in Chapter 3 and Chapter 4. Specifically, Chapter 3 focuses on the improvement of classification to inter-day hand motion recognition to address the limited robustness to inter-day changes by taking advantage of both implicit and explict subclass division based discriminant analysis and a simple convolutional neural network. Chapter 4 improves the robustness in the same application through proposing novel feature extraction and feature combination comprising the merged handcrafted and non-handcrafted features, multi-threshold based feature extraction and computational intelligence based optimisation of feature candidates. Given the difficulty of robust long-term control by unimodal sEMG sensing, multimodal sensing fusion is a promising substitution and proposed. The deficiency of information captured by solely sEMG can be remedied with extra sensory fusion. Specifically, the fusion of myoelectric and ultrasonic sensing will be introduced in Chapter 5. The unique morphological information extracted by ultrasound based sensing provides better discrimination of dexterous finger movement and forms the natural complement to

sEMG signals which only detects the superficial muscle movement. The combination of both myelectric and ultrasound sensing mitigate the inherent drawbacks of singly EMG based sensing like low recognition accuracy of deep muscle related motions and randomness of sEMG signals in inter-day changes. To further enhance the aforementioned improvement, a targeted evaluation benchmark for long-term use of sEMG based hand motion recognition is desired and the absence of a properly defined benchmark of low-density sEMG across multiple days and subjects is finally addressed by building a database in this thesis, about which the detailed data acquisition and experiment protocol are introduced in Chapter 6.

Chapter 3

Conventional Pattern Recognition and Deep Learning Based Classification

Classifier design plays an important role in pattern recognition based applications. Specifically, numerous classification strategies like LDA, SVM and GMM together with their modifications have been applied in sEMG based hand motion recognition. Regardless of the intensive research interest in myoelectric control, the development of classifiers with a specific focus on the inter-day hand motion recognition for long-term use is rarely seen, not mentioning the emphasis on various adequateness of training samples in comparison to the testing ones. In daily life of prosthetic hand or assistive device users, the training process is tedious and time-consuming because of the constrained motor function. And the standard protocol of user training requires the users to repeat the motion paradigm for sEMG signal capturing. Because of the focus on inter-day hand motion recognition in this chapter, the inadequate training is defined as only the data captured on 1 or 2 days will be labelled while the rest unseen days' data are to be recognised, while the adequate training is defined as only 1 day's data are unseen for recognition and the 9 distinct days' labelled data are provided for training. This chapter aims to address this problem by developing both conventional pattern recognition and deep learning approaches. In particular, discriminant analysis frameworks and convolutional neural networks are considered to exploit their advantageous capability in sEMG based hand motion recognition with inadequate and adequate training data respectively.

3.1 Discriminant Analysis Frameworks for sEMG Based Hand Motion Recognition with Inadequate Training Data

One of the most critical factors that impedes the clinical application of current dexterous prosthetic hand control is the discontented long-term usability. The recognition accuracy deteriorates severely when prosthesis donning/doffing or muscle fatigue occurs, thus resulting in a significant rate of misclassified execution that leads to a low acceptance rate by users. Extracted sEMG patterns under different conditions naturally form various overlapping subclasses. An intuitive sketch can be seen in Fig. 3.1, where the first 2 principle components of extracted sEMG TDAR features of 9 hand motions shown in Fig. 3.2 captured from the same subject. The two trials are distinguished by square and dot symbols respectively while different motions are indicated by different colours. Despite the most distinguishable motions, the others are overlapped in the reduced feature space. The hindrance of overlapping has a serious effect on the recognition accuracy when donning/doffing happens for long-term use. A potential solution is to build a hierarchical structure which first divides the overlapping samples of the same distinct motions yet from different trials into subclasses for a further and finer categorisation. Thus importance is attached to the subclass division as a prior step of the hierarchical structure where the adopted algorithm draws inferences from the data and forms subclasses according to their distribution and distance.

LDA has been employed in the sEMG based hand motion recognition for decades and remains the most important baseline for its robust performance in academic research. Liu et al. [40] addressed the reduction of user re-training while preserving an acceptable inter-day recognition accuracy by using LDA with an optimised projection. Vidovic et al. [163] employed supervised adaptation to calibrate the model for inter-day use on both able-bodied subjects and amputees. The aforementioned discriminant analysis methods are mostly based on the assumption that each class is represented by a single cluster. However, separated subclasses are possibly formed because of the nonstationary and stochastic nature of sEMG signals. Overlapping subclasses among predefined classes could go against the assumptions embedded in some classification methods. For example, the distribution of pooled samples might not meet the assumption of having a common covariance matrix but different means for LDA. The potential of subclass division in the cross-day settings has not been addressed yet regardless of the widely developed modifications of LDA.

In our preliminary work, the effectiveness of subclass division has been proved on the force based granular modelling for grasp recognition, where the sEMG signals and forces

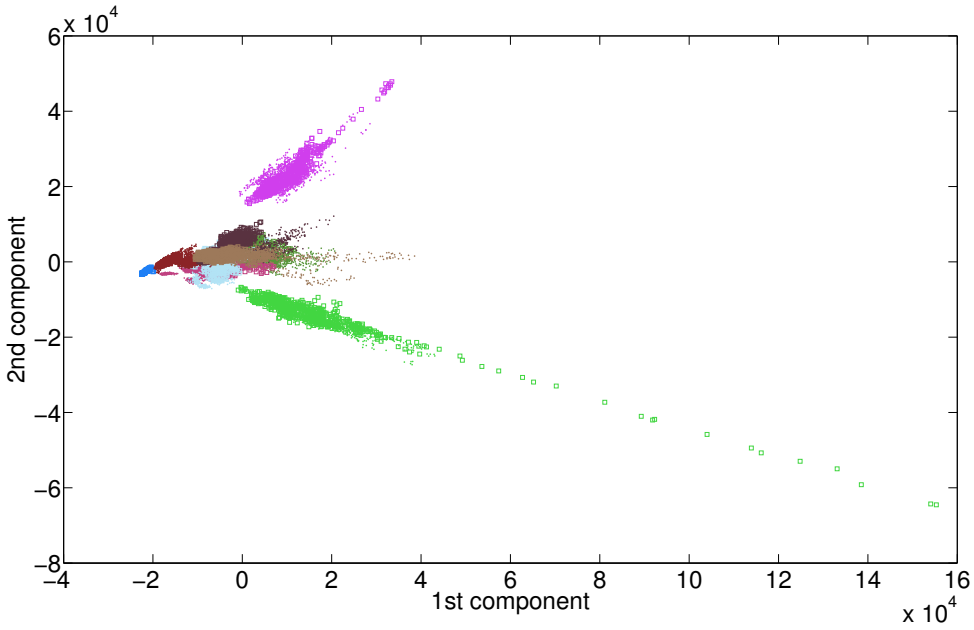

Fig. 3.1 First 2 principle components of sEMG features extracted from 9 motions for 2 different trials captured on the same subject

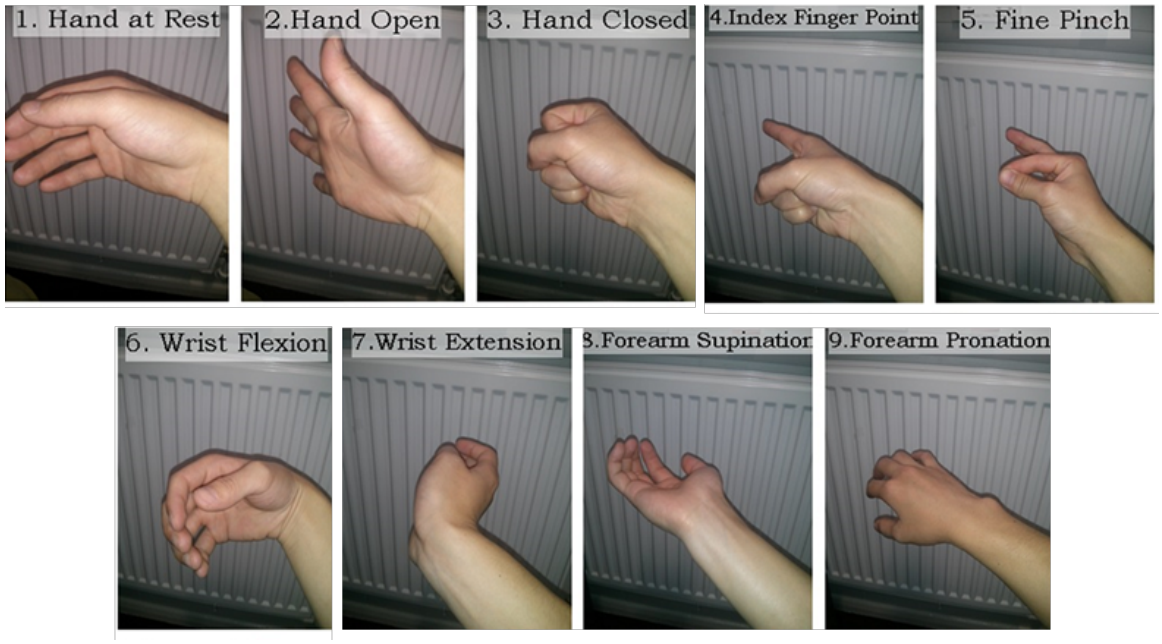

Fig. 3.2 Adopted 9 motion candidates for recognition

of hand grasps were captured synchronously. The grasping force was introduced by the incorporation of an additional force sensor to the sEMG capturing system, as shown in Fig. 3.3. The confusion matrix of the subclass division based hand grasp recognition is provided

in Fig. 3.4. It can be seen that the number of classes is enlarged by dividing each grasp type into 3 subclasses according to the magnitude of forces. The original 8 different grasp types were enriched by the attributes of exerted forces and formed the 24 classes in the intermediate classification. The misclassification among subclasses that belong to the same class will contribute to the improved correct classification through a mapping into the original classes at last.

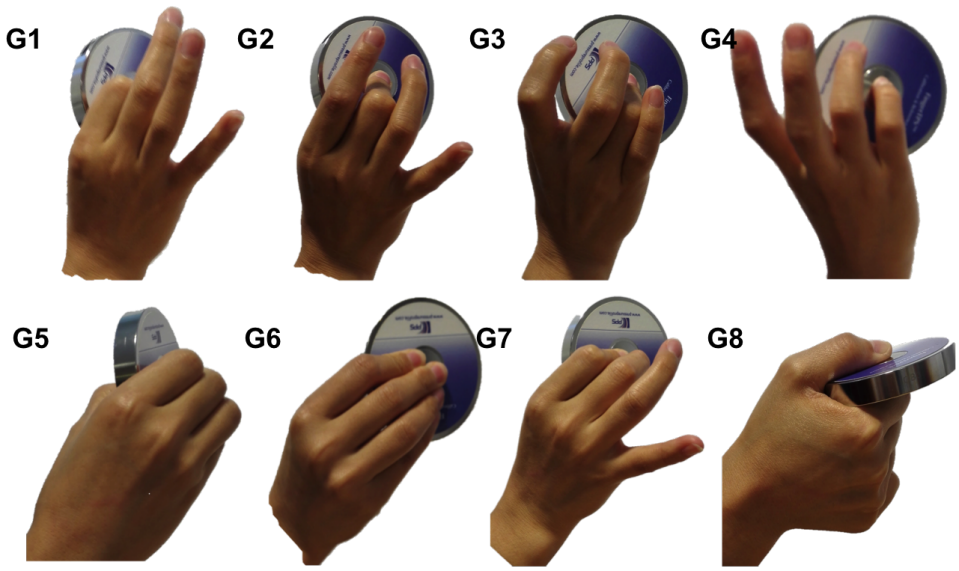

Fig. 3.3 Force sensing of the 8 hand grasps

Despite the improved recognition accuracy, the force driven subclass division is based on an additional attribute of force utilising extra sensory information at an ideal setting and does not reflect the real daily life scenarios, where human-object interaction is conducted without the force sensing. In this section, we further examine the feasibility of subclass division for hand motion recognition using solely sEMG signals across multiple days with inadequate training data, whose subclasses are shaped by the inter-day changes of sEMG characteristics and electrode shift caused by donning/doffing in long-term use. Specifically, the subclass division is combined with discriminant analysis step by step from an explicit and totally unconstrained division to an explicit yet constrained division and finally to an implicit and constrained implementation, with the improved performance of the latter two approaches verified.

3.1.1 Unconstrained Subclass Division Based Discriminant Analysis

In this section, the subclass division is first conducted without a strict constraint of the subclass number. What's more, we consider the fully unsupervised subclass division by pooling all the

	F1	219	34	0	5	1	0	1	0	0	0	0	0	17	0	0	4	0	0	9	0	0	0	0	0
G1	F2	16	179	38	0	0	0	0	0	0	0	0	0	0	0	0	0	0	0	0	0	0	0	0	0
	F3	0	22	207	0	0	0	0	0	0	0	0	0	0	0	0	0	0	0	0	0	0	0	0	0
	F1	4	0	0	200	13	0	3	0	0	0	0	0	4	0	0	2	0	0	1	0	0	0	0	0
G2	F2	0	0	0	41	235	45	0	0	0	0	0	0	0	0	0	0	0	0	0	0	0	0	0	0
	F3	0	0	0	1	28	176	0	0	0	0	0	0	0	0	0	0	0	0	0	0	0	0	0	0
	F1	12	3	0	2	0	0	249	19	0	6	1	0	0	0	0	0	0	0	1	0	0	0	0	0
G3	F2	0	0	1	0	0	0	28	248	21	0	1	0	0	0	0	0	0	0	0	0	0	0	0	0
	F3	0	0	0	0	0	0	0	54	127	0	0	0	0	0	0	0	0	0	0	0	0	0	0	0
	F1	1	1	0	0	0	0	0	2	0	242	29	0	0	0	0	0	0	0	3	0	0	0	0	0
G4	F2	0	0	0	0	0	0	0	0	0	17	259	32	0	0	0	0	0	0	0	0	0	0	0	0
	F3	0	0	0	0	0	0	0	0	0	0	30	134	0	0	0	0	0	0	0	0	0	0	0	0
	F1	2	1	0	0	0	0	0	0	0	0	0	0	192	8	0	17	0	0	0	0	0	0	0	0
G5	F2	0	0	0	0	0	0	0	0	0	0	0	0	15	208	17	11	11	0	0	0	0	0	0	0
	F3	0	0	0	0	0	0	0	0	0	0	0	0	0	29	162	0	9	10	0	0	0	0	0	0
	F1	0	0	0	0	0	0	0	0	0	0	0	0	19	12	0	211	20	0	0	0	0	0	0	0
G6	F2	0	0	0	0	0	0	0	0	0	0	0	0	0	19	31	8	234	21	0	0	0	0	0	0
	F3	0	0	0	0	0	0	0	0	0	0	0	0	0	0	16	0	11	181	0	0	0	0	0	0
	F1	7	0	0	0	1	4	0	0	0	0	0	0	0	0	0	2	0	0	201	19	0	0	0	0
G7	F2	0	0	0	0	0	0	0	0	0	0	0	0	0	0	0	0	0	0	23	272	32	0	0	0
	F3	0	0	0	0	0	0	0	0	0	0	0	0	0	0	0	0	0	0	0	23	168	0	0	0
	F1	3	0	0	0	0	0	0	0	0	0	0	0	1	0	0	0	0	0	0	0	0	193	38	2
G8	F2	0	1	0	0	0	0	0	0	0	0	0	0	0	0	0	0	0	0	0	0	0	49	181	45
	F3	0	1	0	0	0	0	0	0	0	0	0	0	1	0	0	0	0	0	0	0	0	1	52	190
		F1	F2	F3	F1	F2	F3	F1	F2	F3	F1	F2	F3	F1	F2	F3	F1	F2	F3	F1	F2	F3	F1	F2	F3
		G1			G2			G3			G4			G5			G6			G7			G8		

Fig. 3.4 The confusion matrix of the sEMG based hand grasp recognition with force driven subclass division

training data for division without taking advantages of any priori knowledge of their classes. And the self organising technique of growing neural gas (GNG) is firstly combined with LDA for the subclass division based hand motion recognition in an unconstrained way for the sublcass division among all the pooled data. GNG can extract and dynamically change the topological structure of the data based on the relation between adjacent reference nodes and sampling points. The distances between unseen samples and the extracted representation nodes are used as the membership or further fed to the following classifier. The GNG algorithm is implemented following the steps below.

Step 1. The sets of nodes, edges and ages are initialised with two random nodes n_1 and n_2 from the node set N and the corresponding edge between them is saved.

Step 2. A sample point x is drawn from the candidate sample set X for inclusion.

Step 3. The nearest two nodes n_p and n_q to the sample point x are selected out of the node set.

$$n_p = \arg\min_{n_i \in N} \|n_i - x\| \tag{3.1}$$

$$n_q = \arg\min_{n_i \in N \setminus \{n_p\}} \|n_i - x\| \tag{3.2}$$

Step 4. The nearest two nodes n_p and n_q are connected, and the age of their edge is set zero.

$$a_{p,q} = 0 \tag{3.3}$$

Step 5. The local error of the nearest node n_p is increased by its corresponding distance from the sample point x.

$$E_{n_p} \leftarrow E_{n_p} + \|n_p - x\| \tag{3.4}$$

Step 6. The reference vectors of the nearest node n_p and its directly connected nodes are moved towards the sample point x with a moving rate of α_1 and α_2 respectively.

$$n_p \leftarrow n_p + \alpha_1 (x - n_p) \tag{3.5}$$

$$n_i \leftarrow n_i + \alpha_2 (x - n_i), \quad \forall\, i \in \{i | n_i \in N, c_{i,p} = 1\} \tag{3.6}$$

Step 7. The ages of all the edges directly connected to the nearest node n_p are increased by one.

$$a_{i,p} \leftarrow a_{i,p+1}, \quad \forall\, i \in \{i | n_i \in N, c_{i,p} = 1\} \tag{3.7}$$

Step 8. The edges whose ages exceed the predefined threshold ε are eliminated. Nodes without any edges after this operation will be removed from the node set N.

$$N \leftarrow N \setminus \{n_i\}, \quad if\ \nexists a_{i,j}\ for\ \forall j \neq i \tag{3.8}$$

Step 9. For every predefined λ iterations, a new node n_{in} is inserted following the steps.

1. The node n_{e1} with the largest local error is selected. The node n_{e2} which is directly connected to n_{e1} with the largest local error within the subset is selected as well.

2. The reference vector of the new node n_{in} is interpolated by averaging the two nodes with the largest local errors.

$$n_{in} = 0.5(n_{e1} + n_{e2}) \tag{3.9}$$

3. The local errors of the nodes n_{e2}, n_{e1} are decreased by a rate of γ. And the local error of n_{in} is subsequently assigned.

$$E_i \leftarrow E_i - \gamma E_i,\ i \in \{e1, e2\} \tag{3.10}$$

$$E_{in} = \beta(E_{e1} + E_{e2}) \tag{3.11}$$

Step 10. The local errors of all the nodes are decreased by a rate of η.

$$E_i \leftarrow E_i - \eta E_i, \quad \forall\, n_i \in N \tag{3.12}$$

The iteration is continued until the stopping criterion is met.

In the proposed hierarchical classification framework, the classifier training follows the phase of relabelling the given training data. The GNG is first conducted on the pooled training data in an unsupervised way to generate representation vectors of various clusters. The cluster indices and original labels are combined to form the enlarged set of labels. The classifier is trained from the data with their newly assigned labels. The unseen data are assigned with the original labels according to the newly defined labels following the inverse transformation. The relabelling is similar to the fining process in graininess while its inverse transformation is like the coarsening process.

The comparison of recognition accuracy between conventional LDA and hierarchical recognition strategy GNG-LDA for inter-day evaluation is shown in Fig. 3.5. The sEMG data of 3 experienced subjects performing 9 hand motions from Fig. 3.2 in consecutive 7 days are adopted. For each trial of recognition, the training data comprises the labelled 9 out of 10 folded sEMG data of two randomly selected distinct days with the rest candidate days as the testing data, whose combination is not exhausted in this experiment. The preliminary result shows that when the subject 2 and subject 3 are performing relatively consistent patterns with a significantly low average recognition error rate of 5% and 2%, the hierarchical classification GNG-LDA is inferior to solely adopting conventional classifier of LDA. The slight decrease of average recognition error rate can be observed on subject 1. A plausible explanation

of the results is that the totally unconstrained clustering incorporates bias into the newly labelled data. The variant size of GNG induced subclasses is a potentially severe factor for subjects with consistent sEMG pattern exertion and leads to a larger number of samples belonging to certain subclasses. As a result, the unseen data are more favourably assigned with these labels. On the contrary, when the subject is not able to generate repeatable patterns of sEMG signals, the scattering distribution of newly labelled data leads to an improved result with the incorporation of subclass division. Another cause for the uncertain results could be the limited training data that leads to a largely reduced samples for each subclass when they are assigned with new subclass labels in an unconstrained way. For example, in this applications, the number of a subclass under GNG could be half less when compared to the 128-dimensional feature vectors. The limited training data for each unconstrained subclass contributes to an undetermined performance with the pooled subclasses. Despite the improved intra-day recognition shown in the preliminary work, the feasibility of GNG + LDA in inter-day use is not guaranteed according to the preliminary results. Further validation of a strictly constrained subclass division method in combination with classification is needed, and presented in the following section.

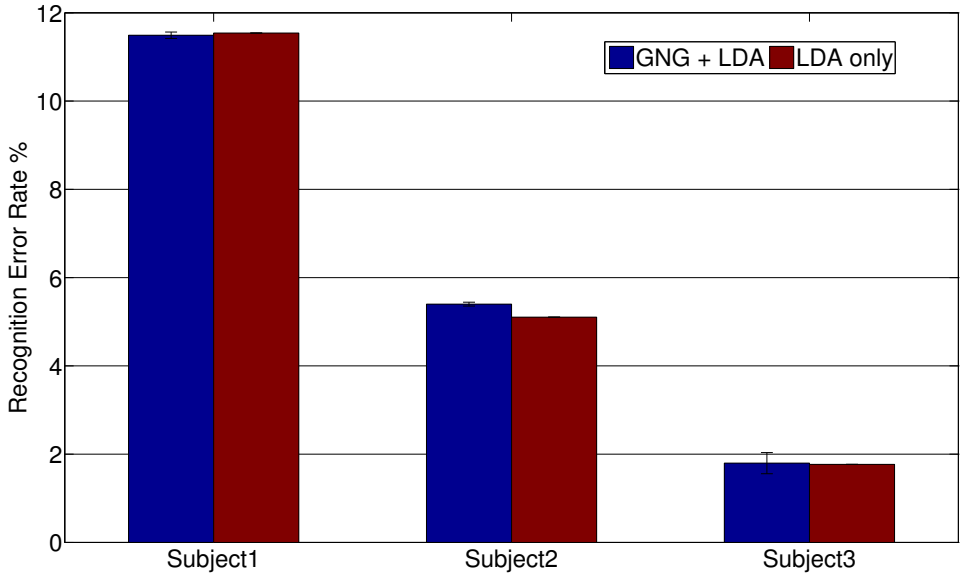

Fig. 3.5 Comparison of inter-day recognition error rate between GNG-LDA and LDA methods for 3 subjects

3.1.2 Constrained Subclass Division Based Discriminant Analysis

GNG-LDA fails to show consistent improvement of hand motion recognition accuracy mainly because of the totally unconstrained subclass division where all the pooled data are simultaneously divided into subclasses without using their original class labels. In contrast to the aforementioned unconstrained subclass division, a constrained subclass division with the hard constraint of the original data labels in the phase of relabelling is adopted in this section to remedy the performance ambiguity. Specifically, the inter-sample distance based sorting and KNN are exploited to divide the samples from a certain class into several subclasses according to their Euclidean distances. The training and and testing are based on the new subclass labels using a LDA classifier, and their original class labels are retrieved by the end of the recognition. The 4-step KNN-LDA is described as follows.

Step 1. Half of the data belonging to a certain class i are first sorted and categorised into C_i subclasses according to their inter-sample distances. A C_i-class KNN classifier is then formed by the samples.

Step 2. For every class out of the total C classes of the training data, the rest half samples belonging to class i are classified by KNN into C_i subclasses. The number of samples in each subclass is set equal. The labels are re-assigned for each sample according to the cluster they belong to, which leads to a total of C_{knn} subclasses.

$$C_{knn} = \sum_{i=1}^{C} C_i \tag{3.13}$$

Step 3. A C_{knn}-class LDA classifier is trained with the relabelled training data and represented by their means and covariance. And the label of an unseen data x is predicted by the Bayesian decision rule, where μ_i is the mean vector of the samples belonging to subclass i, Σ and Σ_i are the pooled covariance matrix of all samples and the sample covariance matrix of samples from subclass i, $p(i)$ is the prior probability of subclass i. And the prior probability is equal for all subclasses in the adopted settings because of the strict constraint of subclass size.

$$\arg\max_i {\mu_i}^T \Sigma^{-1} x - \frac{1}{2} {\mu_i}^T \Sigma^{-1} \mu_i + \ln p(i) \tag{3.14}$$

$$\Sigma = \sum_{i=1}^{C_{knn}} \frac{n_i - 1}{N} \Sigma_i \tag{3.15}$$

Step 4. The C_{knn} predicted labels of testing data are mapped back into the original C labels, which forms the final hand motion recognition results.

The experiments are conducted on the 3 experienced subjects with 2 days' data for training and the rest days' data for testing, which can be considered as training with inadequate data while the total number of testing samples is large enough in an exhausted comparison. And the training phase is repeated with 9 out of 10 folded data from the 2 days' training set. The results shown in Fig. 3.6 and Fig. 3.7 reflect the inter-day hand motion recognition accuracy with and without the preprocessing of normalisation respectively. It can be seen that the KNN-LDA outperforms the single LDA in both cases which validates the feasibility of a constrained and explicit subclass division for long-term sEMG based hand motion recognition. It is worth noting that all the 3 subjects are experienced users of the sEMG based hand motion recognition system, who can exert more consistent muscle contraction than others. A detailed numerical comparison between KNN-LDA and LDA is shown in Table 3.1, where a larger improvement is achieved by the KNN-LDA method for normalised sEMG data than that of the sEMG data without normalisation. Despite the difference between the two settings, a consistent improvement of classification accuracy is seen for the inadequate training of 2 days' data.

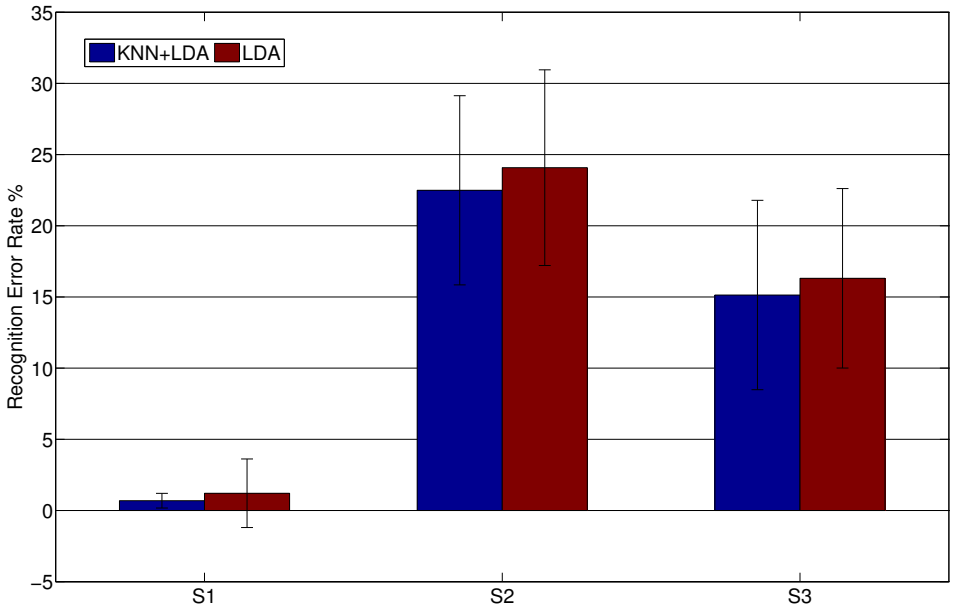

Fig. 3.6 Comparison of inter-day recognition error rate between KNN-LDA and LDA methods for 3 subjects with normalisation

In comparison with the totally unconstrained subclass division based GNG-LDA, the constrained KNN-LDA shows a favourable support to the explicit subclass division. A plausible explanation is that the unconstrained subclass division is conducted on the pooled training

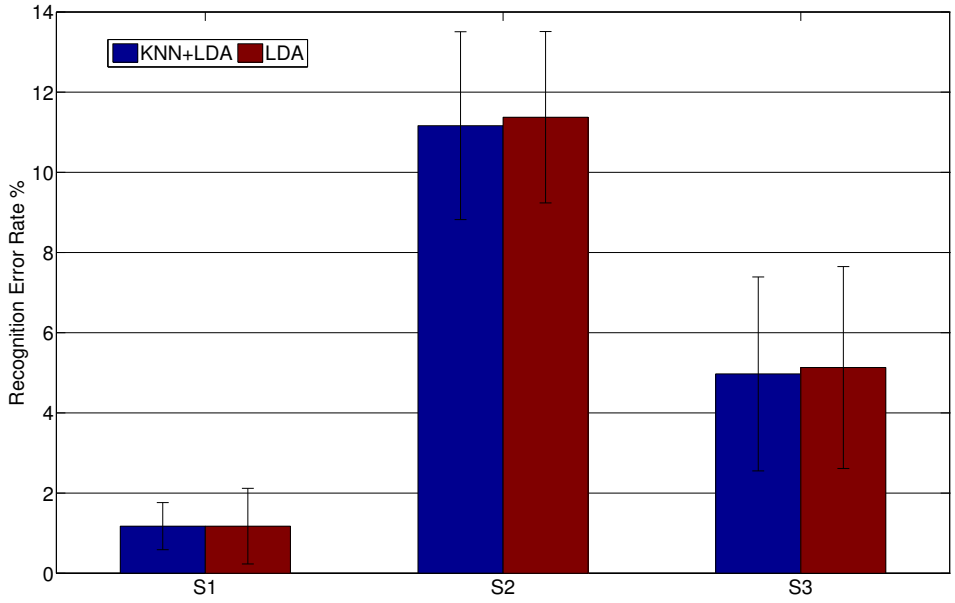

Fig. 3.7 Comparison of inter-day recognition error rate between KNN-LDA and LDA methods for 3 subjects without normalisation

samples without any priori knowledge of their classes, while the constrained operation is confined to those belonging to the same class, which avoids the false label assignment against the given conditions. And the bias incorporated by an imbalanced subclass division is avoided in this scheme. Despite the improvement brought by subclass division, it is worth noting that the number of samples in a subclass can be few when the number of subclassess increases, which potentially leads to an inferior classifier training with the explicitly divided subclasses. Thus it is necessary to further utilise the subclass division implicitly in the discriminant analysis in the next section.

3.1.3 Implicit Subclass Division Based Discriminant Analysis

An implicit subclass division utilises the subclass information without enlarging the class labels in a fining and coarsening scheme, and is realised in the discriminant analysis directly. The discriminant analysis based algorithms classify the samples with a projection of the original data into a reduced subspace with an optimised separability by simultaneously maximising the between-class distance and minimising the within-class distance. Accordingly, a general criterion [167] of separation for most discriminant analysis algorithms is defined as

Table 3.1 Comparison of KNN-LDA and LDA based inter-day hand motion recognition with inadequate training data with/without normalisation processing

Subjects	With Normalisation		Without Normalisation	
	LDA (%)	KNN-LDA (%)	LDA (%)	KNN-LDA (%)
1	97.08±2.41	99.31±0.52	98.23±0.94	98.82±0.59
2	75.98±6.87	77.65±6.64	88.21±2.14	88.86±2.34
3	82.92±6.30	84.87±6.65	94.88±2.52	95.10±2.42
Mean	85.33	87.28	93.77	94.26

$$S = \frac{|\omega^{\mathsf{T}} S_B \omega|}{|\omega^{\mathsf{T}} S_W \omega|} \tag{3.16}$$

where S_W and S_B are the scatter matrices of within-class distance and between-class distance respectively, while ω represents the direction for projection. The discriminant analysis aims to find an optimal projection direction by maximising S. Conventionally the within-class scatter matrix is defined as

$$S_W = \frac{1}{N} \sum_{i=1}^{C} \sum_{j=1}^{N_i} (x_{ij} - \mu_i)(x_{ij} - \mu_i)^{\mathsf{T}} \tag{3.17}$$

where N is the total number of samples, C is the number of classes, N_i is the number of samples that belong to class i, x_{ij} is the j-th sample within the class i, and μ_i is the mean centre of class i.

Different from the previous KNN-LDA solution, an integration of subclass division into the projection determination is adopted instead of using two independent subclass division and linear discriminant stages. The subclass discriminant analysis (SDA) algorithm proposed by Zhu et al. [168] is the first discriminant analysis considering the distance between subclasses instead of the distance between classes. The idea is adopted in combination with the nearest neighbour based division criterion to find the most convenient division of each class into multiple subclasses in an exhaustive scheme. In this thesis, the between-class scatter matrix is defined as

$$S_B = \sum_{i=1}^{C} \sum_{p=1}^{c_i} \sum_{j=i+1}^{C} \sum_{q=1}^{c_j} \frac{n_{ip}}{N_i} \frac{n_{jq}}{N_j} (\mu_{ip} - \mu_{jq})(\mu_{ip} - \mu_{jq})^{\mathsf{T}} \tag{3.18}$$

where C is the number of classes, c_i is the number of subclasses within the class i, N_i and N_j are the number of samples belonging to class i and j respectively, n_{ip} is the number of samples belonging to the subclass p of class i, and μ_{ip} is the mean centre of subclass p of

class i. The distance between subclasses is utilised instead of the distance between classes to extract the distribution information of subclasses attributed to the overlapping classes in long-term use.

Conventionally, once the scatter matrices are acquired, the projection direction is found to linearly separate the pooled data following the generalised eigenvalue decomposition as

$$S_B W = S_W W \Lambda \tag{3.19}$$

where W is the matrix whose columns are formed by the right eigenvectors and Λ is the diagonal matrix whose diagonal elements are corresponding eigenvalues. The first k columns of W with the greatest magnitude of eigenvalues are selected to form the projection matrix W^k for a $k+1$-class classification problem.

Based on the definition in 3.18, the further calculation of projection direction requires an determined subclass division number of each class. The strategy for seeking optimal subclass divisions with the leave-one-out test is adopted on the pooled dataset for both training and testing with only one sample excluded to achieve the global optimum. In this thesis, the selection of separate training and testing samples is adopted to address the inter-day and long-term use instead of solely considering the intra-day use. Specifically, the training samples U_{train} from each class are first divided into subclasses according to their inter-sample distances. The nearest neighbour method is adopted in the distance sorting, which measures the Euclidean distance $D_{p,q}$ between the two samples x_{ip} and x_{iq} within the class i to determine their subclass category. Then SDA classifiers using different subclass division choices are compared with the recognition accuracy on the testing data U_{test}. The one with the highest accuracy is finally selected for further validation on the subclass division number Γ. The testing algorithm is summarised as Shown in Algorithm 1.

The comparison of SDA and LDA based solutions on inter-day use is depicted in Fig. 3.8. The data of 3 experienced subjects performing 9 motions in consecutive 7 days are adopted. The classifiers are trained by only 2 day's data and tested on the rest days' data using the same group of TDAR features, which means the recognition is totally conducted on the unseen data captured in novel days. The number of subclasses is set equal among all classes in opposition to the previous flexible settings in GNG. The average recognition error rate decreases with slight improvement for all the 3 subjects utilising the proposed SDA instead of LDA. However, the performance improvement on subject 1 can be ignored in comparison with the other 2 subjects, which is possibly attributed to either the less variant sEMG patterns exerted by the subject among multiple days or the less flexibility of the adopted subclass division scheme. It is also worth noting that the optimal subclass division is subject dependent with a respectively selected subclass division number of 2, 4 and 7 for

Algorithm 1 SDA algorithm with subclass division tested on inter-day recognition

Dataset: U_{train}, U_{test}
Output: Γ
Initialisation: T, $R = \{r_1, r_2, \cdots, r_T\}$
Calculate the within-class scatter matrix S_W of U_{train} using 3.17
for i=1 to C **do**
  Extract the data from U_{train} belonging to class i, denoted as $X_i = \{x_{i1}, x_{i2}, \cdots, x_{in_i}\}$
  Let $U_{i1} = \emptyset$, $U_{i2} = \emptyset$
  Construct the distance matrix D, whose element is calculated by $D_{p,q} = \|x_{ip} - x_{iq}\|$
  Let $diag(D) = +\infty$
  Retrieve the index of the largest distance element $(a_1, b_1) = \arg\max_{(l,m)} D_{l,m}$
  $U_{i1} = U_{i1} \cup \{x_{ia_1}\}$, $U_{i2} = U_{i2} \cup \{x_{ib_1}\}$
  for j=2 to $\lceil n_i/2 \rceil$ **do**
    $a_j = \arg\min_{a_j} D_{a_{j-1},a_j}$,$b_j = \arg\min_{b_j} D_{b_{j-1},b_j}$
    $U_{i1} = U_{i1} \cup \{x_{ia_j}\}$, $U_{i2} = U_{i2} \cup \{x_{ib_j}\}$
    Let $D_{(b_{j-1},t)} = D_{(t,b_{j-1})} = D_{(a_{j-1},t)} = D_{(t,a_{j-1})} = +\infty, \forall 1 \leq t \leq n_i$
  end for
  $U_i = U_{i1} \cup U_{i2}$
end for
for k=1 to T **do**
  Divide the sorted samples in U_i evenly into k subsets, $\forall 1 \leq k \leq T$
  Calculate the between-class scatter matrix S_B including all U_i using 3.18
  Calculate the generalised eigenvalue decomposition $S_B W = S_W W \Lambda$
  Let $W = [w_1, w_2, \cdots, w_s]$,$\Lambda = Diag(\lambda_1, \lambda_2, \cdots, \lambda_s)$ with sorted eigenvalues
  $\lambda_1 \geq \lambda \geq \cdots \geq \lambda_s$
  Let $W^{C-1} = [w_1, w_2, \cdots, w_{C-1}]$
  Project training data U_{train} and testing data U_{test} to subspace of W^{C-1}
  Predict label for testing data according to the decision boundary
  Calculate the recognition accuracy r_k
end for
Retrieve the optimal subclass division number, $\Gamma = \arg\max_k r_k$

each subject. Thus it is favoured that an optimisation of the subclass division should be conducted on new users to ensure its effectiveness, yet the process of which remains time consuming and to be further improved.

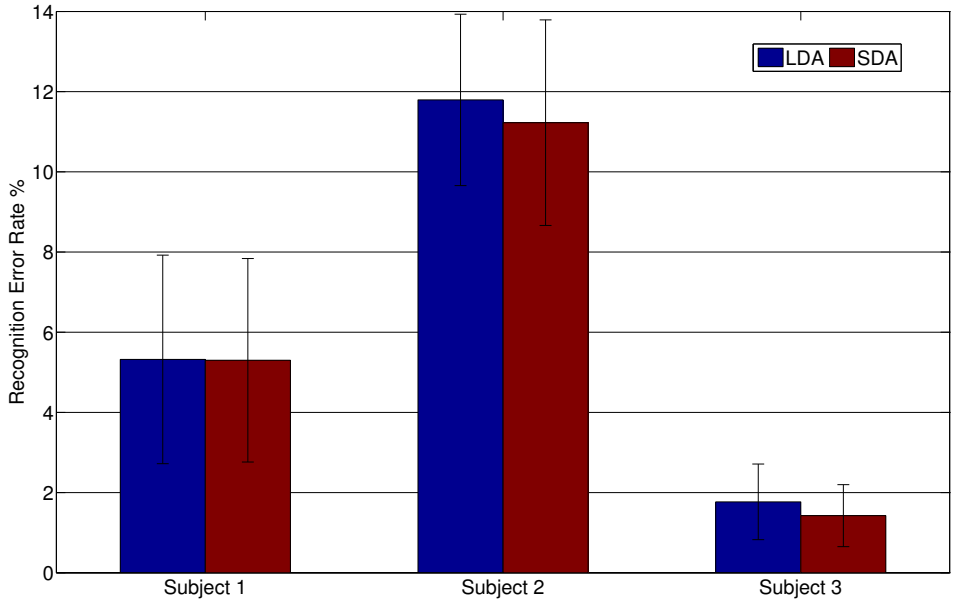

Fig. 3.8 Comparison of inter-day recognition error rate between SDA and LDA methods for 3 subjects

To further validate the feasibility of SDA in inter-day hand motion recognition with inadequate data for the implicit subclass division, a test on another dataset comprising 6 subjects, who are inexperienced at sEMG based hand motion recognition for prosthetic control, performing 13 hand motions in 10 days is utilised, where the training is conducted respectively with 1 day's data in Fig. 3.9 and 2 days' data in Fig. 3.10 whose sEMG are captured at distinct trials and testing on the rest days' data respectively. An improvement of recognition accuracy across the subjects can be seen for the situation with inadequate training of 1 day, and 9 days' totally unseen data for testing, which supports the implicit incorporation of subclass division when inadequate training data are provided.

A detailed numerical comparison of the recognition accuracy and corresponding numbers of testing samples is shown in Table 3.2. It is seen that the recognition accuracy increases by a large extent of around 10% when a new day's data is included for the training which aligns with the intuition. Regardless of the enriched training of 2 days' data, the total samples are still inadequate when compared to the 8 days' unseen data for prediction. When adequate training data are available across multiple days and subjects, instead of the conventional

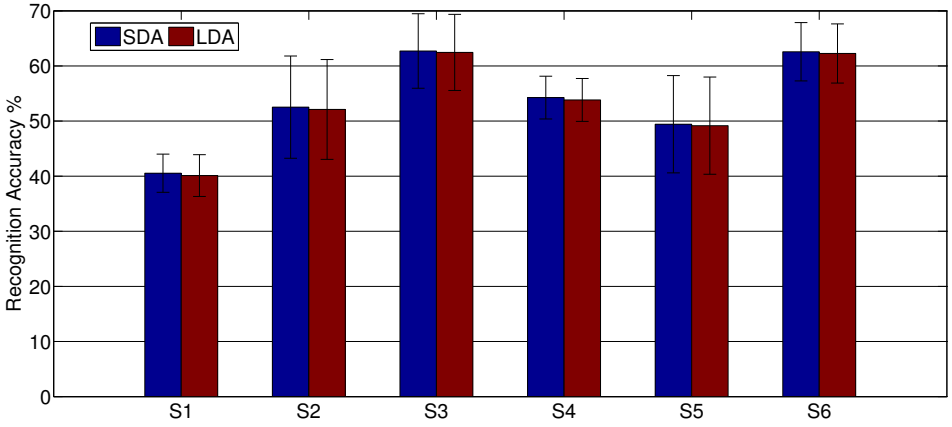

Fig. 3.9 Comparison of inter-day recognition accuracy between SDA and LDA methods for 6 subjects with 1 day for training

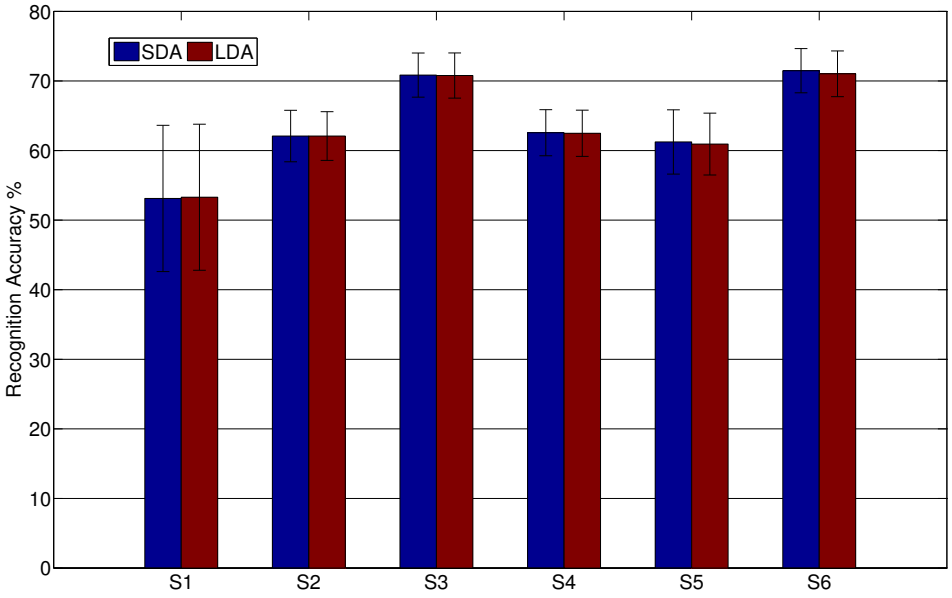

Fig. 3.10 Comparison of inter-day recognition accuracy between SDA and LDA methods for 6 subjects with 2 days for training

pattern recognition approaches, the improved feasibility of deep learning approaches over discriminant analysis is explored in the following sections.

Table 3.2 Comparison of SDA and LDA based inter-day hand motion recognition accuracy with inadequate training data of 1 day and 2 days

Subjects	Training on 1 Day		Training on 2 Days	
	LDA (%)	SDA (%)	LDA (%)	SDA (%)
1	40.11±3.79	40.54±3.46	53.29±10.50	53.12±10.51
2	52.11±9.06	52.53±9.28	62.08±3.50	62.08±3.70
3	62.46±6.91	62.72±6.76	70.78±3.25	70.85±3.18
4	53.83±3.89	54.26±3.88	62.48±3.32	62.56±3.31
5	49.17±8.82	49.43±8.83	60.93±4.45	61.24±4.62
6	62.27±5.37	62.58±5.29	71.03±3.28	71.47±3.18
Mean	53.32	53.67	63.43	63.55

3.2 Convolutional Neural Network for sEMG Based Hand Motion Recognition with Adequate Training Data

Deep learning approaches have been intensively applied in conventional pattern recognition based applications after their promising success in computer vision, natural language processing and other fields. Specifically, significant attention is attached to the deep learning framework of CNN since the milestone achievement in the ImageNet test conducted by Krizhevsky et al. [169]. Though there have been attempts in investigating the capability of CNN for hand motion recognition in several works, because of the fact that current sEMG capturing configuration is not unified as the image processing applications, it inevitably leads to a discrepant performance under various conditions. The usage of a higher density of electrode configuration, a smaller hand motion set, and an adaptive approach usually presents favourable conditions in [149]. Such an ideal experimental setup may see potentially better performance than the low-density ones for the less relative shift of the detection sites while the high-density sEMG signals naturally form the 2-dimensional images for each sampling frame where more information may resides in. Besides, the electrode shift can be alleviated by the image matching techniques to utilise partial grids for recognition. In some studies, the electrode shift is manually avoided by following the guidance of accurate positioning markers for electrode placement to investigate long-term characteristics of sEMG signals [34, 162]. Through the accurate electrode re-positioning approach in multiple days, these studies could normally reach an improved average recognition accuracy, which in turn proves that electrode shift negatively influences the classification performance and highlights the importance of electrode configuration and fixation optimisation. However, when it comes to daily life activities, the markers are hardly employed for the potential inconvenience.

Thus the electrode shift is inevitable in clinical settings and should be incorporated in the research of inter-day recognition. This thesis focuses on the 16-channel sEMG sensing system developed by [22] at a low-density electrode distribution without putting a marker purposely for reference, and utilises a CNN model for inter-day myoelectric hand motion recognition with an emphasis on the performance of solely using the raw sEMG signals as the input without signal preprocessing or handcrafted feature extraction, and the further improvement through merging handcrafted TDAR features into non-handcrafted features extracted by the CNN.

3.2.1 Convolutional Neural Network Architecture

The adopted architecture of CNN is shown in Fig. 3.11 which comprises 2 convolution layers and 2 fully connected layers, and implemented in the deep learning platform of TensorFlow. The choice of such a relatively simple architecture is based on the low-density nature of the input signals, which in turn proves the superiority of the deep learning approaches in such settings.

Raw sEMG signals captured from all the 16 detection channels in a segment of 256 sampling points are first concatenated in the form of a rectangle frame of their amplitudes with the size of 256×16, and fed to the CNN as the input without rectification, filtering, normalisation, standardisation or any other preprocessing. The 2 convolution layers are equipped with the rectified linear units (ReLU) as the activation function. And 32 and 64 filters are applied in the first and second layers respectively with the same filter size of 3×3. A 2×2 filter based max pooling layer with a two-step stride is connected after each convolution layer that down-sample the input feature maps to a quarter of their original size. Following the convolution layers, 2 fully connected layers using a linear activation function are incorporated, which map the extracted convolutional feature from the preceding convolution layers to the final 128-dimensional features. The softmax function is adopted routinely in the output layer to generate classification results. Besides the placement of the multiple layers in the network, both dropout and batch normalisation are employed to improve the CNN performance. The dropout is adopted to reduce the overfitting by dropping units together with their corresponding connections from the neural network during the training process [170]. In the adopted CNN architecture, the dropout is applied following the second convolution layer and the first fully connected layer respectively with a default retained probabilities of each neural unit at p = (1, 0.8, 0.5) going from the input layer to the top during training. The parameter setting is determined by the one with slightly higher accuracy among candidates with fixed-step enumeration based searching such as p = (0.95, 0.8, 0.5), p = (1, 0.8, 0.5), p = (1, 0.9, 0.5), p = (1, 1, 0.5), etc. Batch normalisation is adopted

to accelerate the training of deep networks by removing the covariate shift from internal activations of the network [171]. In the adopted CNN architecture, the batch normalisation is applied directly after the first and the second convolution layers, with the batch size set to 600 during all the experiments. In the adopted configuration, the training of the CNN is conventionally divided into two steps of pre-training and fine-tuning, where pre-training initialises the weights and biases of the network by related but non-targeted databases in either supervised or unsupervised manners [172] while fine-tuning further polishes the pre-trained network by training with samples of the targeted task only. It is reported especially helpful to optimise the parameters of the lower-level layers in deep structured networks [173]. In this thesis, the pre-training is specifically used to train a CNN with sEMG samples from all the subjects or all but the targeted subjects' sEMG signals, and solely the targeted subject's data, and the fine-tuning is to further train the pre-trained network with solely the training samples captured from the targeted subject. As a result, the common knowledge and the invariance across different subjects are first extracted, which can be applied to cross-day and cross-subject use with a compromised performance. Afterwards the fine-tuning contributes to a specific model with the training data from the targeted subject, which specialises the model with an optimal performance using the common knowledge and invariance as the complementary support. The AdamOptimiser algorithm is selected for classifier training with an exponentially decayed learning rate at 0.95, starting from 0.01 and decays every 10 steps and experiencing 500 iterations during the pre-training phase. The learning rate is fixed to 0.0001 with more than 500 iterations in total in the fine-tuning stage. For every targeted subject, the size of training and testing samples are 13650 and 5850 respectively, which provides the setting of adequate training.

3.2.2 Low-density sEMG Based Hand Motion Recognition

The inter-day hand motion recognition is conducted on a dataset comprising the low-density sEMG signals captured by a customised 16-channel sensing system from 6 subjects performing 13 hand motions. The raw sEMG signals are concatenated and fed to the CNN for training and testing, following the routine defined in Section 3.2.1. The classic pattern recognition approach of combined LDA and TDAR is selected as the baseline for comparison. A steady improvement of recognition accuracy can be seen in Fig. 3.12 and remains consistent for all 6 subjects, despite the voluntary performance varying among different subjects. Two baselines of LDA are formed by utilising different training strategies of training solely on samples from the same testing subject, and training on the pooled samples from all the subjects while the CNN is provided with the same set of training samples. The results also show that the performance of LDA degrades when trained by non-targeted subjects, which implies the

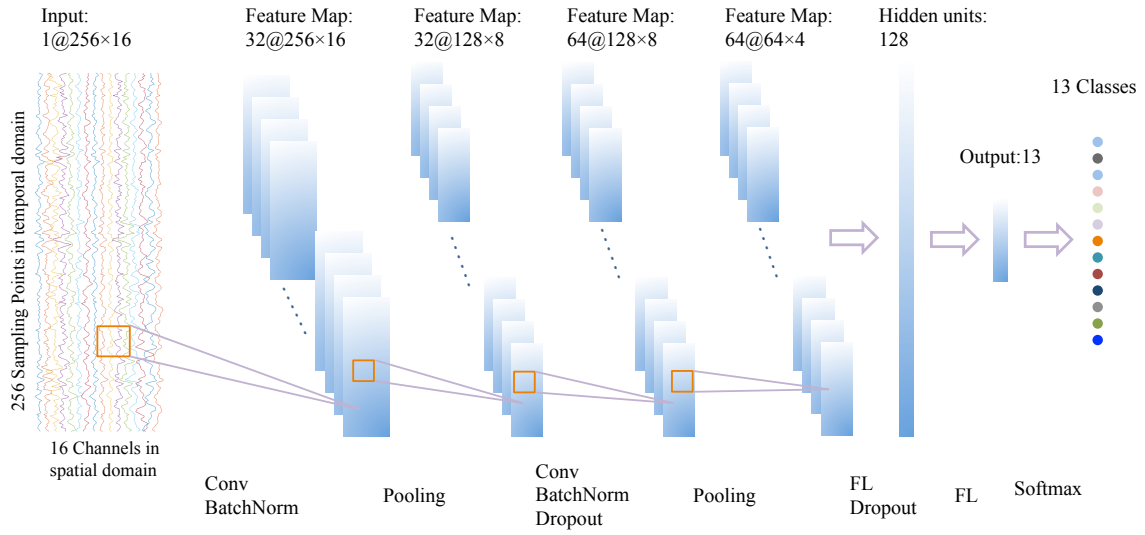

Fig. 3.11 The adopted architecture of convolutional neural network

inferior common knowledge extraction of combined LDA classification and TDAR feature representation in inter-day scenarios. The training is conducted on 7 days' samples while the testing is on the rest days, which is followed for all the comparison in this section.

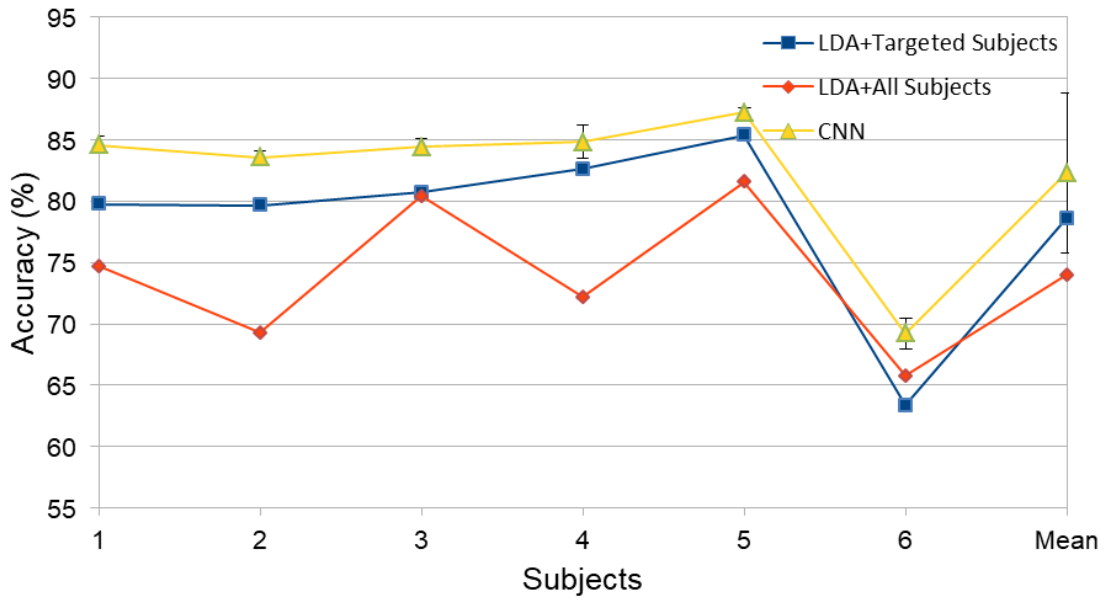

Fig. 3.12 The comparison of inter-day hand motion recognition between CNN and LDA

The detailed numerical comparison of inter-day recognition accuracies with different selections of training samples using respectively SVM with a radial basis function kernel (Rbf-SVM), SVM with a linear kernel (L-SVM), LDA and CNN are presented. Specifically,

the results in Table 3.3 are achieved by training on solely samples from the same testing subject while those in Table 3.4 are achieved by training on the pooled samples from all the subjects. An intuition can be drawn that LDA exhibits a better average recognition accuracy in comparison with SVM based solutions, which aligns with the choice of adopting LDA as the baseline for inter-day applications. It can be concluded in the experiment that the conventional recognition algorithms outperform CNN when the training and testing samples are from the same subject while on the contrary CNN exerts better performance than all the other approaches under the previous setting when the training samples are enriched by other subjects. What's more, the incorporation of sEMG data from multiple subjects contributes to the superiority of CNN in the comparison including both training strategies. A plausible explanation is that the adequate training samples are essential for deep learning approaches to extract useful features since no priori knowledge is provided in comparison with the conventional ones with handcrafted features. The adequacy is identified in both multiple days and multiple subjects in the adopted settings. The CNN operates without restrictions from the priori knowledge, and benefits from an enlarged training dataset of unseen subjects. The automatically extracted features and tuned classifiers contribute to a more robust inter-day recognition accuracy above 80% for 5 out of 6 subjects with less deviation than the conventional strategies as shown in Table. 3.4. A more intuitive understanding of the different responses of CNN and LDA to the inclusion of unseen subjects is illustrated in Fig. 3.13. A further comparison of the recognition accuracies of different number of motion types is conducted between CNN and LDA. It can be seen in Fig. 3.14 that the hand motion recognition accuracy decreases with the increasing number of motion candidates for classification, which complies with with the intuition. Yet the CNN remains consistently outperforming the LDA + TDAR. Despite the same decreasing trend of recognition accuracy, the different degree of degradation is visibly observable with the difference of accuracy between the two approaches varying from 1.33% to 3.41% and then 3.72%. A possible explanation is that the deep learning approaches can extract more distinguishable and repeatable patterns among similar hand motions than the conventional TDAR handcrafted features. When the complexity of application scenarios or the number of motions increases, the degradation of CNN is less severe than that of classic handcrafted TDAR features based LDA.

The two-stage training convergence of the adopted CNN is shown in Fig. 3.15. In the adopted settings, the first 500 iterations are for the pre-training and the rest are conducted for the fine-tuning. It can be seen that the pre-training contributes to an acceptable validation accuracy for 3 out of the 6 subjects, a mildly inferior accuracy for 2 subjects and an unsatisfactory result for the last subject. The capability of CNN in extraction common knowledge and

Table 3.3 Inter-day hand motion recognition accuracy with training on solely samples from the same testing subject

Subjects	LDA (%)	L-SVM (%)	Rbf-SVM (%)	CNN (%)
1	79.78	70.60	77.40	77.40±1.08
2	79.65	74.96	79.56	80.70±0.45
3	80.70	78.89	79.23	76.36±1.20
4	82.65	79.06	83.28	72.86±1.24
5	85.38	84.67	86.75	80.54±0.82
6	63.38	59.45	63.06	58.79±1.75
Mean	78.59	74.61	78.21	74.44

Table 3.4 Inter-day hand motion recognition accuracy with training on the pooled samples from all the subjects

Subjects	LDA (%)	L-SVM (%)	Rbf-SVM (%)	CNN (%)
1	74.68	71.79	77.13	84.59±0.72
2	69.27	65.90	60.22	83.57±0.53
3	80.43	78.50	76.74	84.42±0.74
4	72.21	70.31	78.14	84.83±1.36
5	81.56	79.56	85.68	87.23±0.42
6	65.78	64.70	63.49	69.21±1.23
Mean	73.99	71.79	73.56	82.31

invariance is favourably supported in the preliminary evaluation. However, due to the limited size of involved subjects, it remains to see in an explicit way whether the pre-trained common knowledge and invariance could contribute to a compromised yet acceptable recognition accuracy with less or no re-training regardless of the individual difference in sEMG exertion. And potentially a generalised model can be established by the incorporation of a large group of subjects to simplify the time-consuming data collection procedure for new users. On the other hand, significant improvement can be seen through fine-tuning for those with mildly inferior and unsatisfactory pre-training performance. What's more, the individual differences of improvement attributed to fine-tuning reflect the possible necessity for user training when new subjects are included. In the aforementioned experiments, we use all subjects' data to train a CNN model in pre-training, and further tunes the parameters with the target subject's training data in fine-tuning. To further validate the potential applications of the pre-trained CNN on unseen subjects and fully understand the sensitivity of CNN to the corresponding sEMG pattern distribution, another experiment is conducted to pre-train the model with five

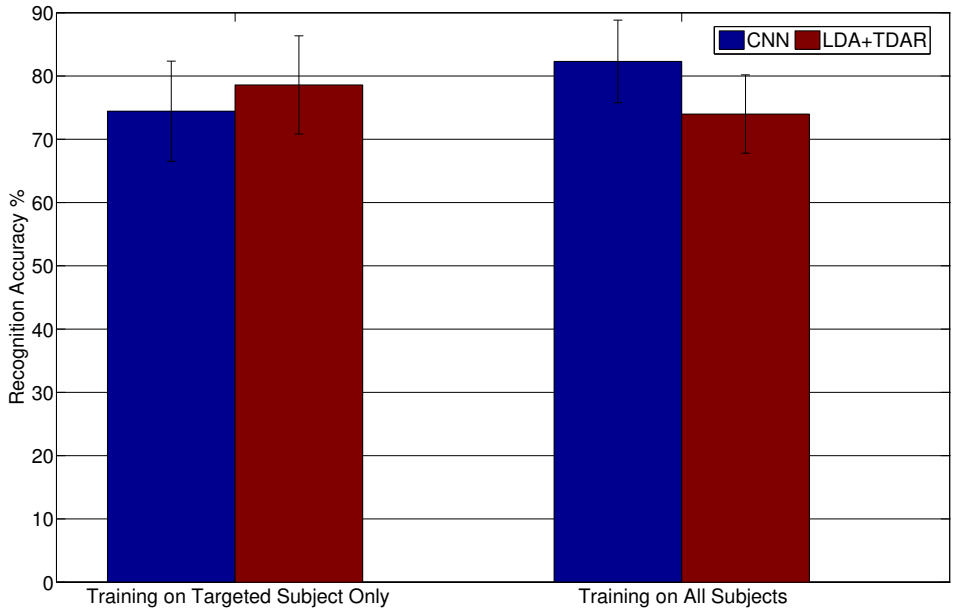

Fig. 3.13 Comparison of average recognition accuracy over subjects using CNN and LDA with different training strategies

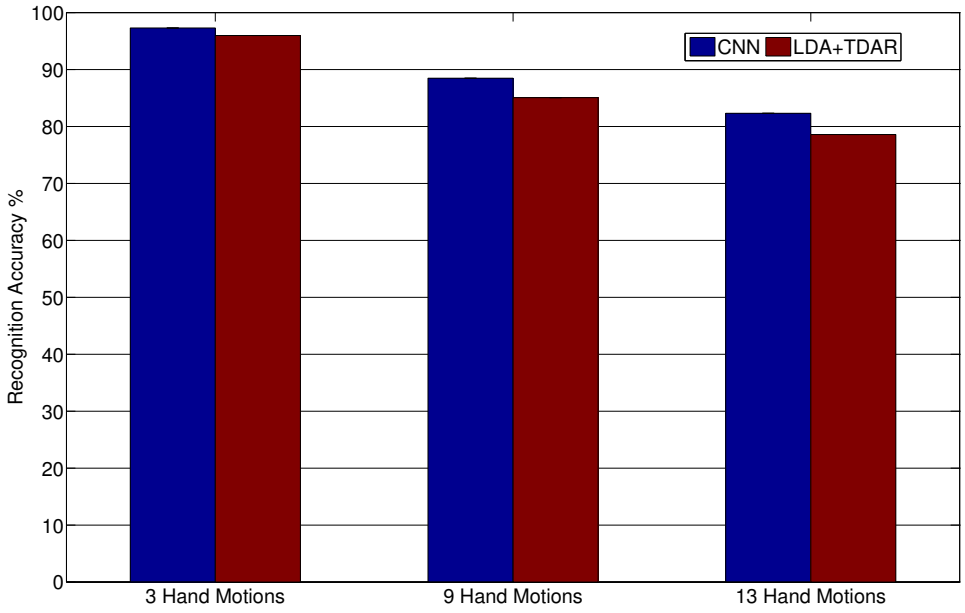

Fig. 3.14 Comparison of recognition accuracy of different motion sizes using CNN and LDA

out of the six subjects' data, excluding the target subject, and then fine-tune the model with training data of the target subject. The experimental results showed an average accuracy across six subjects at $79.96 \pm 6.28\%$, in comparison with the baseline accuracy achieved on the same and solely targeted subject of LDA at $78.59 \pm 7.76\%$. It implies the feasibility of creating a unified pre-trained CNN model that fits new users to achieve an acceptable accuracy.

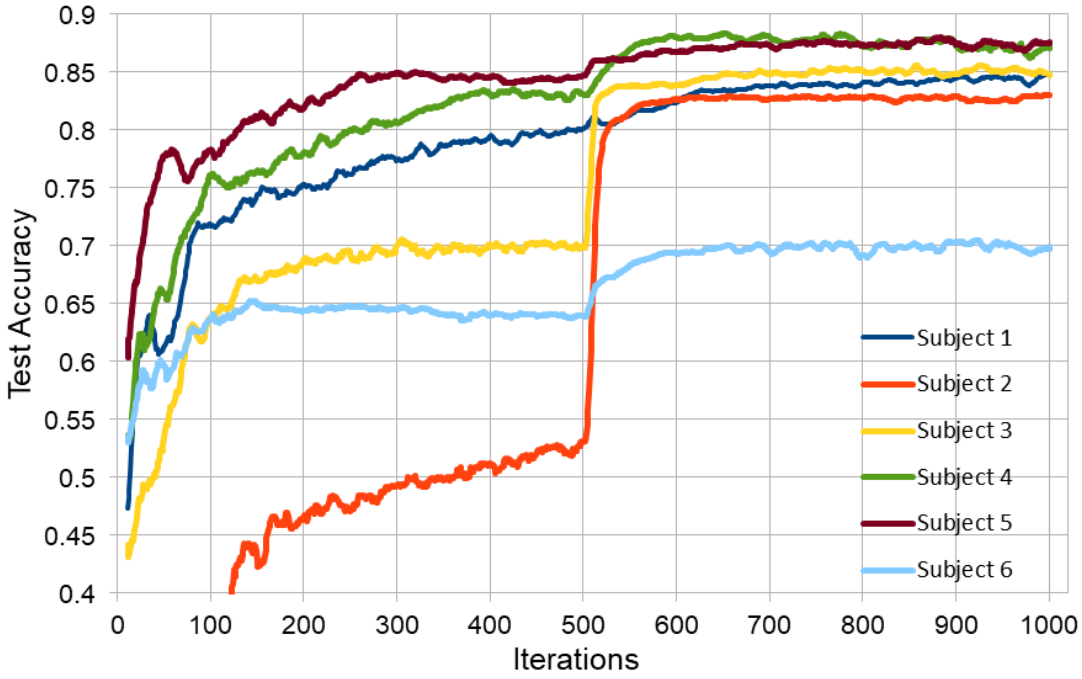

Fig. 3.15 The validation accuracy convergence of CNN training on 6 subjects with the first 500 iterations for pre-training and the rest for fine-tuning

Another comparison of different combinations of features and classifiers for 10 individual trials is shown in Fig. 3.16. The comparison is based on the 3 classifiers of LDA, SVM and CNN. Both LDA and SVM remain the most widely adopted classification methods in sEMG based hand motion recognition for their stable recognition accuracy and simplicity for implementation. The features of TDAR are chosen together with LDA and SVM as the baseline for its state-of-the-art for the last two decades since Hudgins' proposal [12]. The combination of both handcrafted TDAR features and non-handcrafted CNN features are chosen to evaluate their potential complement to each other. Because of the demonstrated difference in the aforementioned comparison between CNN and LDA+TDAR, here the CNN classification is only combined with the merged TDAR and CNN features because the non-handcrafted features are simultaneously learned with the parameters of networks. It is seen

that the averaged recognition accuracy is improved to a large extent by combining the CNN features with traditional TDAR features across classification strategies of LDA, SVM and also CNN. All trials of the algorithms demonstrate a consistent result that the merged features outperform single TDAR or CNN features. The experiments also illustrate that traditional TDAR features slightly outperform the CNN features both in conventional LDA and SVM classifiers. Additionally, LDA achieves better results than SVM with minor but consistent improvement regardless of the choice of single features or merged features which still aligns with the choice of LDA as the baseline classifier. Despite the promising performance of CNN in inter-day hand motion recognition, its uncertainty remains among different trials dealing with the same task and is inevitable especially for the specific application with a limited size of training data which contributes to a slight deviation of recognition accuracy. A variation of about 1% of the recognition accuracy occurs during the 10 individual trials as shown, yet still smaller than that of the conventional approaches.

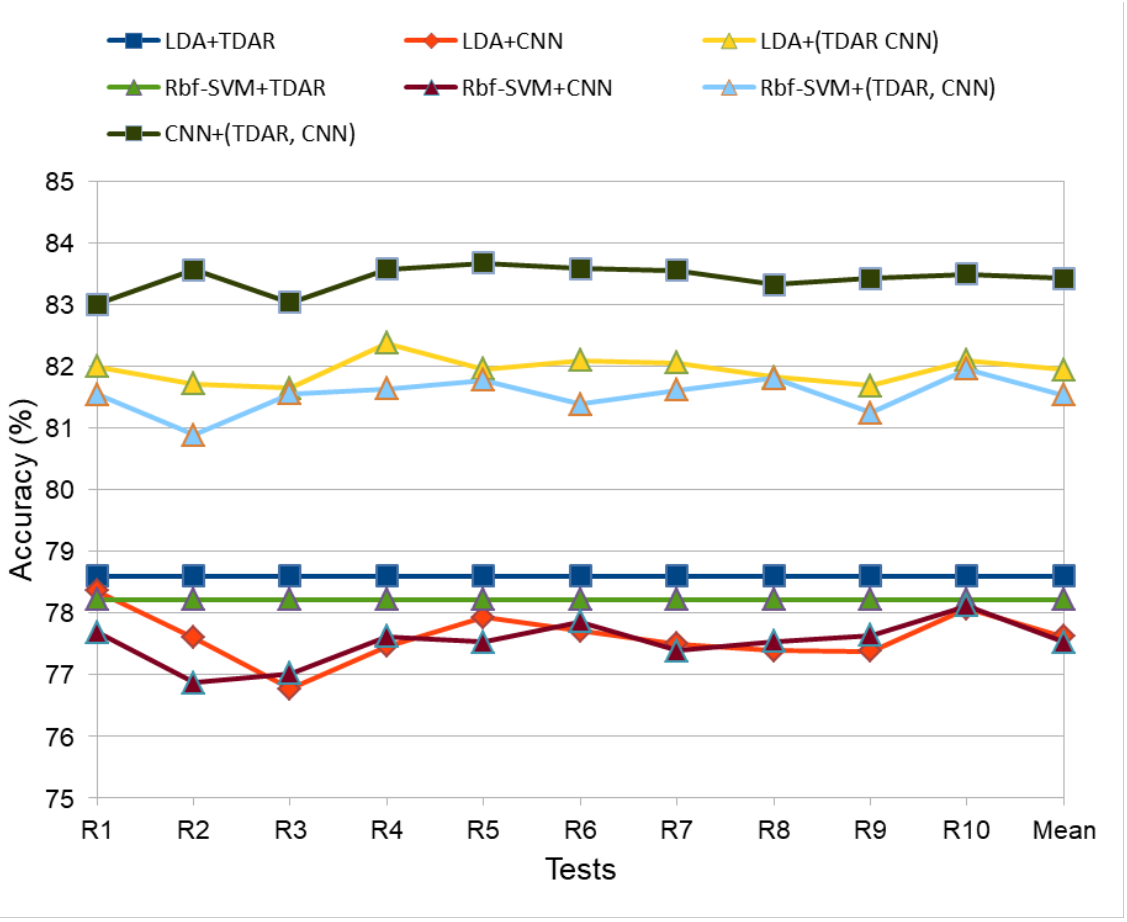

Fig. 3.16 The comparison of recognition accuracy with different combinations of classifiers and TDAR features, CNN features and merged TDAR+CNN features for 10 individual trials

A more detailed discussion of the handcrafted TDAR features, the non-handcrafted CNN features, and their combination will be presented in Section 4.1.

3.3 Summary

In this chapter, both conventional pattern recognition and deep learning classifiers are developed to achieve an improved inter-day hand motion recognition for long-term use. The discriminant analysis frameworks are first step by step developed with subclass division in both explicit and implicit ways. The subclass division is first conducted by GNG in an unconstrained way across all samples instead of using a separated division scheme, which shows an ambiguous inter-day performance. Then the totally unconstrained subclass division is replaced by the nearest neighbour based searching within the separated data belonging to a certain class which leads to the KNN-LDA. The combined subclass division optimisation with a modified definition of the between-class scatter matrix leads to the utilisation of SDA. The recognition results of inter-day evaluation demonstrate the improvement attributed to additional subclass division under the hard constraint of original classes in both KNN-LDA and SDA. The deep learning approach of CNN is adopted for the low-density sEMG sensing based hand motion recognition in inter-day scenarios. Raw sEMG signals are fed to the classifier directly without signal preprocessing or handcrafted feature extraction. The proposed CNN comprising 2 convolution layers and 2 fully connected layers steadily improves the inter-day recognition accuracy in comparison with the baseline achieved by LDA and TDAR and other conventional pattern recognition algorithms with handcrafted features. And the feasibility of the two-step training using the pre-training on multiple subjects to extract the common knowledge and invariance for the reduction of required fine-tuning data from the targeted subject is verified. The merged TDAR and CNN features are combined with multiple classifiers and beneficial for the improvement of inter-day recognition performance. Various choices of the training data including the number of motion types and the inclusion/exclusion of the targeted subject are also evaluated to demonstrate the potential strategies for CNN based hand motion recognition in long-term use.

Besides, the importance of training data size is also identified in this chapter. In the conventional classification development, the evaluation settings are confined to using inadequate training data to test unseen samples in more days. Specifically, the experiments are conducted on the limited training data of 1 or 2 days while the rest days are left for testing. Further evaluation on using adequate training data of 7 days across 6 subjects and testing on the rest days' data is conducted when deep learning approaches are adopted, where significant

improvement can be seen on the combination of CNN with the enlarged pooled training data across days and subjects.

The training process of a CNN are naturally much more time consuming than the training of classifiers like LDA and SVM. And the requirement of adequate training data for a decent CNN will inevitably lead to a large burden of user training. Though the improvement of inter-day recognition accuracy is seen in the proposed classification methods compared to the classic ones, it is reasonable to achieve a well balanced trade-off between the efficiency of both classier training and user training and recognition accuracy for inter-day use.

Chapter 4

EMG Feature Extraction and Selection

In pattern recognition based applications, features play a vital and even dominant role in most cases, where good features can contribute to acceptable classification results with naive classifiers. Feature extraction aims at finding the descriptors that are both consistent and distinguishable for classification. Because of the redundant feature representations and different targets, multiple feature combinations are suitable for a certain application. To efficiently exploit the redundancy, offline feature selection is usually conducted to reduce the burden of feature extraction under various constraints before real applications. In this chapter, the feature extraction and feature selection are addressed simultaneously. In the section of feature extraction, both handcrafted features and the non-handcrafted features will be discussed in details. And a novel feature descriptor is proposed with a specific emphasis on the multi-threshold based time domain feature extraction for an improved average recognition accuracy. In the section of feature selection, both computational cost reduction and recognition accuracy improvement are focused on respectively and implemented by the evolutionary algorithm based feature selection and analysis.

4.1 Feature Extraction

SEMG signals are the sum of electrical activities of the muscle fibers, as triggered by the impulses of activation of the innervating motor neurons and obtained by the convolution of each motor neuron spike train exerted by the MUAPs [58], and the amplitude of the sEMG signals is a zero-mean random process. In pattern recognition based solutions, feature extraction within a sliding window is adopted to transform the stochastic signal to meaningful information that can be effectively classified. Conventional classifiers can obtain a higher classification accuracy with extracted features instead of raw sEMG signals as the input. The sEMG features are commonly extracted in both temporal and spatial domains [174, 175] to

boost the motion recognition performance. Geng et al. [148] reported that repeatable and distinguishable patterns exist in instantaneous sEMG frames leading to a better hand motion recognition, which is intuitively beneficial to deep learning algorithms. The superfluity and redundancy of features are stated by Phinyomark et al. [176] and form a feature reduction and selection problem that remains to be addressed. Thus it is worth conducting research on both perspectives including better exploitation of existing features and proposal of novel features with an emphasis on the combination with both conventional and deep learning approaches.

4.1.1 Merging Handcrafted and Non-handcrafted Features

The feasibility of handcrafted TDAR features has been proved by the extensive research after Hudgins' prominent work [12] in the last two decades. And the priori knowledge driven feature extraction is applicable for the vast majority of users with a promising accuracy under the condition that training samples are well captured in an unseen scenario.

In the previous chapter, it has already been verified that a simply structured CNN with 2 convolution layers and 2 fully connected layers is able to learn sEMG features for inter-day use automatically without the guidance of any priori knowledge. The CNN learns features hierarchically and automatically and allows a system to induce complex functions mapping the input to the output directly from data, without depending heavily on handcrafted features [173]. The results concluded from Chapter 3 imply that the extraction of handcrafted features could be bypassed when CNN is adopted as the classifier. In comparison with conventional classification approaches, the CNN shows significant superiority on the inter-day hand motion recognition when the training dataset is adequate across multiple days and subjects. Based on the fact that specific hand motions are related the contraction of certain muscles and people share similar muscular structures, it is assumed in this thesis that common knowledge or invariance of the sEMG patterns among multiple days can be extracted by CNN through a proper pre-training approach. And the extracted common knowledge can accommodate the varying conditions for long-term use. This belief can be preliminarily verified by the acceptable inter-subject recognition accuracy with a pre-trained CNN across all the 6 subjects, and reflected by the comparison between the pre-trained feature maps and the fine-tuned feature maps in Fig. 4.1 where most elements of the maps remain similar. Specifically, an example of the pre-trained and fine-tuned feature maps captured from an individual subject whose pre-trained model could achieve an acceptable recognition accuracy is shown in Fig. 4.2. The differences between the two feature maps can hardly be visually identified. It implies that the pre-trained feature maps hold the most information that remains unchangeable with a user-targeted fine-tuning if the common knowledge is well extracted. This assumption is

also supported by the training convergence plotting in Fig. 3.15, where the hand motion recognition accuracy for all subjects steadily improves along iterations in the pre-training phase, which acts as a proof of effective extraction of common knowledge or invariance. CNN is a powerful tool for feature extraction from the raw sEMG signals as demonstrated in Section 3.2.

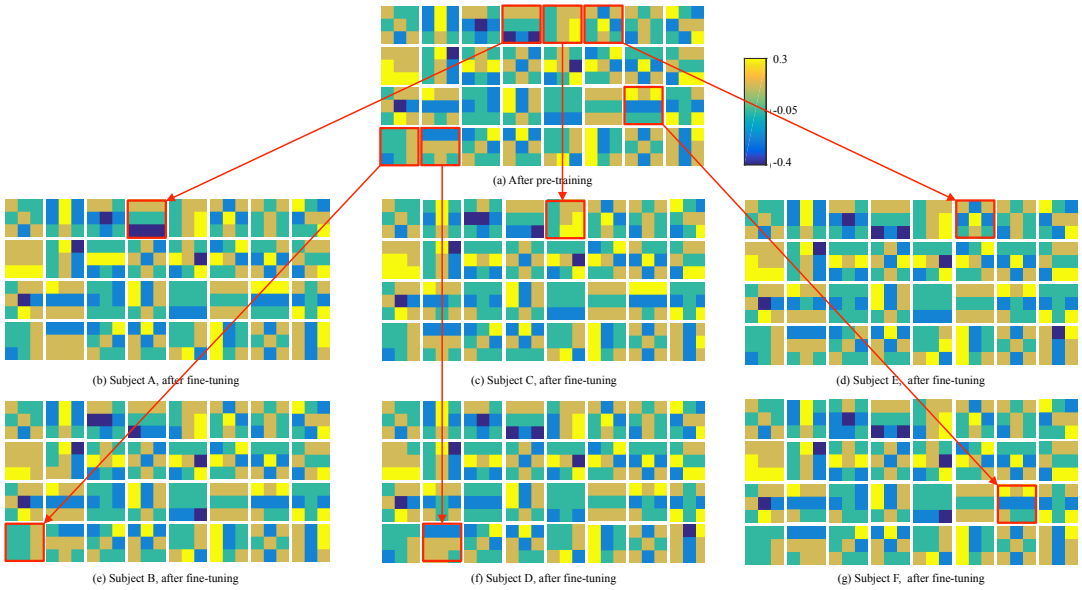

Fig. 4.1 The learned 32 feature maps by the first convolution layers, obtained from pooled samples from all subjects after pre-training and fine-tuning

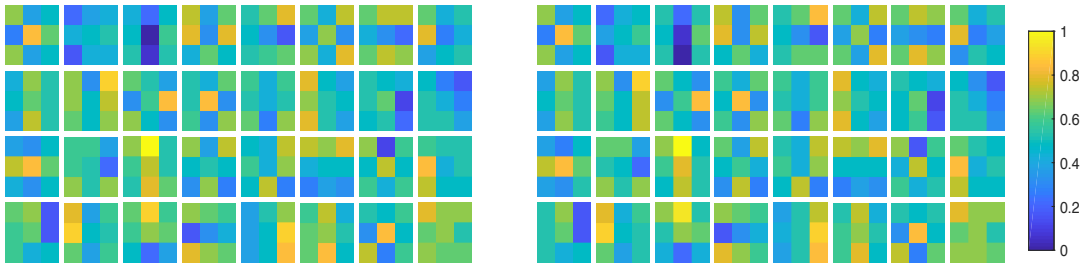

(a) After pre-training (b) After fine-tuning

Fig. 4.2 The comparison of learned 32 feature maps after pre-training and fine-tuning for a single subject whose pre-trained model achieves an acceptable recognition accuracy

However, despite the merits of CNN, conventional TDAR features outperform the CNN features in the test when the size of training samples is limited. Handcrafted TDAR features

exhibit a promising performance with the training and testing on solely the targeted subject, which is also verified in last chapter. Thus an intuitive idea is whether the two kinds of features can be utilised simultaneously to take advantages of them both. The scatter plot of the principal components of extracted sEMG features for 5 motions in multiple days is depicted in Fig. 4.3. It can be seen in Fig. 4.3a that there exist several clear clusters for hand motions like hand rest, hand open, wrist flexion and wrist extension with only 3 dimensions after PCA of TDAR features. And the feature distribution within multiple days exhibits significant variation which potentially leads to degradation of the long-term performance. In contrast, the distribution of the first 3 principal components of CNN features share consistency among multiple days and the scatter within each hand motion remains similar to those of other motions as shown in Fig. 4.3b, which means the common knowledge and invariance of inter-day sEMG patterns could be extracted by CNN features without any priori knowledge. As a result, the inter-day recognition with CNN features outperforms using solely TDAR features. The merged features of both handcrafted TDAR features and non-handcrafted CNN features are proposed to take advantage of them both as demonstrated in Fig. 4.3c. Thus the fused features are possible to improve for long-term use even with the classic non-deep learning based classifiers, which is verified and illustrated in Fig. 3.16. An intuitive idea is formed that TDAR features can be separated better than CNN features with naive classifiers for certain motions while CNN features exert better robustness against the inter-day scenarios but can only be well distinguished with more complex classifier such as the CNN itself, which coincides with the recognition results in Section 3.2.

4.1.2 Multi-threshold Based Time Domain Feature Extraction

To fully exploit the TD features for an improved long-term performance, a lot of efforts have been seen in academia. Kamavuako et al. [177] investigated the optimal threshold of typical Hudgins' TD features like ZC and SSC using metrics of classification error, separability index, scatter matrix separability criterion and cardinality of the features, and verified the parameter settings with the data captured in 2 days from 8 able-bodied subjects in an inter-day recognition scenario. Though the optimal threshold is highly data-dependant and subject-dependent, which does not generalise well, it is claimed the results showed a strong evidence to support that keeping the threshold equals zero provides a good trade-off between system performance and generalisation. Determining the optimal window length for pattern recognition based myoelectric control seeks to balance the competing effects of classification error and controller delay [121]. Taking the importance of segment length and the TD feature threshold into account, the research instance of simultaneously considering both the factors is still missing and remains to be addressed. The threshold and sub-segments

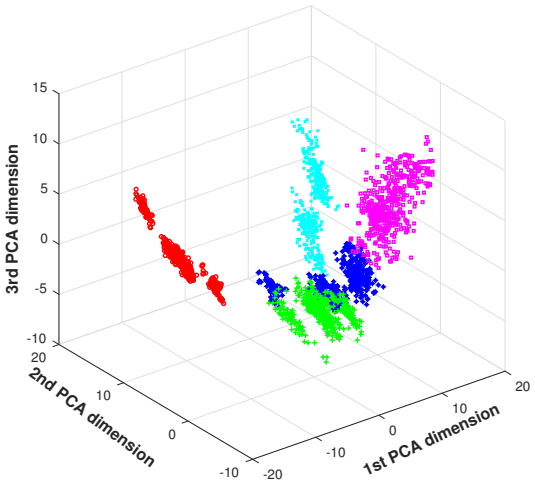

(a) TDAR Features

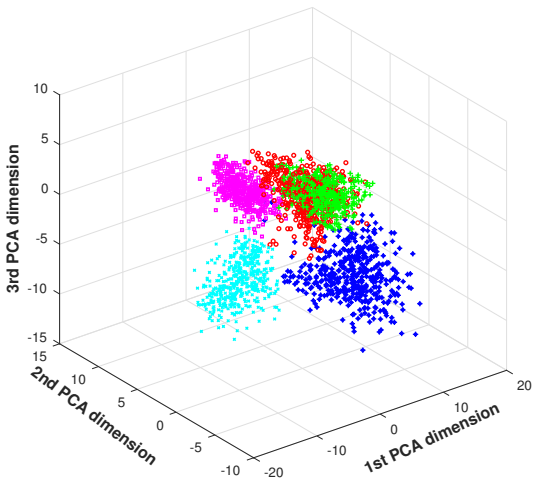

(b) CNN Features

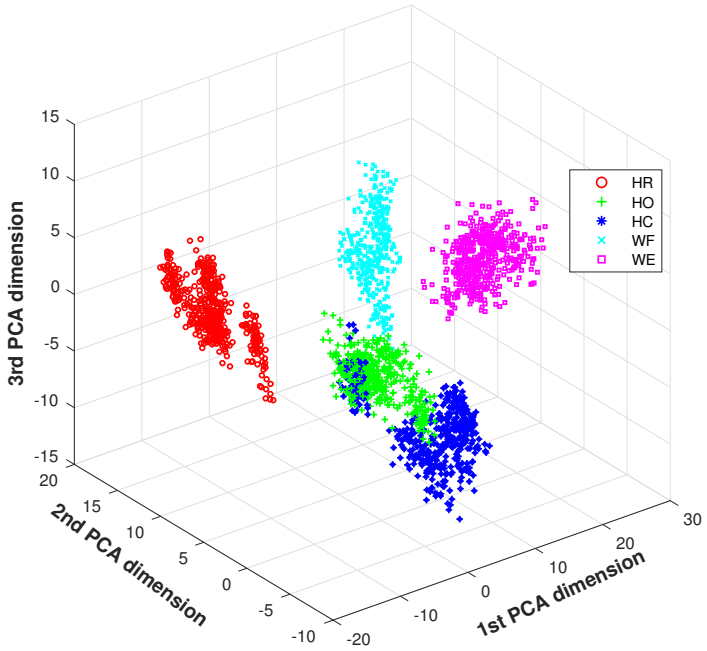

(c) TDAR+CNN Merged Features

Fig. 4.3 Principal component scatter of the TDAR, CNN, and merged TDAR+CNN features of 5 motions in multiple days

are considered respectively in this section and the following section. And the enumeration of

SSC and ZC with multiple thresholds is considered in this section to provide a novel feature vector named TDARM.

Conventionally, the threshold of 0 or an relatively small integer is applied for the ZC and SSC feature extraction as reviewed in Section 2.2.2 and controls the counting of zero crossings and slope sign changes. The evaluation of multiple thresholds in this thesis is conducted across the subjects and utilises 2 days' data for training and the rest for testing. The choice of the 2 days' combination is exhausted in the experiment to verify the feasibility of TDARM features. A 3-threshold extraction scheme is adopted in this thesis, which contributes to 3 additional pairs of ZC and SSC to the original TDAR features. The first set of threshold is selected as (0,10,20) and (10,20,30) respectively for the ZC and SSC while the other two increased thresholds of (0,15,30) and (10,30,50), (0,20,40) and (10,40,70) are chosen, which reflects different scales of amplitude change division. The comparison of the 3 different choices of TDARM and TDAR features is illustrated in Fig. 4.4. It can be seen that the average recognition accuracy over all subjects is improved by around 1% for all 3 different TDARM features. Another finding is that a smaller scale of division plausibly contributes to a more improvement despite the slight difference of 0.1% between the adjacent TDARM feature vectors. An intuitive understanding of ZC and SSC features is that they reflect the waveform variation within an sEMG segment. A single threshold based counting of slope sign changes and zero crossings simply enumerates the changes that exceed the predefined amplitude differences of sEMG signals without a finer categorisation. The multiple-threshold based TDARM features proposed in this thesis aim to address the diversity of signal changes by dividing them into multiple subsets. A well designed threshold naturally leads to the incorporation of both stable changes and significant variations of the sEMG signals and potentially illustrates different stages during the muscle contraction. For example, our proposed 3-threshold selection categorises the sEMG amplitude changes into 3 sets of small, medium and large variations respectively, which provides more description of the EMG patterns than that of a single threshold based features. Besides, the multiple threshold based extraction is potentially improvable with an additional optimisation process through feature selection, which will be addressed in our future work. Let alone the emphasis on multiple thresholds, the other aforementioned property of multiple sub-segments is addressed in Section 4.2.3.

4.2 Feature Selection

SEMG signals are the electrical manifestation exerted by a group of superficial muscles and detected over the skin surface, which inevitably comprise more information from the muscle

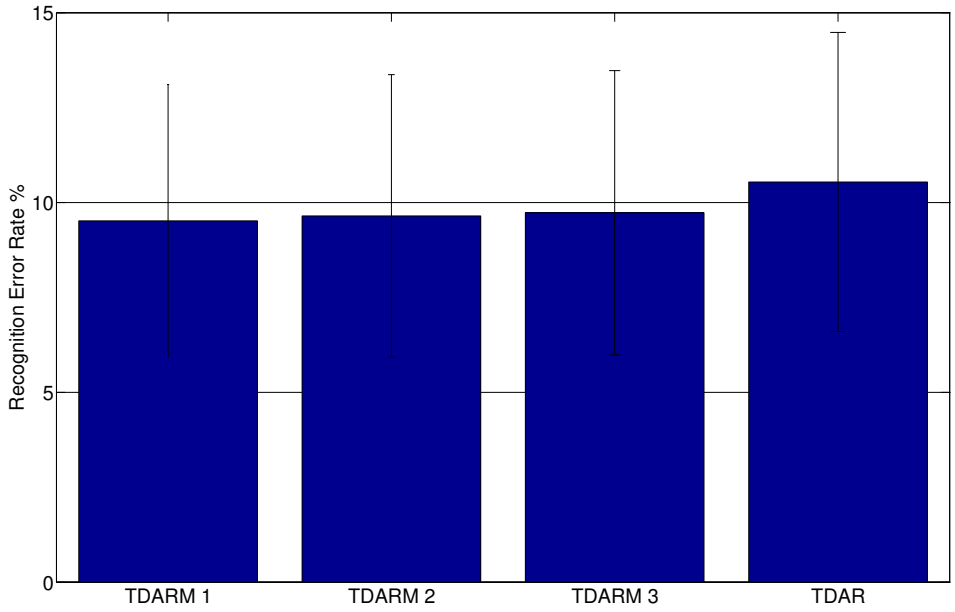

Fig. 4.4 Comparison of the TDARM features with different thresholds and TDAR features

contraction nearer to the electrodes and less from the contraction of more distant muscles. Thus intuitively a denser distribution of more electrodes without exceeding the limit of electrical interference in the sEMG capturing system could contribute to the acquisition of more physiological information. However, despite the potential use of informative patterns brought in by incorporating more physiological signals with extra detection sites, the extraction of more features could be time-consuming for real-time applications. Furthermore, redundant pooled feature sets, especially the ones comprising the handcrafted features, sometimes degrade the recognition performance because of the overfitting of classifiers against the non-consistent features. Besides, Phinyomark et al. [176] evaluated a group of candidate features captured by a system equipped with 5 electrodes and stated the superfluity and redundancy of TD features within. Though only a limited number of detecting sites can be allocated over the forearm muscles with current low-density sEMG capturing systems due to the size constraints of the electrodes and their mutual electrical interference, it has been pointed out by numerous research that the required number of channels is quite low compared to the availability. For example, Khushaba et al. [133] utilised the particle swarm optimisation to evaluate the feature and channel combination to gain the minimum number of channels and features required to achieve the demanded recognition accuracy, and found that only 3 channels were enough to generate an acceptable recognition accuracy.

As a result, let alone the aforementioned numerous research on feature extraction, feature selection is also addressed by researchers seeking for an optimised feature combination. Among all the research, Oskoei et al. [132] first applied the genetic algorithm in sEMG based hand motion recognition. In their application of recognition among 6 motions, the optimal subset of features was selected for their 4-channel and 6-channel myoelectric systems respectively instead of exploiting the pooled feature ensemble. After the initial work conducted by Oskoei et al., a trending research on the feature selection to reduce the computational complexity and maintain the accurate recognition under various constraints has been seen in the last decade, such as in scenarios with the varying contraction forces and limb positions. Al-Timemy et al. [178] considered the finger movement classification and achieved a comparable accuracy with a group of selected channels instead of utilising all channels, and further found that the classification accuracy under limb variation was improved with the selected subset out of 10 feature candidates [128]. And Adewuyi et al. [179] aimed to optimise the sEMG feature combination under varying wrist positions for subjects with partial hand amputation and identified the optimal number of wrist positions needed for classifier training, which was realised by sequential forward searching with Bhattacharyya distance as the separability index. Besides the focus on the varying status of the subjects, the most recent research of feature selection has been seen on the constraint of different characteristics of the capturing system. Phinyomark et al. [180] specifically selected sEMG features that provide better recognition for the emerging low-sampling rate systems such as the prevalent MYO armband.

In summary, the importance of feature selection for sEMG based hand motion recognition has been addressed in various publications since last decade. Despite their constructive findings, the selection was confined within the combination of feature types and channels without considering long-term use as the target. The selection of optimal feature subsets for a reduced computational cost at a compromised yet comparable recognition accuracy or for an improved performance with additional attributes respectively in long-term use remains to be investigated. This section will introduce the adopted feature selection algorithm and the feature candidates together with the verification of the ideas.

4.2.1 Bacterial Memetic Algorithm for Feature Selection

In this thesis, the bacterial memetic algorithm (BMA) is adopted for feature selection. BMA is an evolutionary memetic algorithm inspired by the nature of microbial evolution that combines both global and local search for optimisation [181]. BMA comprises basic operations including mutation, transfer and local search, taking advantages of both evolutionary and memetic approaches. The optimisation problem of feature selection aims to seek the optimal

or quasi-optimal combinations of feature candidates. In BMA, the possible combinations of features are encoded by the chromosomes with integer indices. And the evaluation of the feature subset is to test each chromosome according to the predefined metrics such as the recognition accuracy for a classification problem or the computational cost. After the random initialisation of chromosomes, mutation, transfer and local search operations will be sequentially conducted on the chromosomes according to the calculated evaluation metrics. The loop of three operations will be continued till the termination criteria are met. The chromosome with the best evaluation result will be finally retrieved as the output and decoded into the selected feature combination.

Encoding and Evaluation

In the initialisation stage, a total of N_{ind} individual bacteria are created as the whole population to be processed in the following stages. The chromosome length of each bacterium is first randomly initialised within a predefined length and filled with a string of non-negative integers mapping to the feature candidates. In our case of feature selection, each integer in the chromosome represents the index of an individual feature from the pooled sEMG TDAR features of all channels. Features denoted by chromosomes will be examined on their inter-day hand motion recognition for the performance evaluation in each evolutionary memetic loop. The chromosome with the best evaluation result in the last loop is exported as the optimal or quasi-optimal feature set. In our feature selection problem, the recognition accuracy obtained from the retrieved features and the predefined LDA classifier is adopted as the fitness. In our application the chromosome length is variable and extended or reduced with a fixed probability P_{bm} in each loop of bacterial mutation and transfer operations to explore a broader search space. Referring to the priori knowledge of the scenario, the size of a constrained search space is controlled by lower and upper boundaries of the chromosome length.

$$S = \sum_{i=n_L}^{n_U} \binom{N}{i} \tag{4.1}$$

where N is the total number of candidate features, and n_U and n_L represent the upper boundary and lower boundary of the chromosome length.

An alternative constraint is to combine the penalty function as a regulariser on the chromosome length in the evaluation. To constraint the complexity of the model, the regularised fitness function is adopted.

$$\sigma_{\varepsilon_i} = \frac{1}{N} \sum_{(x,t)\in T} \delta[f(x) - t] + \lambda \frac{l_b}{U}$$
$$\delta(x) = \begin{cases} 1, & x = 0 \\ 0, & x \neq 0 \end{cases} \tag{4.2}$$

where σ_{ε_i} is the fitness of i-th bacterium chromosome ε_i, N is the size of testing data, $f(x)$ is the classification function which outputs the category, (x,t) is the sample from the testing domain T, l_b is the current chromosome length, U is the upper boundary of chromosome length, λ is the regularisation parameter to tune the evaluation with different emphasis and $\delta(x)$ is the Kronecker delta function.

Mutation

BMA searches for the global optimum through mutation in the chromosomes, which imports new information in a randomly selected space. Similar to other evolutionary algorithms, individuals from the population are mutated, evaluated and replaced or preserved.

The mutation operation is performed for all N_{ind} chromosomes one by one in each loop. The mutation starts with the duplication of the objective chromosome for N_{Clone} times. Then a random length of l_{bm} is generated to indicate the segments to be mutated in the chromosome. Despite the mutation in the clones, the original chromosome remains the same as the unaltered source chromosome in this stage. The evaluation operation is conducted on each chromosome and the source one is replaced by the one with the best result whereas the inferior ones are eliminated. In our application, the mutation epoch of one bacterium is set adaptive to its length to guarantee that all the segments are mutated at least once and only once in every loop. During the mutation process, the length of each chromosome varies by a predefined length l_{cl} or remains unchanged according to the predefined probability P_{bm}. The mutation operation and length modification is illustrated in Fig. 4.5, where $N_{Clone} = 3$, $l_{bm} = 2$, $l_{cl} = 1$, and Eva is the fitness function of accuracy and a larger Eva is to be achieved in the selection.

Local Search

After the mutation, the local search operators will randomly function on the individuals from mutated population with a probability of P_{ls}. A predefined local search space is explored to find the best neighbouring solution among one or grouped segments. Memetic algorithms incorporate the local search operation to accelerate the whole searching process with exploitation of the priori knowledge attained in the certain field. In our thesis, the local

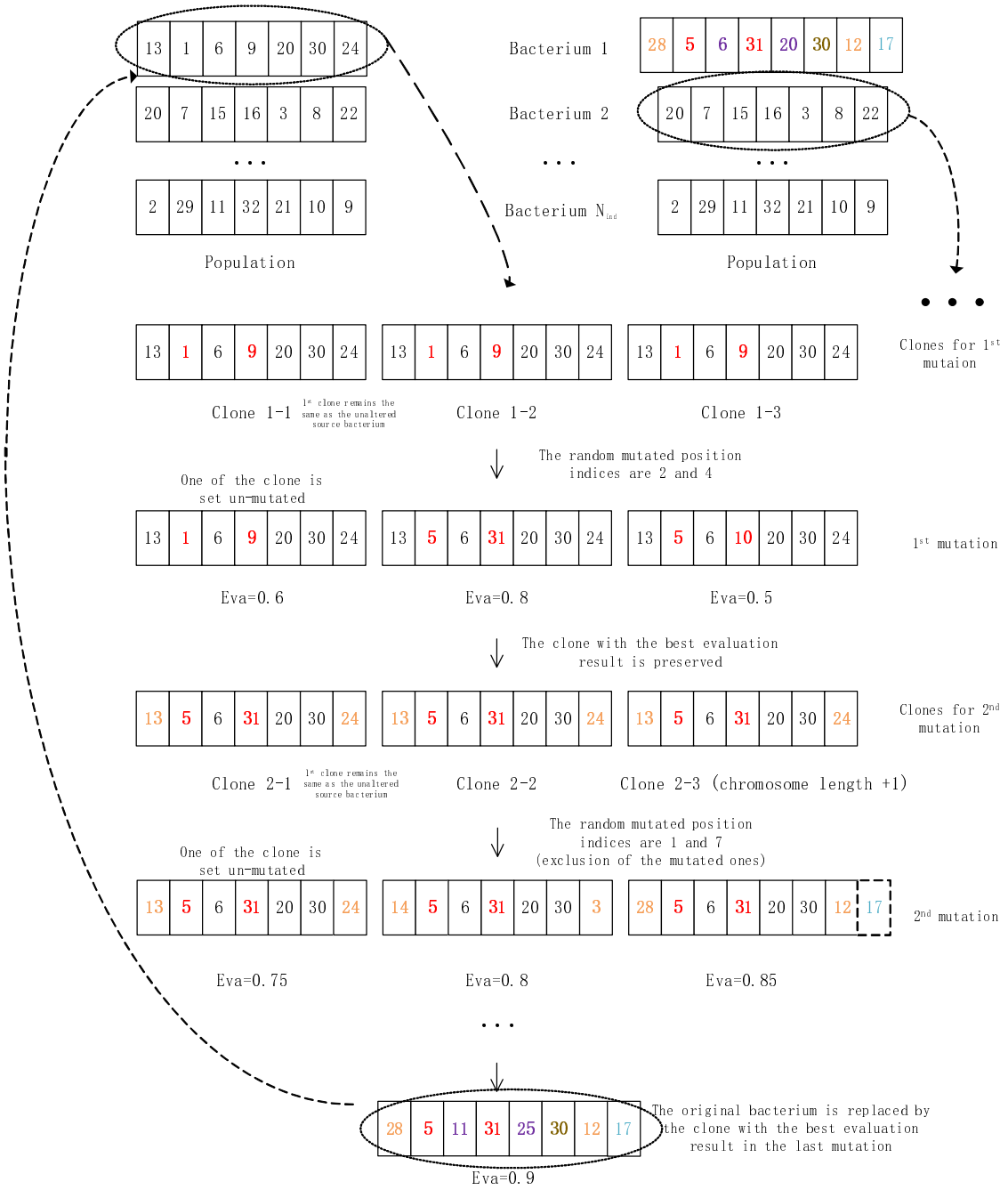

Fig. 4.5 Mutation operation in BMA

search space is defined in alignment with the consistent choice of channels, feature types and additional attributes like window lengths for segmentation to narrow down the search range. The local search space needs to be carefully determined to balance the acceleration of the convergence rate and the avoidance of the local optimum.

In our case, the priori knowledge is the physiological manifestation influencing the exerted sEMG signals and the anatomical deformation of the forearm muscles for certain hand motions. For each feature in the searching space, its index possesses the properties of the sEMG acquisition site and the extraction strategy. As a result, the local search space is naturally defined with either fixed channel or fixed extraction domain. Depending on the design of signal acquisition system, which is either muscle targeted or untargeted, two different views can be generalised in the local search protocol. For a fixed channel in untargeted sEMG capturing system, only features extracted from the same signal source can be viewed as the candidates for a certain operation of local search. It is intuitive that certain hand gestures only involve the contraction of certain muscles, and it is more reasonable to compare the information acquired from the corresponding detection sites. While the muscle untargeted detection normally covers an overlapped area with muscle synergies, a muscle targeted detection only gathers the sEMG signals from certain muscles with negligible influence by others. In this situation, the candidate group of channels will be enlarged by those who are related to the same motions. For a fixed domain only the features computed in the same scheme like TD, AR or others are included for the selection because of their own characteristics to facilitate different physiological conditions. As indicated in previous research, spectral features are good indicators for muscle fatigue and the entropy based indices perform robustly under circumstances where small contraction and noise are included [34]. Besides, additional attributes of the feature extraction are considered including segmentation length and overlapping increment, which contribute to a more detailed exploitation of the sub-segments. In the end of each local search, the chromosome is either preserved or replaced by the alternative with the best evaluation performance in its predefined neighbourhood.

Transfer

Mutation and local search are followed by the operation of transfer, which allows the exchange of information between two bacteria and contributes to incorporating new features from a better chromosome for performance improvement. The goal of the mutation and local search operations is to explore the unknown searching space and bring in unseen and beneficial information while transfer operation aims to preserve the incorporated features instead of introducing new ones by passing them to multiple bacteria within the existing population.

First the population is divided into two sorted halves including a superior set and an inferior set according to their evaluation results. Then one bacterium is randomly selected from both superior and inferior halves as the transfer candidates. A group of segments with a predefined length of l_{gt} from the source bacterium are assigned to the targeting bacterium in

a point-wise matching scheme. This process mimics the infection process of the bacteria and will repeat N_{inf} times in each generation. During the transfer operation, the chromosome length is also modified at a fixed probability, yet implemented in a different way from the mutation operation. The difference between the two modifications lies on the concept that transfer operation only preserves the existing information without incorporating unseen features. To preserve the improvement of the target bacterium, the updated population will be divided again according to another evaluation after each transfer. The transfer process with the length change involved is shown in Fig. 4.6, where $l_{gt} = 1$, $l_{cl} = 1$ and the chromosome length remains the same.

The BMA parameter settings are investigated with various combinations of lengths and probabilities. Specifically, the simplified comparison of convergence rate and the recognition accuracy for feature selection process of the the same subject with two different parameter settings are depicted in Fig. 4.7. The conventional TDAR features from 16 channels are considered as a pooled set of 128-dimensional candidates. It can be seen that the evaluation has reached a quasi-optimal performance with around the 10 generations of evolution and searching in both settings. No obvious differences in convergence rate or accuracy are witnessed in the comparison, which indicates that the application of BMA in this specific sEMG based feature selection is not sensitive to the parameter settings.

4.2.2 Computational Cost Reduction Targeted Feature Selection

In the test of computational cost reduction targeted feature selection, the aim is to find a subset of features whose number is reduced by more than half of the original feature vector while preserving a compromised yet acceptable inter-day hand motion recognition performance. In the experiments the transient phase between two motions is excluded and the feature selection of solely stationary signals during hand motion conduction is carried out. An overlapped windowing strategy is adopted to segment the sEMG signal stream with a window length of 250 ms and an increment of 50 ms to meet the real-time requirement despite its nature as an offline validation. The classic TDAR features with 4-th order AR from 16 low-density distributed channels contribute to the total 128-dimensional feature candidates for selection and are all tested under the classification approach of LDA. The results achieved by LDA in combination with the original TDAR set and PCA for the dimensionality reduction are used as the baseline for comparison.

A detailed enumeration of 5 candidate bacteria for a single subject who is experienced in the myoelectric prosthetic control in a random trial after the entire evolutionary process is shown in the Table 4.1. It should be noted that the average evaluation result for all bacteria including the omitted ones is $97.09 \pm 0.60\%$ that almost every individual would perform

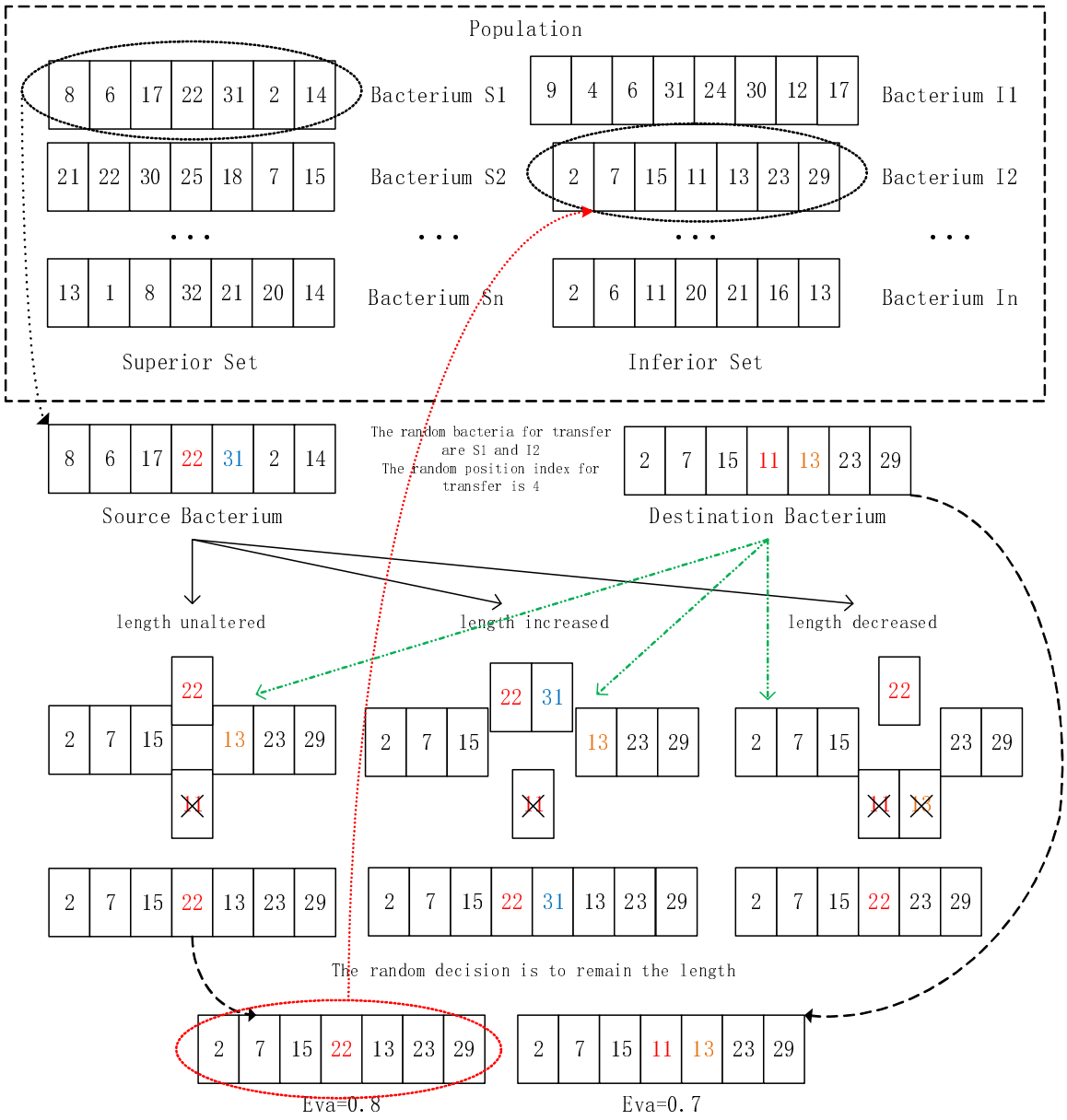

Fig. 4.6 Transfer operation in BMA

comparable results to each other without a large variation. It can be inferred that redundancy exists among the candidate features to be exploited. In other words, it is practical to extract a small number of feature candidates instead of the fully pooled combination of all channels and feature types to meet the real-time requirement without much compromise in recognition accuracy in clinical application. Besides, a denser stream can be formed in combination with the postprocessing techniques like majority vote to obtain an improved performance. Specifically, the two selected subsets with a similar size of 25 features lead to different

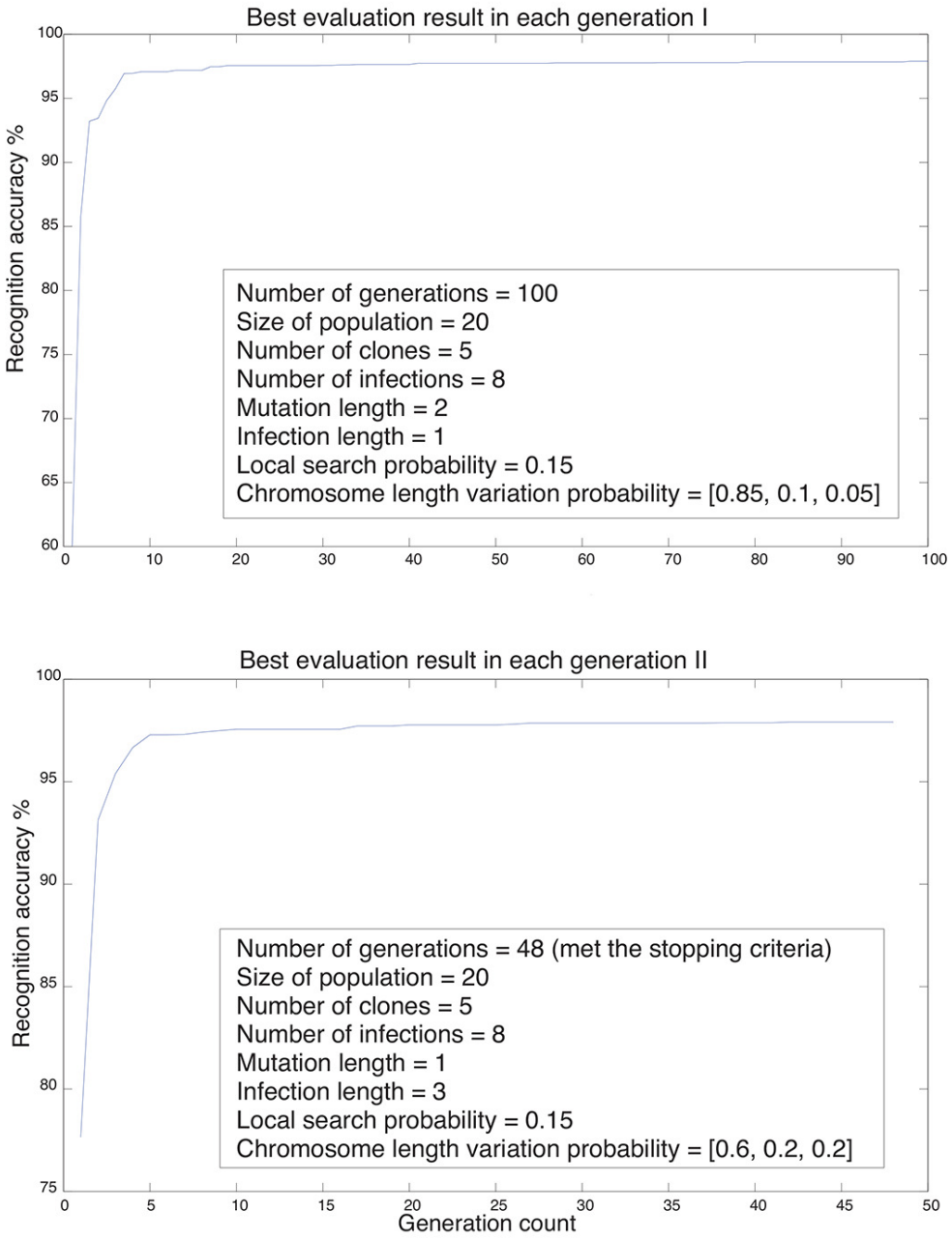

Fig. 4.7 Convergence sensitivity to parameters of the BMA

recognition accuracies of 97.52% and 96.28% respectively, which indicates that the same computational cost leads to a difference of more than 1% on the recognition result. What's more, the feature subset with a total number of 25 achieves a higher recognition accuracy than the one with 32 features included. The same fact is also validated by the comparison between the 23 features and the 25 features. It can be concluded that the a larger number

of features do not necessarily contribute to a better performance, which in turn provides the significance of offline feature selection prior to the online feature extraction. It is worth noting that the experiment is conducted within the selection of TDAR features with an original dimensionality of 128. There are a plenty of feature extraction strategies in TD, FD and TFD domains, whose diversity could be more than the 50 feature types examined in [34]. Thus the preliminary results in this section will be even more useful when applied in a larger pooled feature set.

Table 4.1 Selected feature subset examples for feature reduction for a single subject in a random trial

Indices of selected features	**Number**	**Evaluation accuracy** %
3 6 10 13 18 20 25 26 37 44 53 58 59 63 71 72 83 91 92 96 110 112 122	23	97.04
5 10 13 18 20 22 25 33 41 44 45 49 56 57 63 66 76 82 84 91 92 96 113 122 123	25	97.52
1 2 11 13 18 20 22 26 30 37 44 53 58 63 71 76 83 92 96 99 110 118 122 123 128	25	96.28
5 6 8 11 13 15 16 17 18 19 20 22 24 26 27 29 43 44 53 56 58 76 82 84 91 92 97 101 105 119 121 123	32	97.10
5 6 10 11 13 16 17 19 20 22 25 27 29 31 33 34 35 41 44 45 49 52 55 58 63 65 76 82 84 87 88 91 92 103 104 111 113 122 123 124 128	41	97.90

The experiments for inter-day hand motion recognition are conducted in comparison with PCA based dimensionality reduction, with the results shown in Fig. 4.8. In BMA based feature selection, the first 2 days' labelled data are utilised in the feature selection stage to generate the feature subset. The LDA classifier is later trained by the labelled selected features extracted from the sEMG signals solely on the first day and adopted for the inter-day application on the rest days' data in an offline scheme. The PCA based solution calculates the projection matrix on the first two days' data and tested on the same data with BMA based ones. The test on the fatigue data captured from one of our subjects follows a similar routine but in an inter-trial scheme instead of the inter-day way. Between adjacent trials, the subject

exhausts his forearm strength with multiple rounds of muscle contraction as much as possible to cause muscle fatigue, which would be another critical issue to impede the recognition accuracy in long-term use. It can be seen that the BMA based method leads to an increase of near 1% in the error rate for inter-day experiments, which is acceptable when compared to the computational reduction in the number of extracted features shown in Table 4.2, which would largely reduce the burden of online computation. A further reduction of feature dimensionality is expected because only a limited set of 128 feature candidates are adopted in the experiments. However, the results already reveal the efficiency of the feature selection approaches. Taking into account the fatigue test, the reduced extracted features through BMA even outperforms the whole feature set PCA based method in both computation cost and average accuracy, shown as the last error bars in Fig. 4.8, despite the large degradation by both methods in this scenario. A plausible explanation for the improvement of recognition accuracy under fatigue test is that the occurrence of large variation in sEMG pattern by exhausted voluntary muscle contraction leads to the failure of some certain feature types in classifying the motions. As a result, the incorporation of the whole group of features inevitably hinders the classifier training as a result of overfitting against the failed features. And some selected features instead of the whole feature pool could be more robust to such sEMG inconsistency caused by muscle fatigue. However, because that there is only a single subject employed, it remains to be determined whether the assumption holds when a more reasonable group of subjects are involved under a dedicated experimental protocol. It has shown that the PCA based feature reduction outperforms the BMA based one with 1%, which is because of the additional information despite the potential redundancy and increased computational cost.

Table 4.2 Comparison of trade-off between feature dimensionality reduction and average accuracy

Subject	**Number of extracted features**		**Average accuracy %**	
No.	**BMA**	**PCA**	**BMA**	**PCA**
1	41	128	90.99	92.04
2	33	128	98.71	98.81
3	37	128	92.54	93.80
4 (fatigue)	30	128	63.87	62.97

Furthermore, the preliminary inter-subject test is conducted to investigate the feasibility of the transfer of feature selection results between different subjects. The best subset of candidate features from each subject is applied to the other two subjects in our experiment following the same training and testing paradigm. A comparable and even improved perfor-

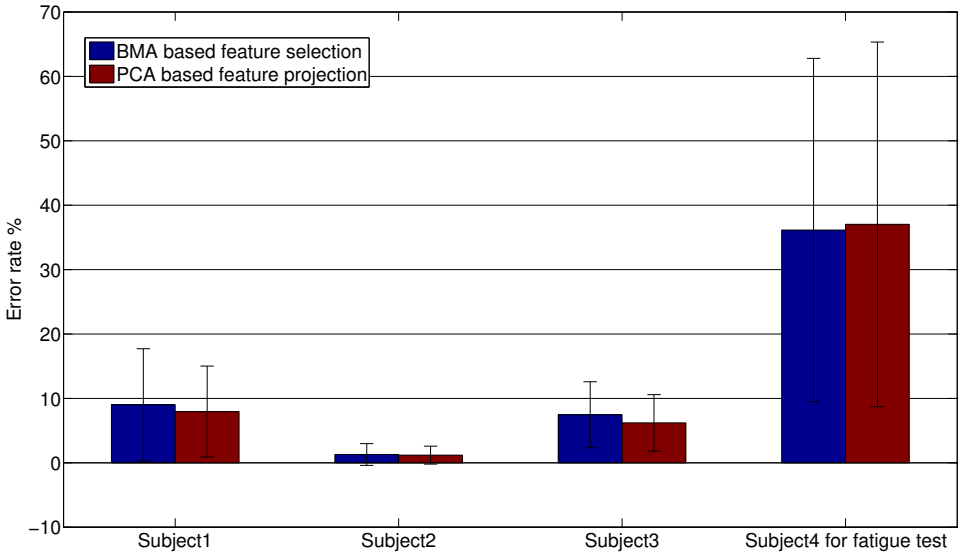

Fig. 4.8 Comparison of features selection results on 4 subjects

mance of the inter-subject feature set transfer could be seen in Fig. 4.9 utilising the feature subset selected from other subjects, which supports the incorporation of feature selection to form the optimal or quasi-optimal subsets for unseen users without extra offline selection burden on them.

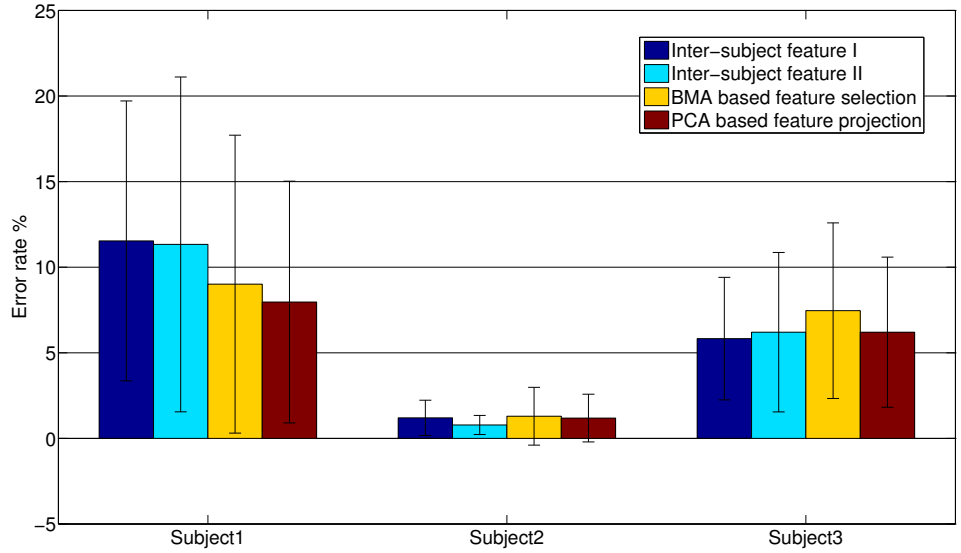

Fig. 4.9 Comparison of features selection results for inter-subject use

A further enumeration of corresponding channels of selected features is shown in Fig. 4.10. Here the statistics is based on the pooled subset selection of the whole population of the 2 subjects, where each of the bacteria has reached an acceptable evaluation result at a

largely reduced dimensionality. An approximately similar chance of selection for all the channels is observed, which implies that there is no preference towards specific channels in our scenarios. Apparently, the enumeration result confirms the necessity in adopting all the 16 detection sites, but with a limited features from each of them for achieving an acceptable recognition performance at a lower online computational cost.

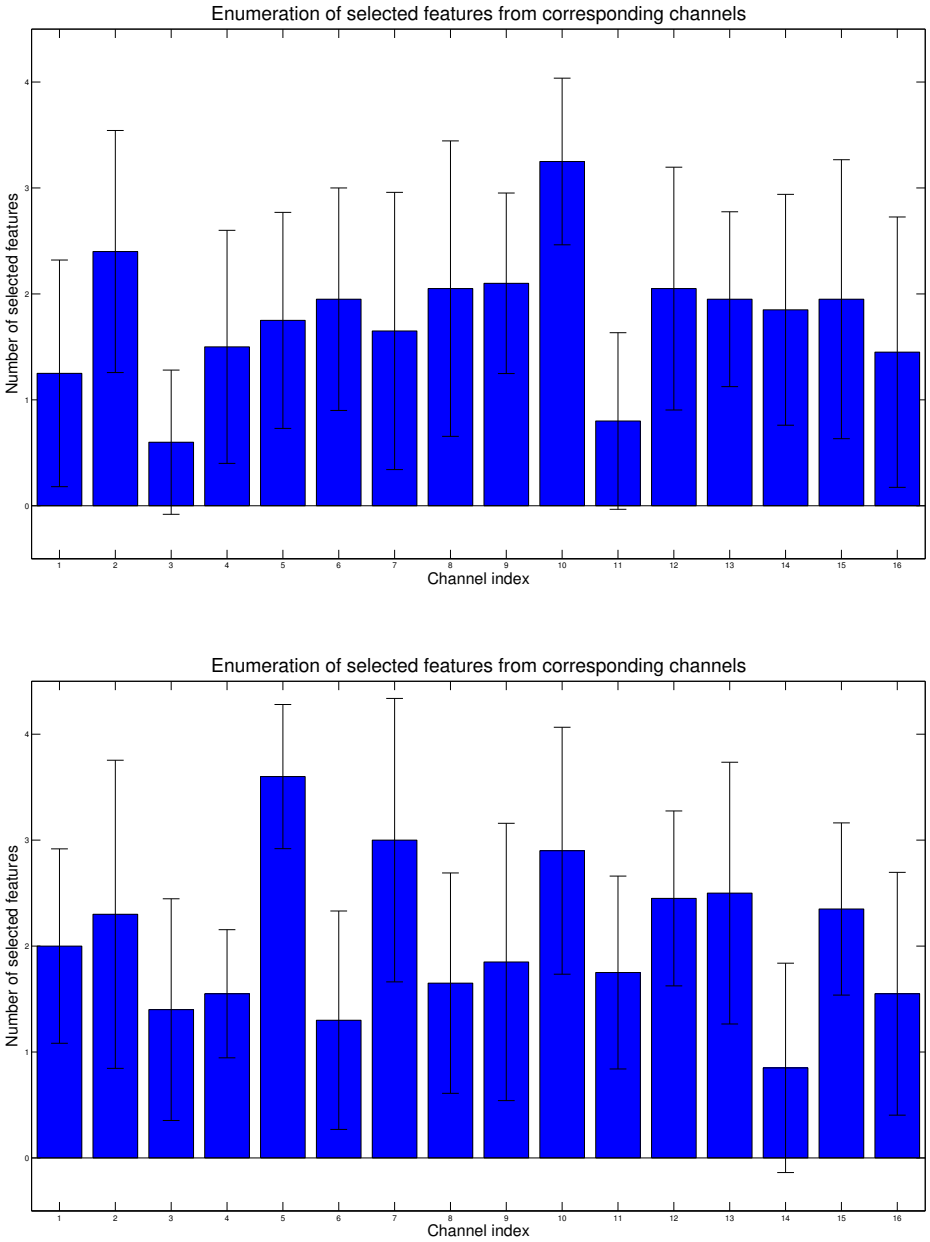

Fig. 4.10 Enumeration of selected channels after feature reduction

4.2.3 Recognition Accuracy Improvement Targeted Multi-length Windowed Feature Selection

Besides the computational cost reduction achieved by the offline feature selection, we further look into the possibility of improving recognition accuracy with the same techniques in this section. The importance of the data segmentation with various window lengths of sEMG stream is addressed by [121]. A longer segment of sEMG signals naturally contributes to a better recognition accuracy as illustrated in Section 2.2.2. However, the real-time constraint only allows a window length of less than the perceivable delay of 300 ms, where the existing research are solely conducted on the selection of a fixed segment lengths. And the research in extracting more knowledge within the fixed window length is commonly ignored. Despite proposing more feature extraction strategies, it is timely deriving deeper insights into the data segmentation itself. An intuitive idea is to further utilise the shorter sub-segments within each windowed sEMG segment. Within the current knowledge, no studies have yet investigated the feature subset selection with fused multiple window lengths. The subset selection that simultaneously concerns feature type, detecting site and window segmentation is still missing. In this thesis, the feature selection algorithm BMA is adopted for the multi-length windowed feature selection targeting at an improved sEMG based hand motion recognition in long-term use.

In our settings, the filtered stationary sEMG stream is first segmented by the windows of 250 ms with an overlap of 200 ms. Subsequently, all the segments of 250 ms are further segmented with the sub-length/overlap combinations of 200 ms/190 ms, 150 ms/130 ms and 100 ms/50 ms as multi-length candidate sub-windows. Based on the prior results, the difference of window lengths at 50ms is selected. The sub-windows are then concatenated and the feature extraction of TDAR is performed on every one of them. For each window and sub-window, a total of 128 dimensional features of 16 channels are extracted which leads to the final 2176 candidate features. Prior to the succeeding classification, the features extracted on the same group of data are routinely normalised. To exploit the most of a segment, the 128 features of the 250 ms window are kept as the basis while the selection is conducted among those sub-windows. The feature selection is carried out utilising BMA with the inter-day recognition accuracy as the fitness following the same routine in Section 4.2.2. Finally the features will be dimensionally reduced by PCA to collect the first 20 components as the input to LDA for classification. The convergence of the recognition accuracy with multiple subsets during the multi-length sub-windowed feature selection process is shown in Fig. 4.11. It can be seen that the ones with a quick convergence have an inferior performance compared to the others. Yet it is still worth noting that the improvement could happen at any iteration, which is formed on the nature of evolutionary algorithms in seeking for the

global optimum. Besides, the intrinsic randomness of such methods contributes to diverse recognition accuracies with a large variance of 2% at most, which confirms the necessity of conducting multiple trials of feature selection to gain the quasi-optimal subsets with an acceptable performance.

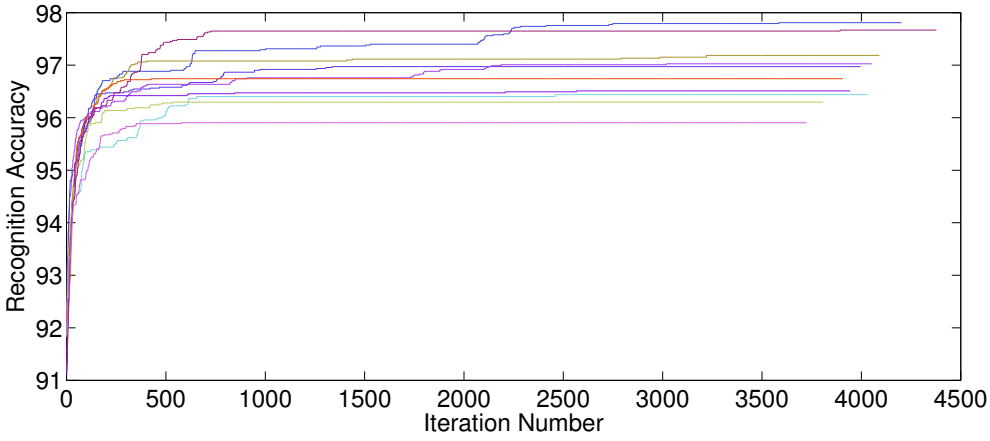

Fig. 4.11 Convergence for 10 trials of the BMA based multi-length sub-windowed feature selection process

The feasibility of multi-length sub-segmented feature selection is illustrated by the inter-day recognition performance respectively, on both testing and validating data from all three subjects in Fig. 4.12, and on the testing data only captured from the two subjects shown in terms of training on 1 day and testing on the rest days in Fig. 4.13. Specifically, 3 different optimised feature subsets are first selected from the 3 subjects respectively and then applied in the testing on each subject, in comparison with the same 128-dimensional TDAR features as shown from left to right in Fig. 4.12. It can be deducted that the selected feature subset can be utilised among distinct subjects, which in turn reduces the time consumption for potential inter-subject applications. A special case of using both training and validation is conducted on Subject 3 due to the subject's fully experienced capability of consistent sEMG signal exertion. The trend can be seen that the average errors decrease by adopting the selected features in comparison with solely using the single-length windowed ones. However, a discrepant case occurs for subject 2 when the data captured on day 2 is adopted for training and tested on the remaining days. It is also obvious that the inter-day hand motion recognition heavily depends on the selection of training data. For example, the data of day 2, 3, 6 from subject 1 and day 3 from subject 2 significantly outperform the rest when adopted for training the classifier in the same data acquisition scheme. Thus a further validation on an enlarged dataset of more recruited subjects and more fused trials in multiple days is needed to investigate the generalisation capability of the sEMG signals in future research.

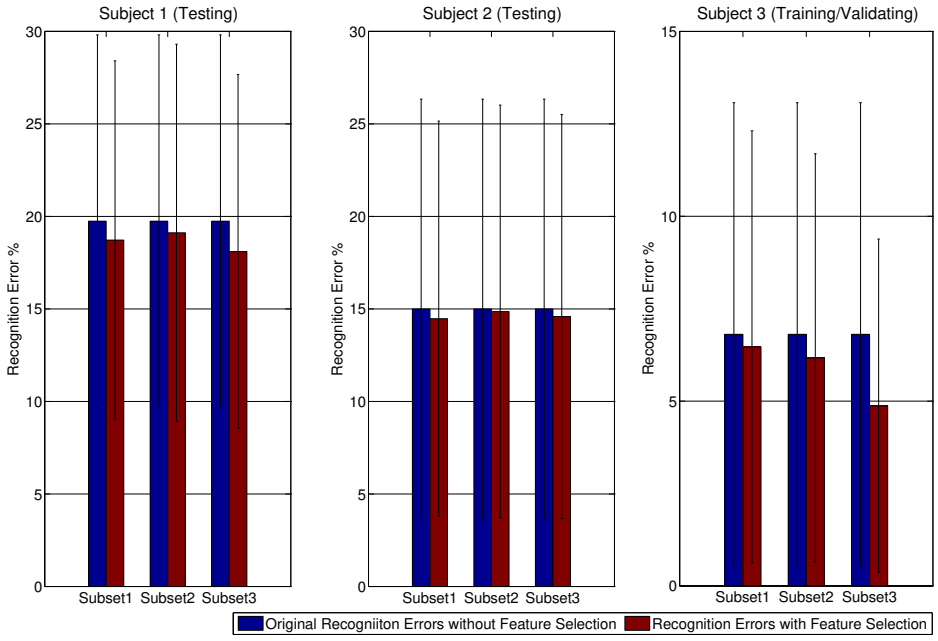

Fig. 4.12 Comparison of average recognition results on both testing and validating data with/without feature selection

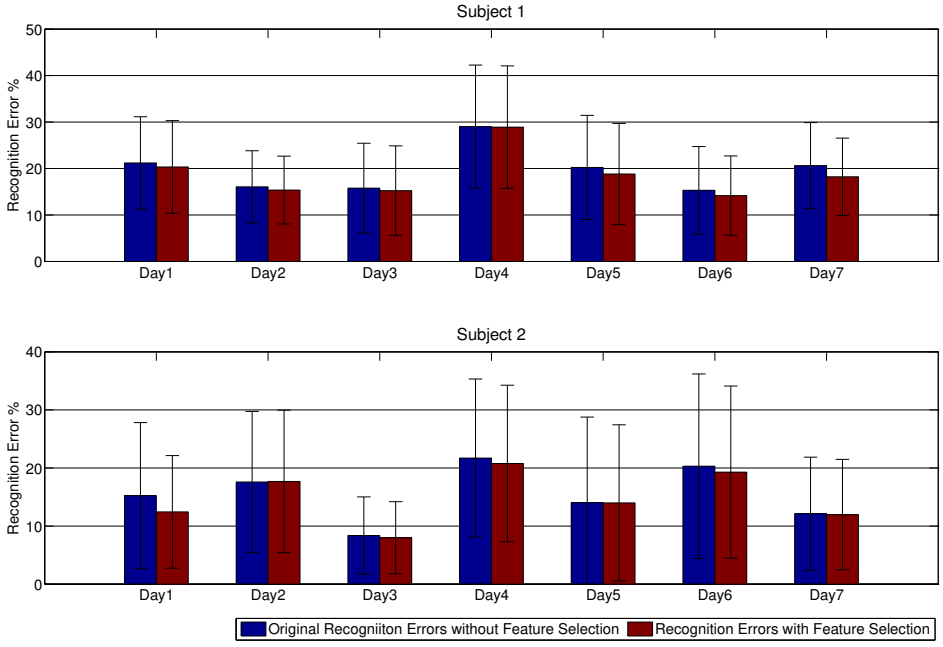

Fig. 4.13 Comparison of average recognition results with/without feature selection for inter-day use

The general enumeration of the selected channels, window lengths and feature types for the 3 subjects is demonstrated in Fig. 4.14 respectively and summarised in Table 4.3. An intuitive selection preference can be deducted by the results that windows with a longer segment length are more likely to be selected. The TD features especially the WL and SSC features and the first 2 components of the AR features are more favoured in the selection. The last 2 AR components are least preferred during the selection. The preference towards a larger segmentation is seen when using accuracy as the evaluation criteria, which coincides with the previous research [2] that an increased window length will provide features with less statistical variance and a better recognition accuracy. However, due to the restriction of processing time, a trade-off has to be considered between the time consumption and the classification accuracy. No explicit preference in the channel selection coincides with the findings in previous section, and is possibly attributed to the preconditions of keeping all features extracted from all channels with 250 ms, where the baseline of an acceptable recognition accuracy can be achieved.

Table 4.3 Enumeration of window lengths and feature types

Category	**Subject A**	**Subject B**	**Subject C**
Window length 200 ms	47	49	45
Window length 150 ms	26	46	38
Window length 100 ms	20	27	29
Feature WL	12	28	20
Feature MAV	9	12	14
Feature ZC	11	11	9
Feature SSC	18	19	28
Feature AR1	19	26	19
Feature AR2	13	13	13
Feature AR3	7	6	6
Feature AR4	4	7	3

A further detailed enumeration for each attribute of all the selected subsets for a single subject is depicted in Fig. 4.15, 4.16, and 4.17 as follows. Features of all the 16 channels are employed at a comparable chance without a significant preference towards a single channel. But it can be seen that there exists an observable difference between the two halves of the detecting sites. A possible explanation to this result is that the split of the two halves of electrodes addresses different coverage of grouped muscles to monitor the muscle contraction of the anterior and posterior forearms respectively. In other words, more sensing data from the posterior compartments of forearm muscles is essential to an improved recognition of the 9 hand motions involved in the proposed evaluation. The enumeration of sub-window

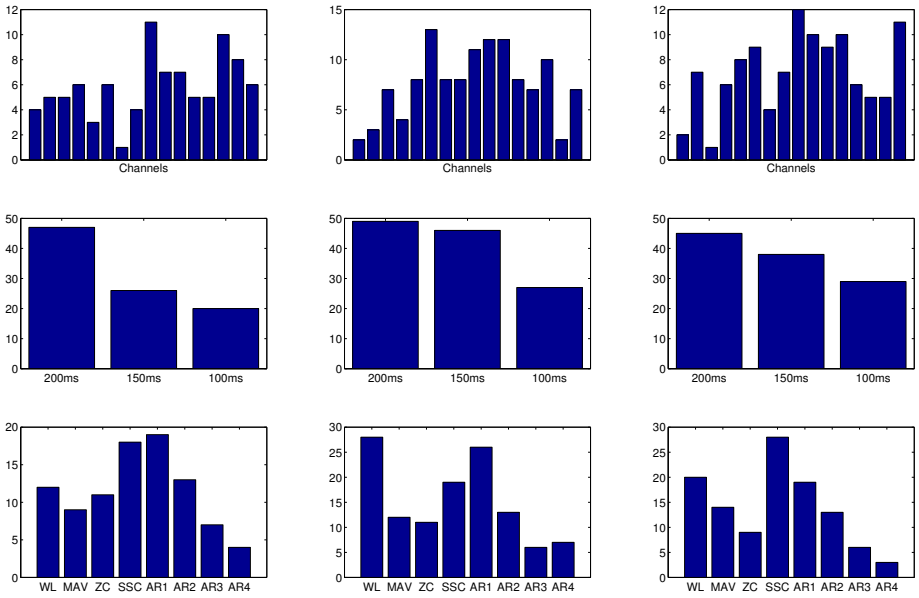

Fig. 4.14 Enumeration of the selected channels, window lengths and feature types for 3 subjects with the best performance

lengths favours the adoption of all sizes of sub-windowed segments and those with longer segments are more selected than the others, which is in alignment with the optimal subsets of the 3 subjects. All the 8 feature types are necessary for the inter-day hand motion recognition as depicted by the enumeration despite the slight more adoption of WL and SSC out of TD features, and the first 2-order coefficients out of AR features. In summary, the attributes comprising but not limited to window length, feature type and detection site are all essential to be taken into consideration for the sEMG based inter-day hand motion recognition instead of utilising the pooled features without a pre-selection.

4.3 Summary

In this chapter, sEMG features are investigated from both perspectives of extraction and selection. Better exploitation of existing feature candidates is achieved through merging the features and taking advantages of both the consistency of non-handcrafted feature distribution across multiple days and the priori knowledge driven distinguishability of handcrafted features. Specifically, in this chapter, the human knowledge based handcrafted feature extraction is utilising the famous Hudgins' TDAR features while the non-handcrafted features are shaped by the automatically learned features in the feature layer of the CNN prior to

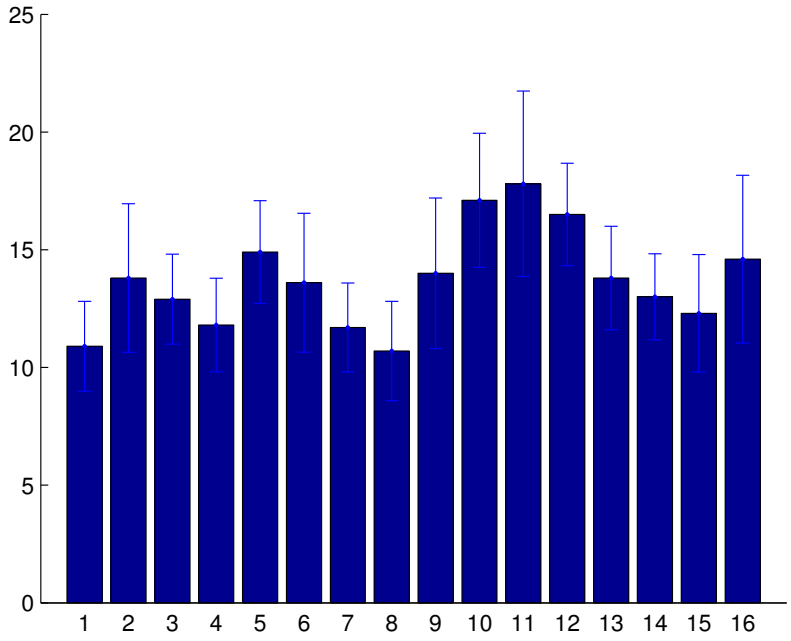

Fig. 4.15 Enumeration of selected channels for a single subject from 10 subsets

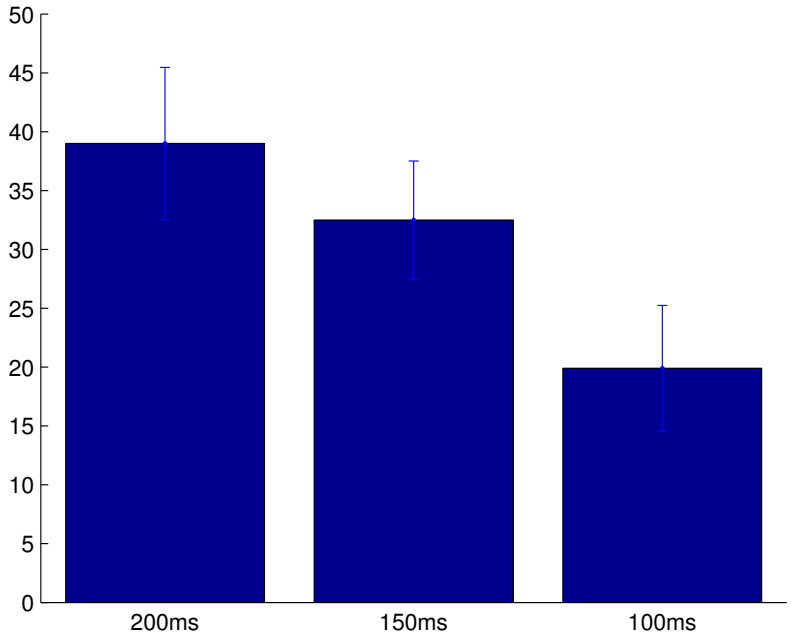

Fig. 4.16 Enumeration of selected sub-window lengths for a single subject from 10 subsets

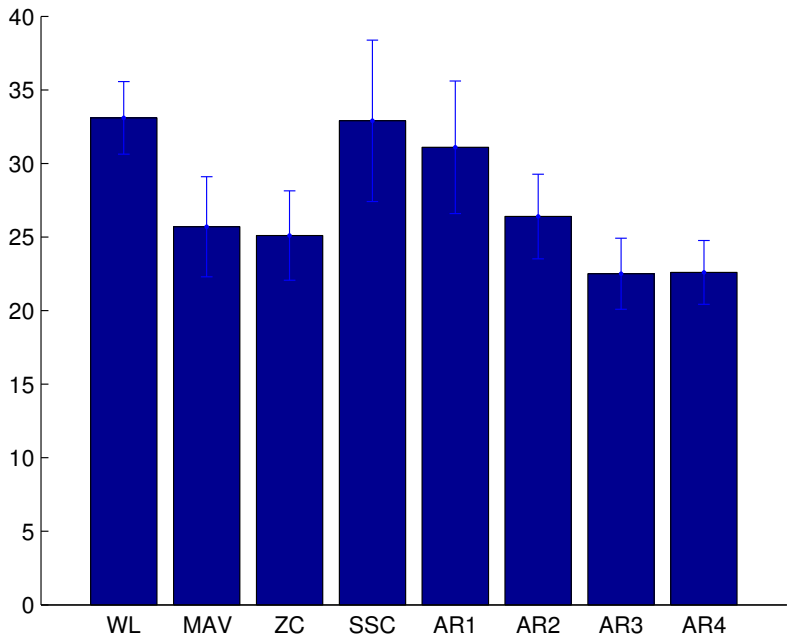

Fig. 4.17 Enumeration of selected feature types for a single subject from 10 subsets

the output layer. And a simple concatenation is performed to combine the TDAR and CNN features into single feature vectors and then the dimensional reduction is conducted on the resulted vectors. The combination of TDAR features and CNN features contributes to an improved inter-day hand motion recognition accuracy with either CNN or conventional classifiers like LDA and SVM. A novel multi-threshold based feature extraction strategy funcionting on the current TD features is also proposed to enrich the feature candidates, whose feasibility has been verified in inter-day experiments. The BMA is adopted for feature selection for its capability of simultaneous global and local search. In the case of sEMG based hand motion recognition, the region for local search is constrained by channel and feature relation. Thus the optimisation will be guided by implicit physiological information instead of a fully random exhaustion. The proposed feature selection is targeting at computational cost reduction and recognition accuracy improvement respectively. A comparable recognition accuracy is achieved with various TDAR feature subsets of which the feature vector length is less than a quarter of the original full set. The idea of combining TDAR features extracted with multi-length windowed sub-segments leads to an improved inter-day hand motion recognition by acquiring more information from the same segment. It is worth noting that a limited number of sEMG feature attributes like channel, feature type and window length are concerned in this thesis, yet to be enriched in later applications. Both proposed feature

selection and extraction methods can be applied to further enhance the existing approaches in long-term use.

Chapter 5

EMG Driven Multimodal Fusion Based Sensing and Analysis

Given the fact that sEMG hardly detects the deep muscle activity, related dexterous finger movements can not be properly distinguished by solely myoelectric sensing based solutions. Ultrasound imaging naturally allows the detection of deep muscle activity at a low level of voluntary contraction [182]. There have been attempts to utilise ultrasound [71] as an alternative modality for muscle activity sensing in assistive device control. The superior local information of targeted muscles permits an intuitive, simultaneous and proportional control of the involved DoFs, as reviewed in Section 2.1. And because of the inherent immunity to electrical crosstalk and interference, ultrasonic sensing forms a suitable fusion modality for the integration with current myoelectric sensing. With an emphasis on portability and the merits of ultrasound sensing, a wearable A-mode ultrasound acquisition device has been developed in [63]. Despite its significance as a cornerstone work for the wearable ultrasonic sensing based hand motion recognition, only naive template matching based recognition algorithms have been applied in the pattern analysis without an explicit feature extraction strategy. Further development of the recognition algorithms is required together with a proper sensory fusion scheme for sEMG and ultrasound. This chapter evaluates the feasibility of ultrasonic sensing based hand motion recognition and fused myoelectric and ultrasonic sensing based hand motion recognition for an amputee subject as a case study.

5.1 Ultrasonic Sensing Based Hand Motion Recognition

Ultrasound imaging allows the detection of morphological changes caused by muscle and tendon movement, which are directly related to corresponding motions. The evaluation of

multimodal sensing fusion relies on the success of the dexterous finger motion recognition of the incorporated ultrasound sensing. In this thesis, the evaluation of ultrasound sensing based hand motion recognition is first conducted on the conventional non-portable ultrasound sensing, and then on the 1-dimensional ultrasound signal captured by the A-mode ultrasound probes shown in Fig. 5.1 with a frequency at 20 MHz for sampling within each frame of the spatial resolution penetrating into muscle tissue at 3.86×10^{-3} cm. A flowchart of the 1-dimensional ultrasound signal processing adopted in our work is shown in Fig. 5.2. The ultrasonic echo signals are first preprocessed by multiple steps including time gain compensation, Gaussian filtering, Hilbert transform and log compression. The preprocessing aims to remove the noise and provide the analytic representation of the morphological changes during muscle contraction based on ultrasonic sensing. The preprocessed ultrasound signals are subsequently segmented with disjoint windows at a length of 15 samples. The features are then extracted by concatenating the two linear fitting coefficients (LFC) of the waveform within each segment. Thus for each frame, a total of 392 features are extracted from the 4 channels with 49 pairs of LFC1 and LFC2 coefficients for each channel. The LFC features reflect the approximation of the ultrasonic waveform and morphological changes during muscle contraction, which is solely determined by the hand motions and exerted forces. A more intuitive understanding of an A-model ultrasound sample frame and the corresponding signal processing is illustrated in Fig. 5.3. And the feature vectors are finally fed to the classifiers for hand motion recognition.

The feasibility study of intra-session recognition on wearable ultrasonic sensing based hand motion recognition has been first conducted in our preliminary work in comparison with the sEMG sensing based solutions. The comparison is carried out among 8 able-bodied subjects with 14 different finger motions using ultrasound and sEMG respectively. The results in Fig. 5.4 indicate that the ultrasonic sensing provides a better consistency of hand motion patterns in intra-session scenarios than the myoelectric sensing among all the involved subjects. It reflects that the pattern of ultrasound signal within a trial under no probe shift is consistent, which is attributed to the consistent muscular deformation. On the contrary, intrinsic randomness resides in sEMG signals, and the feature extraction with priori knowledge is normally considered as a practical tool to alleviate the interference of randomness. Besides, the force variation exists to a large extent when subjects try to maintain the same motion in the signal capturing process. The morphological changes of muscles viewed by ultrasonic sensing is more related to the posture of each joint rather than the isometric contraction force. As a result, ultrasound sensing contributes to a promising recognition result under various force exertion, which intuitively complies with the recognition under varying finger force in [92].

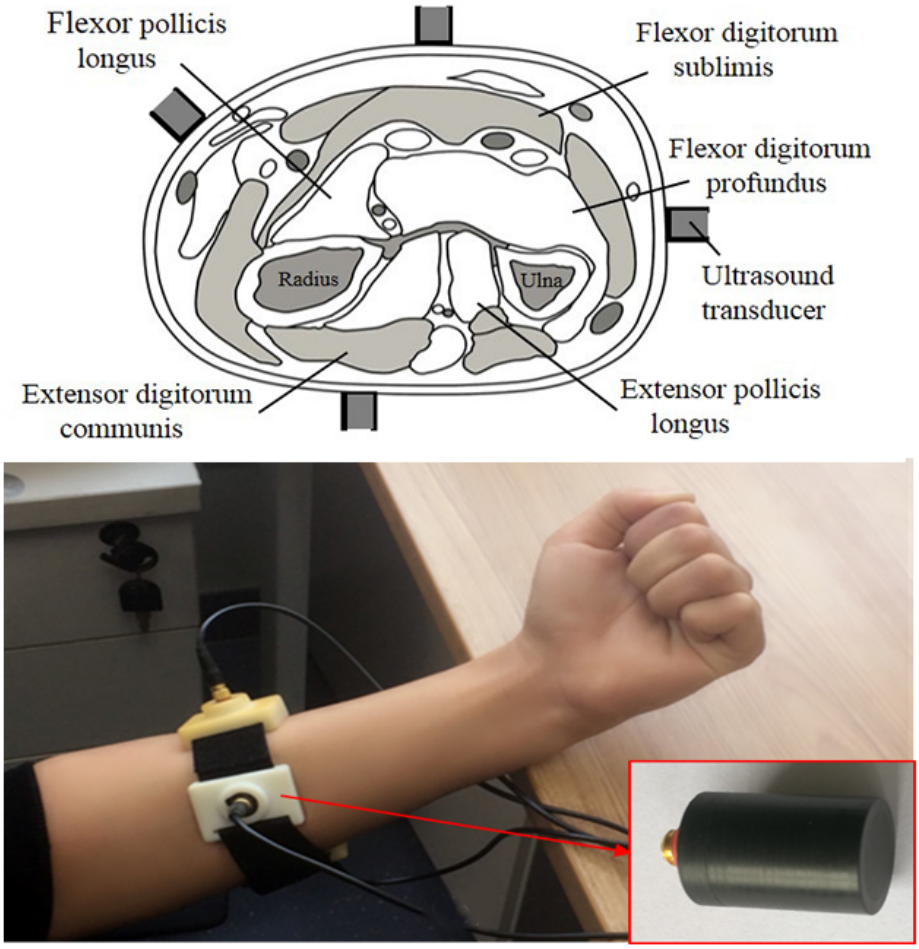

Fig. 5.1 Distribution of adopted A-mode ultrasound detection probes over forearm muscles

However, it is worth noting that the shift of ultrasound detection probe is not considered in the comparison while the shift between the ultrasound probe and the targeted skin surface significantly degrades the performance of the hand motion recognition. The degradation is mainly attributed to the nature of A-mode ultrasound that the detection is limited to a single dot of the muscle. A slight shift of the probe would lead to the extraction of muscular deformation of a totally different set of muscle fibres. Though electrode shift remains a hindrance for myoelectric sensing as well, it suffers less as shown in the comparison depicted in Fig. 5.5. The intra-session test is conducted on the data captured within a session where no donning/doffing of the wearable sensing device occurs and only inappreciable limb movement happens. In the intra-session test, the ultrasound based solution achieves approximately fully accurate recognition of the hand motions while a significantly inferior performance is seen for the sEMG based solution. The inter-session tests incorporate the factor of donning/doffing

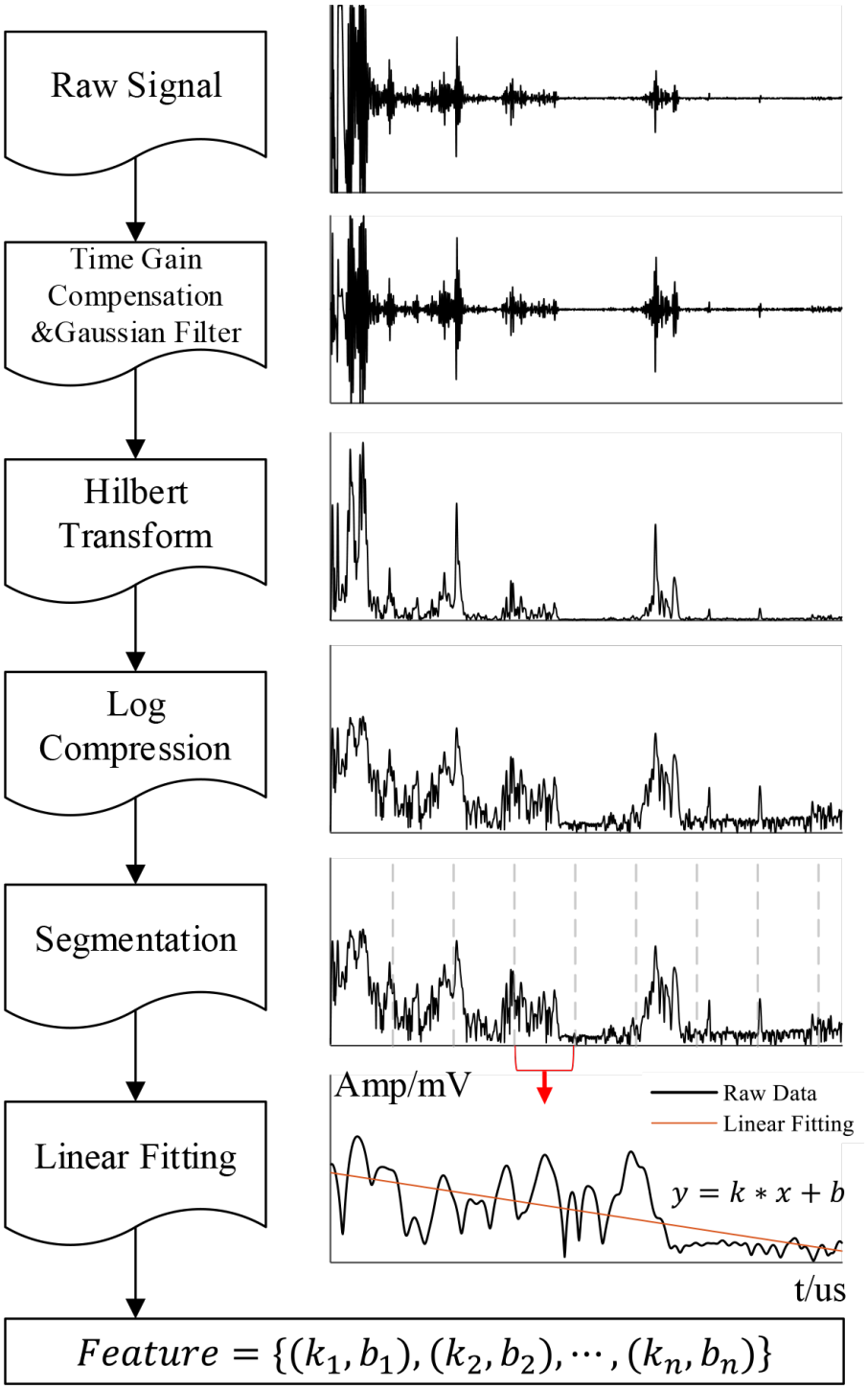

Fig. 5.2 Flowchart of preprocessing and feature extraction of the A-mode ultrasound signal

between two groups of trials including the training and testing sets. An opposite result is seen that the performance of ultrasound based solution deteriorates by a large extent of more than

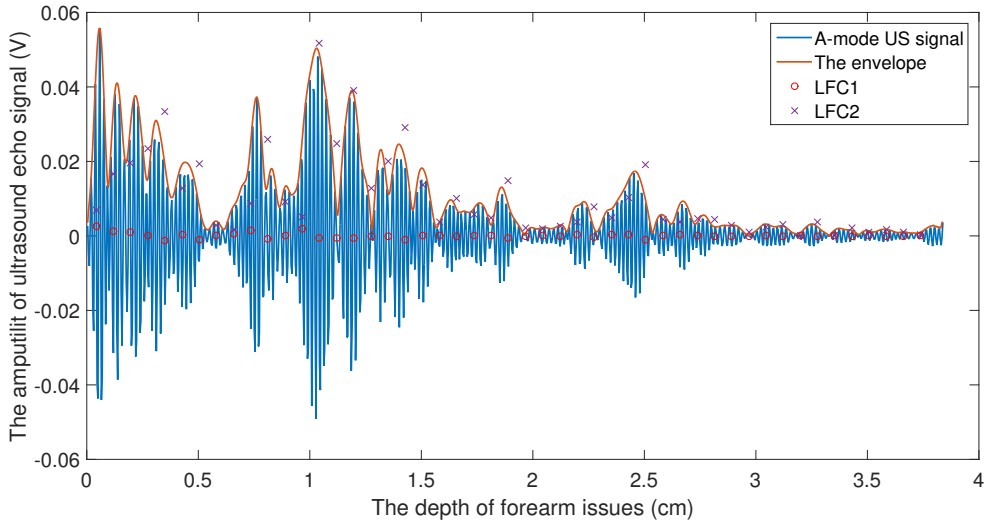

Fig. 5.3 A sample frame of the 1-dimensional ultrasound signal

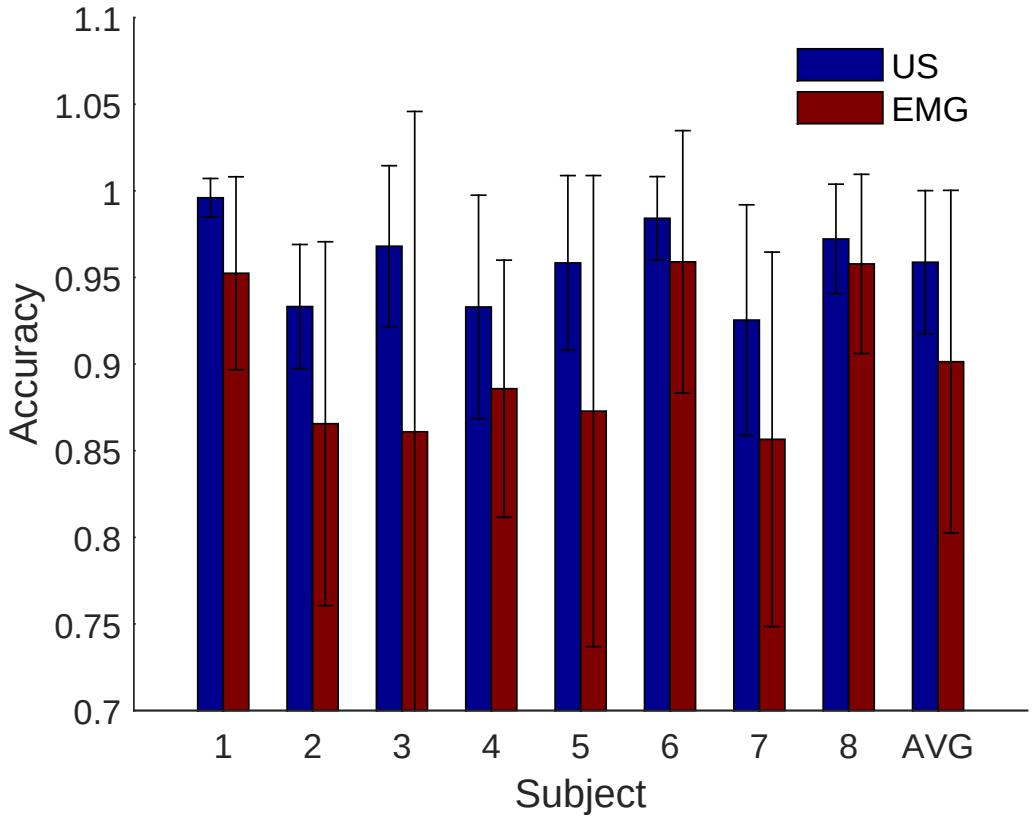

Fig. 5.4 Comparison of intra-day hand motion recognition accuracy between using SMG and sEMG

60%, worse than the sEMG based one. This phenomenon is mainly because of the intrinsic property of sEMG as the electrical manifestation comprising the weighted contributions mainly from a group of superficial muscles covering a large area, which is less affected by the shift of detection sites in comparison with the single dot targeted A-mode ultrasound. A specific case that can explain the mentioned phenomenon is the motion of hand rest. During hand rest, sEMG signals captured from all channels remain approximately zero magnitude regardless of the electrode shift. On the contrary, the difference of morphological changes is less obvious when compared to the myoelectric patterns.

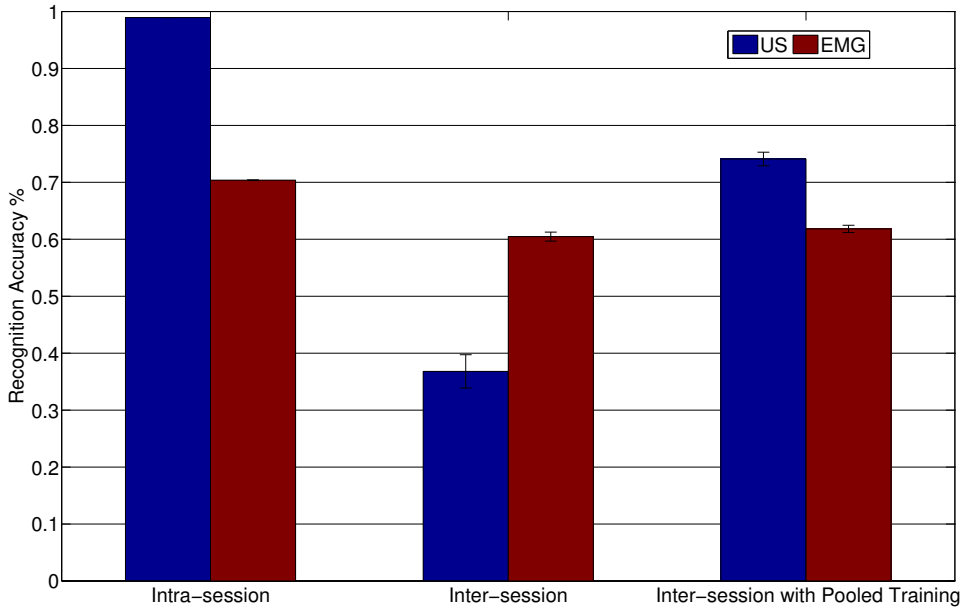

Fig. 5.5 Comparison of intra-session and inter-session recognition reflecting the performance under shift of detection sites

Besides the solely recognition accuracy based offline evaluation, the online performance is also investigated with 4 commonly adopted metrics in EMG sensing based online performance evaluation including motion selection time, motion completion time, motion completion rate and real-time accuracy as referred to in Table 5.1. Motion selection time is the description of recognition system responsiveness reflected by time interval between the motion onset and the first right prediction of the target motion. The selection time of 6 out of 8 subjects remains lower than 300 ms while that for the other 2 subjects merely exceeds 300 ms indicating that the delay caused by motion recognition is not perceivable to users, which is crucial in an intuitive prosthetic control. Completion time is the descriptor of recognition system stability reflected by the total time consumption for 10 times correct recognition of

Table 5.1 Online performance evaluation of ultrasound based hand motion recognition

Metrics	S1	S2	S3	S4	S5	S6	S7	S8
Selection Time (s)	0.246	0.170	0.214	0.317	0.245	0.273	0.165	0.31
Completion Time (s)	1.233	1.087	1.286	1.407	1.243	1.240	1.097	1.256
Completion Rate	0.933	0.983	0.933	0.867	1	0.983	1	0.933
Accuracy	0.899	0.984	0.900	0.856	0.894	0.927	0.987	0.926

the current motion type. A completion rate measures the usability of the recognition system and is defined as the rate of completed motions within 5 seconds, where a completion is regarded as 10 correct predictions of the same motion in 5 seconds. The real-time recognition accuracy is defined as the average classification accuracy from the first correct prediction to the end of the motion conduction. It can be seen that the online performance evaluation results are promising and consistent across the subjects involved, which in turn supports the clinical usability of the ultrasonic sensing based hand motion recognition.

5.2 Multimodal Sensing Based Hand Motion Recognition

As stated in the Section 2.1.2, the fusion of sensing modalities is generally categorised into two approaches. One is the hierarchical approach utilising a dual-stage or multi-stage scheme, which first identifies the predefined hierarchy or indices using one single modality, and then recognises targeted hand motions through analysis of the rest modalities. The other approach simply extends the feature vectors of the original modality with additional features of the fused ones. Regarding our application of myoelectric and ultrasonic fusion, the pattern recognition based approach with merged features is utilised to exploit both the consistent patterns of ultrasound based morphological deformation from a unique dot of muscles and the robust detection of EMG over a covered area of muscle groups. The simplified fusion scheme that concatenate the features of both myoelectric and ultrasonic signals together is proved successful.

A customised multimodal detection site of 3 sEMG electrodes and 1 ultrasound probe shown in Fig. 5.6 is adopted in the proposed research. A case study of an amputated subject is specifically given here with 4 detection sites equipped to verify the feasibility of myoelectric and ultrasonic sensing fusion based hand motion recognition. Both myoelectric and ultrasonic features including TDAR and LFC features are extracted and concatenated to form the feature vector for classification for the multimodal fusion test while the single modality test is conducted under the LDA + TDAR and LDA + LFC respectively. Two different training strategies are followed to examine the suitable scenarios for fused sensing

based hand motion recognition. One of them is the leave-one-trial-out test, where all but one unseen trials are used for the training of the classifier while the unseen trial is left for testing. The leave-one-trial-out test is to examine the feasibility of the fusion scheme in application of totally unseen data caused by observable shift of detection sites. The recognition of unseen trials is a compromised evaluation of the inter-day recognition performance because of the limited involvement of the amputated subject in 1 day. The other one is the cross-validation based pooled training test, where samples of all the trials are grouped together and a randomly selected fold of the samples are used for training while the rest are for testing. A 10-fold validation and a 5-fold validation are both adopted with 10% and 20% of the data for testing respectively, and each of them is repeated for 10 times.

The recognition results of the multimodal sensing based and unimodal sensing based hand motion recognition on the amputee subject are shown in Fig. 5.7. It can be seen that the ultrasound based sensing exerts an inferior performance to EMG based sensing for recognition of the unseen data with shifted detection placement. When the shift of detection sites can be ignored, the ultrasound based sensing significantly improves the recognition accuracy in both unimodal and fused sensing schemes. A steady improvement is observed for the fusion based sensing than the unimodal ultrasound sensing, which suggests that the TDAR features of EMG signals could always provide complementary information to the ultrasonic manifestation. In other words, it is suggested that the ultrasound is used in combination with the EMG. Though we see that the fusion based sensing shows a slightly lower recognition accuracy than the unimodal EMG sensing for unseen scenarios, the deviation of the fused sensing based recognition accuracy indicates that the degradation varies among different trials. Thus it is essential to further enlarge the dataset to reach a more concrete conclusion. Above all, the myoelectric and ultrasonic fusion based sensing is strongly favoured by the pooled training strategy, which in turn forms the requirement of either the adequate user re-training or a better fixation of the detection sites.

Detailed confusion matrices regarding individual motion types for the unimodal myoelectric sensing, the unimodal ultrasonic sensing and the multimodal myoelectric and ultrasonic sensing based hand motion recognition results are given in Fig. 5.8, 5.9 and 5.10. It can be seen that the sEMG based recognition of M4 (Index Finger Point, seen in Fig. 3.2) is significantly worse than other motions. Pointing the index finger is naturally related to the extensor indicis that lies in the deep layer of forearm muscles. Due to the insufficient detection of deep muscle activity by sEMG, the unimodal recognition fails to reach comparable results as other motions. Another finding is that the combined sEMG and ultrasound steadily contributes to an improved recognition of all the individual motion types, which means the two modalities adopted are mutually complementary. Thus the fusion based sensing scheme

Fig. 5.6 Distribution of fused myoelectric and ultrasonic sensors over the residual limb

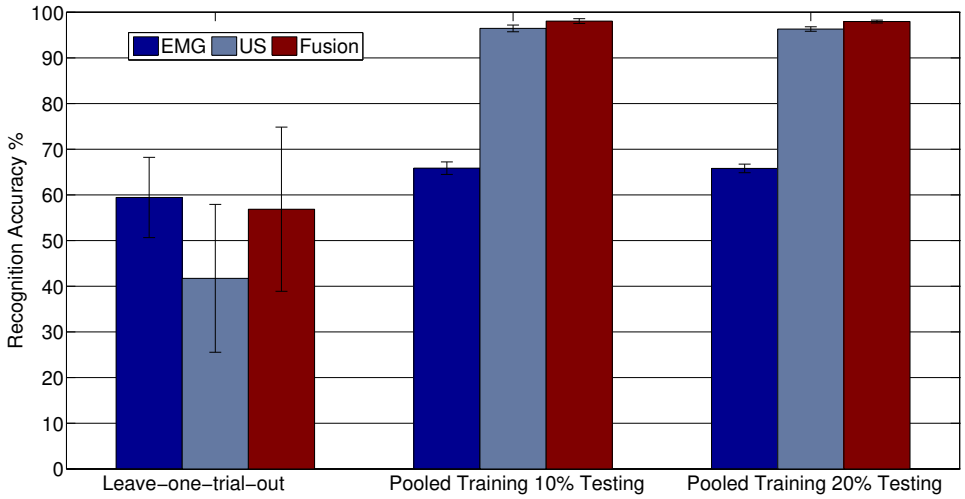

Fig. 5.7 Comparison of multimodal sensing based and unimodal sensing based hand motion recognition on an amputee subject

is favourably supported by the case study on our targeted limb-impaired group of users. Despite the promising overall recognition accuracy of unimodal ultrasonic sensing and fusion based sensing, it is worth noting that an obvious misclassification between M3 and M6 (Hand Closed and Wrist Flexion in Fig. 3.2) can be seen in both their confusion matrices. The two motions are quite different in the force exertion yet similar in a moving direction and the observable morphology. And the subject who has lost his own hand motor function for years will find the two motions similar in performing the imaginary movement of his phantom limb. It is intuitive that the finger gripping remains the medium for both motions following

the visual hint in Fig. 3.2. The amputee subject suffers from the loss of both wrist and hand, which in turn prevents his proprioception to continuously make an explicitly different control of muscles when a similar avenue of muscle contraction should be reached.

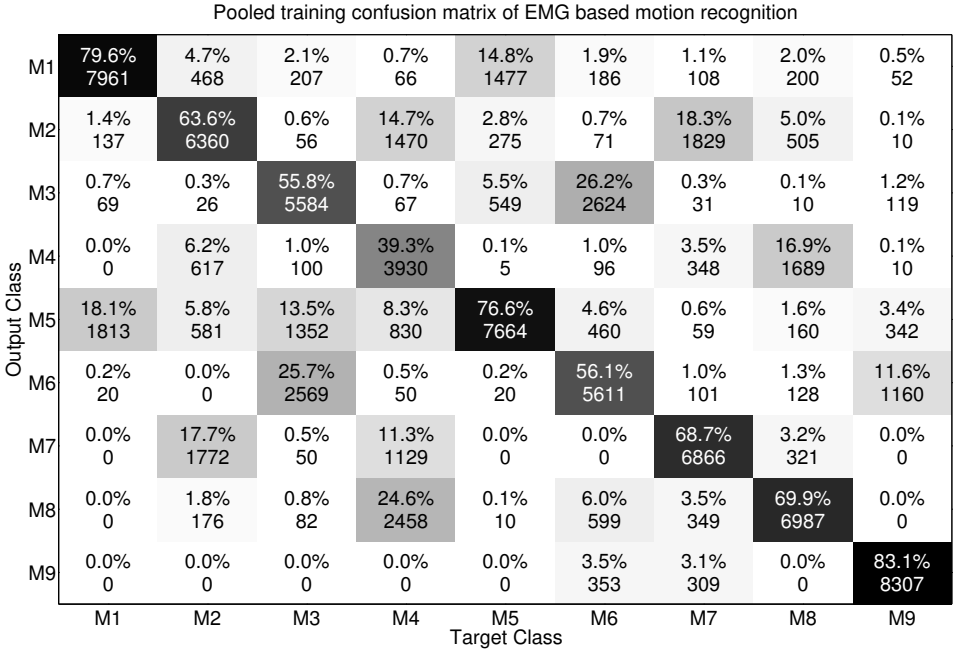

Fig. 5.8 Confusion matrix of EMG based hand motion recognition for an amputee subject using pooled training

5.3 Summary

In this chapter, the feasibility of wearable ultrasonic sensing based hand motion recognition as both single modality and part of multimodal fusion is explored respectively with a customised A-mode ultrasound capturing device. The ultrasonic sensing system is first introduced with corresponding signal preprocessing and feature extraction strategies. Both offline recognition accuracy and online performance metrics like motion selection time are used for its usability evaluation. The offline recognition accuracy describes the distinguishability of the adopted method on segmented stationary sEMG signals, which reflects the accurate recognition of individual action. The online metrics illustrate the accurate execution of activities instead of a single action and emphasise the time consumption of completion of certain tasks. The offline and online metrics demonstrate the effectiveness of the proposed sensing method in different scales. The significant improvement of intra-session motion recognition accuracy by using

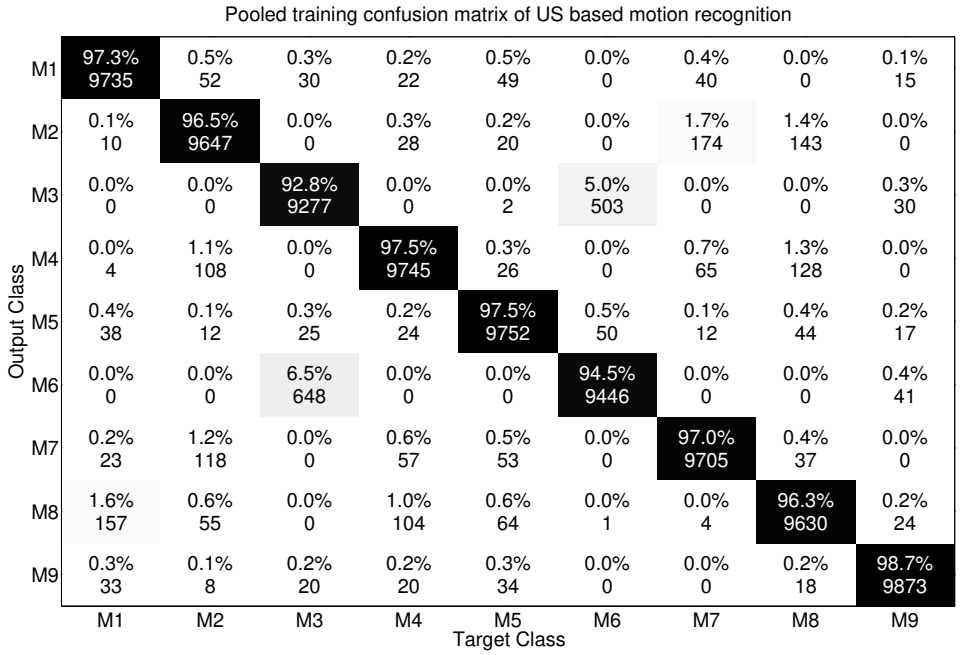

Fig. 5.9 Confusion matrix of ultrasound based hand motion recognition for an amputee subject using pooled training

ultrasound instead of sEMG is verified under the constraint without donning/doffing induced probe shift. And the drawback of wearable ultrasound is identified as the extreme sensitivity to probe shift in comparison with the sEMG based solutions. Following the verification of ultrasound's capability in dexterous hand motion recognition across able-bodied subjects, the ultrasonic sensing modality is further incorporated into the current singly myoelectric modality based muscle activity sensing and hand motion recognition. A pattern recognition framework is proposed to facilitate the multimodal sensing based solution. And the merits of myoelectric and ultrasonic fusion based hand motion recognition are validated with a case study on an amputated subject. The utilisation of both ultrasonic and myoelectric strengths including the detection of deep muscle activity, muscular morphological pattern consistency, robust electrical manifestation baseline under various changes contributes to the promising feasibility of sEMG driven hand motion recognition with only 4 incorporated electrode detection sites.

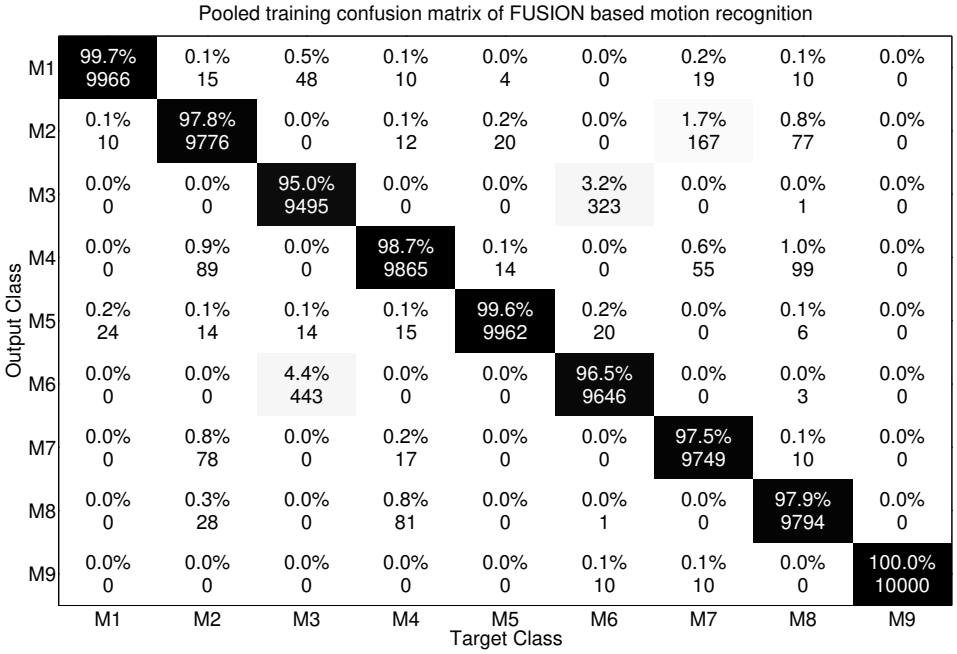

Fig. 5.10 Confusion matrix of myoelectric and ultrasonic fusion based hand motion recognition for an amputee subject using pooled training

Chapter 6

Long-term sEMG Database Building and Benchmark Evaluation

The research community of sEMG based hand motion recognition has seen a trending interest in benchmark building in recent years. Some well accepted dataset including Ninapro [155], CSL-HDEMG [156] and CapgMyo [149] have been published and made publicly available. However, despite the fact that Ninapro remains the most successful public dataset, it is not suitable for inter-day hand motion recognition in long-term use due to its inherent drawback that the database only consists of data captured in 1 single day for all the subjects involved. Similarly, the data are captured for only 5 days and 2 days respectively in CSL-HDEMG and CapgMyo, which reflect limited inter-day variation of sEMG signals in long-term use and lack the flexibility in the division of training and testing sets. Besides, the two datasets are solely made up of high-density sEMG signals while most commercial prosthetic devices are equipped with a low-density sEMG sensing module. Thus, it is timely and essential to build a suitable low-density sEMG database targeted for the evaluation of inter-day hand motion recognition algorithms in long-term use.

Irrespective of the long-term property within the adopted local data for verification of our proposed approaches in previous chapters, a publicly available self-contained benchmark requires the improvement in several aspects. The size of recruited subjects, the days accounted for a prolonged usage and the sufficiency of inexperienced user training protocol are potential for further improvement. This chapter aims to build a benchmark with the locally captured low-density sEMG data of hand motions across multiple days. The benchmark is proposed for the evaluation of sEMG based hand motion recognition algorithms in long-term use. In this chapter, the data acquisition paradigm is first described in details to provide an insight into the long-term settings. Specifically, the 16-channel sEMG data are captured from 10 subjects performing 13 hand motions in consecutive 10 days. Then the classic

pattern recognition and deep learning methods are applied for the preliminary analysis of the database, which form the potential baselines in terms of the hand motion recognition accuracy. The existing problems for long-term hand motion recognition are reflected by the benchmark and identified in alignment with priori knowledge in related publications.

6.1 Database Description

6.1.1 Acquisition Setup

A customised 16-channel sEMG capturing system as seen in Fig. 6.1 [22] is adopted for the forearm sEMG acquisition, with its detailed configuration given in Table 6.1. The 16 bi-polar electrodes are formed by sharing each electrode with two neighbouring channels, and embedded in a stretchable sleeve to cover both the anterior and posterior compartments of forearm muscles with an optimised zig layout. The acquisition system is equipped with a sampling frequency of 1000 Hz, a gain of 3000 and an ADC resolution of 12 bits. The captured sEMG signals are bandpass filtered between 20 Hz and 500 Hz by a Butterworth filter and separated from the power line noise with a notch filter. Another empty sleeve is used to cover the electrode sleeve to ensure a firm contact between the electrodes and the skin surface to alleviate movement artefacts. The digitalised sEMG signals are transmitted to a personal computer via USB connection for data recording and processing. A graphical user interface is designed to display the motion hints and corresponding 16-channel filtered sEMG signals.

Table 6.1 Configuration of sEMG acquisition setup

Property	**Configuration**
Channel	16 bi-polar electrodes
Electrode layout	Zig layout
Lower cutoff frequency	20 Hz
Upper cutoff frequency	500 Hz
Sampling rate	1000 Hz
Amplification gain	3000

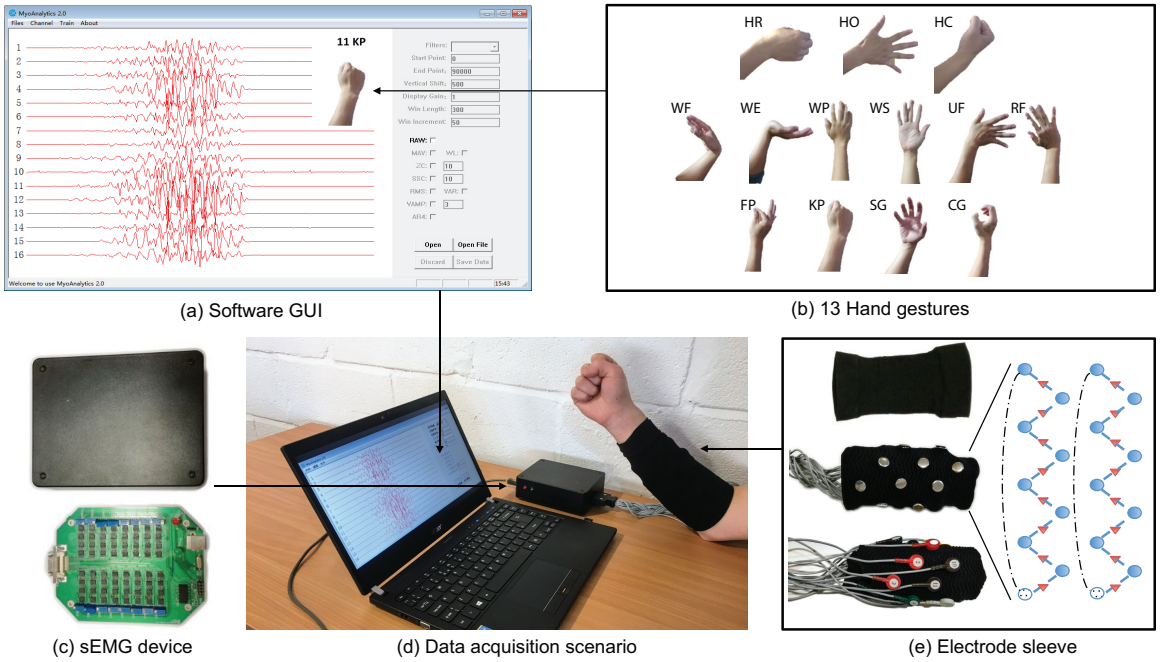

Fig. 6.1 The sEMG capturing system for database building

6.1.2 Experimental Protocol

Hand Motion Candidates

A total of 13 hand motion candidates are included in this database, comprising 3 basic palm movements of hand rest (HR), hand open (HO) and hand close (HC), 4 wrist movements of wrist flexion (WF), wrist extension (WE), ulnar flexion (UF) and radial flexion (RF), 2 forearm movements of pronation (PR) and supination (SU), and 4 basic grasp types of fine pinch (FP), key pinch (KP), spherical grasp (SG) and cylindrical grasp (CG), as depicted in Fig. 6.1. In comparison with the 9 motions in local data adopted in Fig. 3.2, 2 novel grasps of CG and SG and 2 wrist movements of UF and RF are incorporated.

Participants

A total of 10 able-bodied subjects (2 females and 8 males, ranging in age from 22 to 35 years) are recruited in the database building. The subjects are all with intact limb motor function and do no suffer from any neurological or muscular disorders. The subjects are all unfamiliar with the prosthetic control and sEMG based hand motion recognition. The data acquisition is approved by the ethics committee of University of Portsmouth with written informed consent obtained from all subjects.

User Training

The user training protocol proposed in our previous work is adopted to improve the consistency of sEMG patterns from users' voluntary hand motions prior to their participation in the on-site database building. It has been proved that the clustering-feedback user training interface shown in Fig. 6.2 contributes to a consistent online performance. The user training protocol encourages the subjects to adjust their muscle contraction and force control in each intra-day trial, which removes the adverse artefacts of voluntary contraction and confines the variation of sEMG signals to inter-day physiological changes.

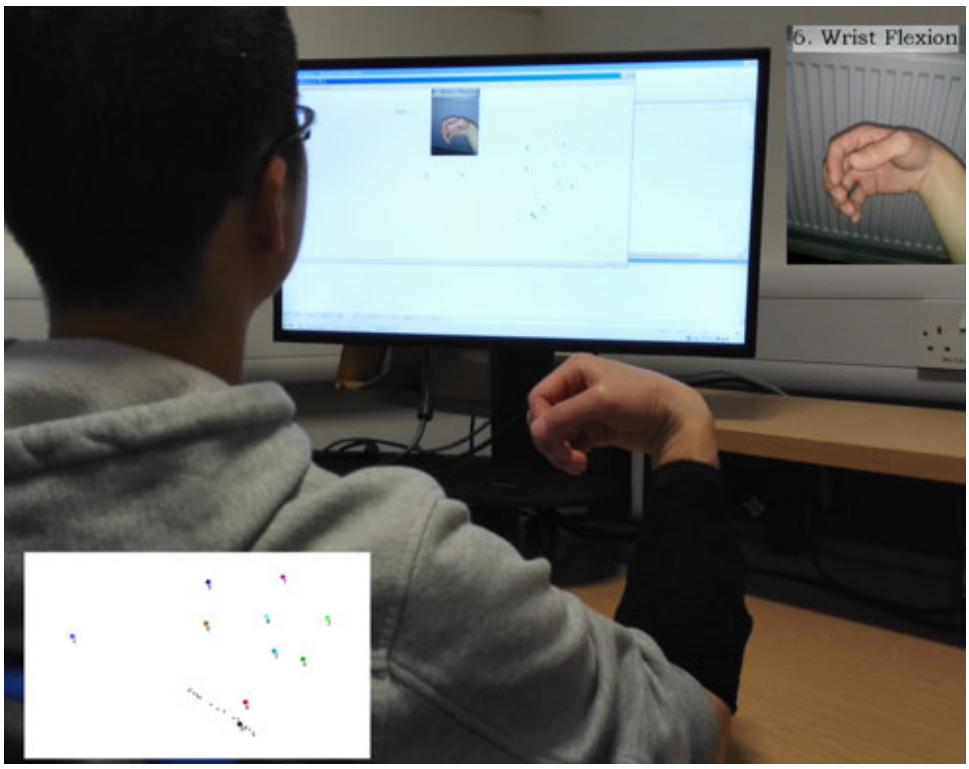

Fig. 6.2 Clustering-feedback user training interface

On-site Data Capturing

Prior to the on-site data capturing, the subjects are informed of a detailed participant information sheet and a demonstration to familiarise themselves with the experiment steps. The forearm skin of the subjects is cleansed before they wear the electrodes, following the routine in related studies [183]. Then the subjects are asked to wear the electrode embedded sleeve with a rough reference that the two ground electrodes are placed on the ventral side of the forearm and the sleeve is pulled right above the elbow. During the signal capturing stage, the

subjects are seated in a relaxed position with their forearms rest on the desk. The subjects are asked to follow the visual hints displayed on the monitor to conduct the hand motions out of the 13 candidates in a random order. For each day, 4 sessions are conducted to represent the intra-day scenario. Within each session, every motion candidate is conducted and maintained for 10 seconds with a relatively steady muscle contraction. A transition period of 5 seconds between two adjacent motions and a rest of 10 minutes between two adjacent sessions are arranged. The everyday donning/doffing, which leads to electrode shift, is considered not only in the inter-day sessions but also the intra-day sessions, where a donning/doffing of the sleeve is arranged each day between the two halves of all sessions. The sEMG capturing are repeated with the same steps in consecutive 10 days.

6.2 Benchmark Evaluation

As reflected in previous chapters, the long-term hand motion recognition accuracy heavily depends on the choice of combined classifiers and features. Both LDA + TDAR and CNN are adopted to produce the baseline of inter-day recognition in long-term use for future research. And the inter-subject performance baseline is achieved by utilising both CNN and CNN + TDAR despite the further improved performance shown by CNN + TDAR because of the diverse handcrafted features which are not incorporated yet. The evaluation is based on the training of 7 days' data while the rest days are left for testing. An average recognition accuracy of 13 hand motions across subjects and trials are seen in Table 6.2. The comparison is conducted on the handcrafted feature and conventional pattern recognition based classification, singly non-handcrafted feature and deep learning approach based classification and the merged handcrafted and non-handcrafted features and deep learning based classification. Here only the recognition accuracy is considered for comparison without the focus on computational cost. It is because that the offline training burden for classifiers and computers is less critical when compared to the user training burden or the high-precision performance. The results coincide with our conclusion reached in previous chapters indicating a favourable support towards the utilisation of CNN classifiers and combined handcrafted TDAR and non-handcrafted CNN features. And the results of a further evaluation based on CNN and CNN + TDAR are shown in Table 6.4 and 6.5. It is noticeable that individual differences exist and are reflected by the average recognition accuracy. A varying accuracy from 60% to 90% is seen on different subjects while most of them exert a similar recognition accuracy around 85%. It is worth noting that the subjects are inexperienced with the prosthetic control though provided with a quick user training phase to improve their consistency of muscle contraction as introduced in the previous section. Thus

the physiological difference such as the muscle contraction control plays another important role in the diversity of performance besides the development of pattern recognition schemes, which in turn validates the significance of a user training protocol allowing a more consistent sEMG pattern exertion.

Table 6.2 Average recognition accuracy of the benchmark across subjects and trials

Classification Approaches	**LDA+TDAR**	**CNN**	**CNN+TDAR**
Accuracy %	77.84	81.43	82.80

Table 6.3 Benchmark evaluation with LDA+TDAR

No.	**S1**	**S2**	**S3**	**S4**	**S5**	**S6**	**S7**	**S8**	**S9**	**S10**
Accuracy	79.78	79.66	80.70	82.65	85.38	63.38	60.15	81.07	85.73	79.93

Table 6.4 Benchmark evaluation with CNN

No.	**S1**	**S2**	**S3**	**S4**	**S5**	**S6**	**S7**	**S8**	**S9**	**S10**
R1	85.75	82.86	83.81	85.19	87.57	68.86	64.00	78.43	91.43	86.06
R2	83.72	84.40	84.29	87.30	87.19	69.38	64.71	76.69	92.72	86.80
R3	84.50	84.26	83.91	84.02	87.56	70.35	64.11	77.18	92.08	84.55
R4	84.95	83.24	85.45	84.15	86.86	69.33	64.26	79.90	91.33	88.28
R5	84.10	83.04	85.33	83.87	86.32	70.46	62.88	76.63	90.16	86.68
R6	84.61	83.10	84.77	86.91	87.11	69.83	67.73	77.74	88.86	84.88
R7	83.77	84.08	83.52	84.45	87.51	68.72	63.76	78.34	91.75	87.02
R8	84.75	83.50	84.62	83.74	87.79	68.71	65.13	79.21	91.68	85.66
R9	85.70	83.44	83.42	83.29	87.07	66.27	65.65	78.08	91.30	86.57
R10	84.04	83.75	85.07	85.38	87.28	70.21	64.34	78.04	92.31	87.19
Mean	84.59	83.57	84.42	84.83	87.23	69.21	64.66	78.02	91.36	86.37

Table 6.5 Benchmark evaluation with CNN+TDAR

No.	S1	S2	S3	S4	S5	S6	S7	S8	S9	S10
R1	86.08	83.83	85.00	85.41	87.81	69.90	67.29	81.23	91.14	87.44
R2	86.17	84.46	86.36	86.34	86.83	71.24	68.04	79.35	91.48	87.26
R3	86.29	84.14	85.72	85.28	86.71	70.07	66.64	81.05	90.37	88.23
R4	86.61	85.10	85.69	85.39	86.82	71.80	67.28	81.68	92.01	87.53
R5	85.85	83.93	85.59	87.84	87.01	71.82	66.28	80.23	91.91	87.92
R6	87.14	85.00	85.87	85.57	87.15	70.78	68.46	81.28	93.14	87.14
R7	86.35	84.46	84.77	87.04	87.35	71.35	65.68	81.68	91.17	86.94
R8	86.77	83.73	85.71	85.49	86.95	71.30	67.83	81.05	91.32	86.99
R9	86.02	84.07	85.35	87.54	87.54	70.00	67.41	80.52	91.92	88.09
R10	86.60	83.50	84.99	88.20	87.18	70.50	67.43	82.14	92.14	87.47
Mean	86.39	84.22	85.51	86.41	87.14	70.88	67.23	81.02	91.66	87.50

Chapter 7

Conclusions and Future Work

7.1 Summary and Contributions

This thesis focuses on the research of sEMG driven hand motion recognition in long-term use with an emphasis on the pattern recognition based solutions. Existing challenges that reside in the pattern recognition approaches lacking robustness to inter-day changes and the inherent limitations of noninvasive unimodal myoelectric sensing are addressed by the development of long-term hand motion recognition targeted pattern recognition methods, multimodal fusion sensing and the benchmark building for evaluation.

First, both conventional pattern recognition and deep learning approaches are developed to accommodate the long-term use. Here the conventional pattern recognition algorithms are categorised as the classification methods where classifier training and feature extraction are conducted separately while the deep learning methods perform both simultaneously. Specifically, the discriminant analysis in combination with TDAR feature extraction and the convolutional neural networks with concatenated raw EMG input are adopted. Subclass division based discriminant analysis methods including KNN-LDA and SDA and a simple yet efficient deep learning architecture of CNN fitting our low-density sEMG acquisition are proposed and adopted respectively in our research, with an improved long-term hand motion recognition performance facilitating various inter-day and inter-subject constraints. Specifically, the discriminant analysis models are proposed to accommodate the training with inadequate data while the CNN based approach deals with the scenario where adequate training of multiple days across subjects is available.

And the importance of features is reflected in our development of feature extraction and selection. The feasibility of merging handcrafted TDAR features and non-handcrafted CNN features is validated in the long-term recognition where each evaluation is conducted on distinct inter-day scenarios out of 10 days' data capturing. A multiple threshold based

feature extraction induced TDARM features are further proposed as the incorporation of finer categorisation of EMG changes to existing TDAR features. Specifically, the TD features of zero crossings and slope sign changes are determined by the threshold where different thresholds provide multiple reflections of the sEMG changes. The BMA based feature selection achieves respectively a compromised yet comparable recognition at a reduced computational cost and an improved recognition accuracy by selection of sub-segments of multiple lengths within each segment. More concretely, the drop of recognition accuracy is within 1% when compared to the reduction of 3/4 of the total feature dimension, which leads to a quarter of the original time consumption of feature extraction.

And the multimodal sensing scheme is adopted by merging the myoelectric and ultrasonic signals to overcome the limitations of unimodal sEMG based sensing such as the lack of deep muscle activity sensing for certain finger movement recognition, and the misclassification between certain motions due to its inherent randomness. Besides, the sensitivity of wearable ultrasound to probe shift is mitigated by the sEMG signals at the same time. The mutual complement between myoelectric and ultrasonic signals favours the integration of both modalities in forming an sEMG driven solution reflected by an improved recognition accuracy using both morphological and bio-electrical information during muscle contraction.

Finally, the limitations in both public benchmarks and our existing dataset are addressed by building a dataset captured under a standard protocol with low-density electrode distribution in comparison to the publicly available ones comprising the long-term sEMG signals captured from 10 subjects of 13 hand motions in consecutive 10 days. Detailed data acquisition protocols and the recognition baseline based on both LDA + TDAR and CNN is provided to form a self-contained benchmark to the research community.

7.2 Future Work

The directions for future work are pointed in this section.

Evaluation benchmark for sEMG based long-term hand motion recognition has been established in this thesis and will be publicly available. However, due to the nature of prosthetic control as a clinical application, the controlled experiments in a lab environment do not effectively reflect the real-life scenarios, where dynamic change of sEMG signal is excluded. And currently the subjects are seated at a comfortable position without moving their forearms freely, and arranged purposely with the rest period to avoid muscle fatigue. The future work of building the benchmark for both training and evaluation will start with including amputees and real-scenario usability despite the individual difference of amputation degree. Thus all the subsequent data acquisition will be conducted under varying conditions such as allowing

free moves of the residual limb, experiencing diverse physiological factors, and physical artefacts interference. First a large amount of able-bodied subjects will be recruited for the generalisation of the common knowledge of sEMG signals. And to further progress the clinical robustness of prosthetic hand control, amputee subjects will be employed to address the variant degree of amputation with corresponding sensing configurations. Meanwhile, the standardisation of the data acquisition and experiment setup will be collaboratively proposed to build a transferable paradigm for the research community.

Pattern recognition frameworks for hand motion recognition have been developed with an emphasis on the long-term use in this thesis. The promising results achieved by the CNN based hand motion recognition allow us to reveal the hidden and consistent patterns of sEMG signals exerted from forearm muscle contraction. Particularly, the full exploitation of the deep learning approaches heavily depends on the adequate or even redundant training data. It is anticipated that more data will be captured under a standardised protocol with the same configuration, similar to the ImageNet in the computer vision community. In that case, more sophisticated architectures could be utilised instead of the simple one used in this thesis. Training a more complex neural network tends to be computationally expensive and requires large amount of data for training. Thus the application of further developed deep learning architectures on hand motion recognition and the establishment of a standarised protocol for sEMG sample acquisition of predefined motion template will shape a major research task for in the future.

Handcrafted features extraction and selection have been investigated, and the combined TDAR and CNN features contribute to an improved hand motion recognition result. Regardless of the improvement, the incorporated handcrafted features are confined within the 8-dimensional TDAR extraction, compared to the large pool of feature candidates proposed so far [34]. We will focus on the utilisation of selected feature subset to enhance the combination of both handcrafted and non-handcrafted features. A more efficient feature selection algorithm will be looked into and applied in the enlarged set of features, concerning the scenarios under variant arm positions, exerted forces and various levels of muscle fatigue simultaneously. A novel dataset including such variation under well thought out constraints is essential in our future work, which also aligns with the aforementioned need of dataset establishment.

Multimodal sensing based hand motion recognition by addressing both myoelectric and ultrasonic modalities has been proposed in this thesis. Despite the plausible dexterous hand and finer motion recognition accuracy, it remains a critical problem to enhance the robustness of signal capturing with the development of numerous sensing techniques. First, our future work will aim at the configuration optimisation of the myoelectric and ultrasonic sensing

fusion in terms of the detection site distribution, which leads to the acquisition of more informative physiological signals. Then the inevitable shift of detecting electrodes or probes should be remedied with the well designed fixation of sensors or compensation schemes. What's more, other noninvasive and non-electric modalities such as NIRS [62], IMU [80] and FSR [66] will be further examined, to exploit the unique capability of each modality. For example, sEMG signals are susceptible to muscle fatigue which can be detected by NIRS, sensitive to limb positions which can be recognised by IMU, unstable under large voluntary contraction which can be measure by FSR. In other words, the selection of an optimal sensing modality combination is another prior concern in the future work.

Implementation in real control system is not addressed in this thesis yet. It is still a must task to transfer a trained models especially the deep learning one from personal computers to a mobile or embedded system for real-time myoelectric control. Recent advancement of system-on-chip solutions for deep learning, such as Jetson [184] and CEVA [185], has opened the way for an embedded algorithm implementation. What's more, the most recent lightweight deep learning architectures of MobileNet [186] and YOLO [187] would allow the real-time performance with limited computational resources. The future task is to utilise the development of both hardware and software in deep learning and ascertain their practicality in a prosthetic control system.

Online adaptation has been proven feasible with the instances of transfer learning [40] domain adaptation [149] or self-calibration [152] in hand motion recognition, where the sudden changes of physiological condition and the severe electrode shift are excluded. The application of adaptive techniques relies on the basic assumption that the sEMG pattern variation is within an acceptable extent. As a result, an adaptive system suffers most from sudden and large variation of sEMG signals due to the abrupt changes in internal physiological mechanisms and external physical conditions. Therefore, it is our future work to incorporate the sudden changes in an adaptive system to deal with the real scenarios in daily life where abrupt interferences becomes one of the critical challenges for sEMG based hand motion recognition.

Closed-loop control has not been successfully realised in the sEMG based prosthetic control systems so far. It is necessary to bring in a proper sensory feedback module and make the prosthetic control a closed loop [188], which is not considered in this thesis but remains to be investigated in the future work. Current sEMG based recognition is an open control or a pseudo closed-loop control that relies solely on the visual feedback. Though vision is a natural feedback path, the perception of tactile, pressure, stiffness and temperature over the residual limbs is more beneficial for a quick response to external variation. Therefore, it is necessary to incorporate sensory feedbacks to prosthetic hand control and make the

control process more intuitive for the restoration of motor function. One of the potential way is to transfer feedback information into the stimulus over skin surface of the residual limbs by vibrotactile, mechanotactile and electrotactile stimulation as reviewed in [189]. Besides the sensory development, a further enhancement of the proprioception and engagement is equally necessary following our previous work of user training in [165].

With the fruition of a reliable sEMG driven hand motion recognition system for long-term rehabilitation use, the accurate motion intention recognition can also be applied in other fields of remote robot control, human-computer interaction, physiological condition evaluation and compliant inspection of labour work.

References

[1] Lizhi Pan, Dingguo Zhang, Ning Jiang, Xinjun Sheng, and Xiangyang Zhu. Improving robustness against electrode shift of high density emg for myoelectric control through common spatial patterns. *Journal of neuroengineering and rehabilitation*, 12(1):110, 2015.

[2] Kevin Englehart and Bernard Hudgins. A robust, real-time control scheme for multifunction myoelectric control. *IEEE Transactions on Biomedical Engineering*, 50(7):848–854, 2003.

[3] Manfredo Atzori, Matteo Cognolato, and Henning Müller. Deep learning with convolutional neural networks applied to electromyography data: A resource for the classification of movements for prosthetic hands. *Frontiers in neurorobotics*, 10:9, 2016.

[4] Manfredo Atzori and Henning Müller. The ninapro database: a resource for semg naturally controlled robotic hand prosthetics. In *Engineering in Medicine and Biology Society (EMBC), 2015 37th Annual International Conference of the IEEE*, pages 7151–7154. IEEE, 2015.

[5] Ann M Simon, Levi J Hargrove, Blair A Lock, and Todd A Kuiken. The target achievement control test: Evaluating real-time myoelectric pattern recognition control of a multifunctional upper-limb prosthesis. *Journal of Rehabilitation Research and Development*, 48(6):619, 2011.

[6] Todd A Kuiken, Guanglin Li, Blair A Lock, Robert D Lipschutz, Laura A Miller, Kathy A Stubblefield, and Kevin B Englehart. Targeted muscle reinnervation for real-time myoelectric control of multifunction artificial arms. *Jama*, 301(6):619–628, 2009.

[7] NHS England. Hand and upper limb reconstruction using vascularised composite allotransplantation (haul-vca). https://www.england.nhs.uk/commissioning/wp-content/uploads/sites/12/2015/07/d00pa-hand-transplnt-forearm-loss.pdf, 2015.

[8] NHS England. Complex disability equipment – prosthetic specialised services for people of all ages with limb loss. https://www.england.nhs.uk/commissioning/wp-content/uploads/sites/12/2015/01/d01-serv-spec-dis-equ-prosth.pdf, 2015.

[9] Francesca Cordella, Anna Lisa Ciancio, Rinaldo Sacchetti, Angelo Davalli, Andrea Giovanni Cutti, Eugenio Guglielmelli, and Loredana Zollo. Literature review on needs of upper limb prosthesis users. *Frontiers in neuroscience*, 10:209, 2016.

[10] RN Scott, PA Parker, and VA Dunfield. Myo-electric control. *IEE Medical Electronics Monographs*, 7(12):141–169, 1974.

[11] RN Scott and PA Parker. Myoelectric prostheses: state of the art. *Journal of medical engineering & technology*, 12(4):143–151, 1988.

[12] Bernard Hudgins, Philip Parker, and Robert N Scott. A new strategy for multifunction myoelectric control. *IEEE Transactions on Biomedical Engineering*, 40(1):82–94, 1993.

[13] Marco Controzzi, Christian Cipriani, and Maria Chiara Carrozza. Design of artificial hands: A review. In *The Human Hand as an Inspiration for Robot Hand Development*, pages 219–246. Springer, 2014.

[14] Hong Liu, Dapeng Yang, Li Jiang, and Shaowei Fan. Development of a multi-dof prosthetic hand with intrinsic actuation, intuitive control and sensory feedback. *Industrial Robot: An International Journal*, 41(4):381–392, 2014.

[15] Hong Liu, Dapeng Yang, Shaowei Fan, and Hegao Cai. On the development of intrinsically-actuated, multisensory dexterous robotic hands. *ROBOMECH Journal*, 3(1):4, 2016.

[16] RARC Gopura, DSV Bandara, Kazuo Kiguchi, and George KI Mann. Developments in hardware systems of active upper-limb exoskeleton robots: A review. *Robotics and Autonomous Systems*, 75:203–220, 2016.

[17] Christian Cipriani, Christian Antfolk, Marco Controzzi, Göran Lundborg, Birgitta Rosén, Maria Chiara Carrozza, and Fredrik Sebelius. Online myoelectric control of a dexterous hand prosthesis by transradial amputees. *IEEE Transactions on Neural Systems and Rehabilitation Engineering*, 19(3):260–270, 2011.

[18] Dario Farina and Sebastian Amsüss. Reflections on the present and future of upper limb prostheses. *Expert review of medical devices*, 13(4):321–324, 2016.

[19] Tommaso Proietti, Vincent Crocher, Agnes Roby-Brami, and Nathanaël Jarrassé. Upper-limb robotic exoskeletons for neurorehabilitation: a review on control strategies. *IEEE reviews in biomedical engineering*, 9:4–14, 2016.

[20] Mohammadreza Asghari Oskoei and Huosheng Hu. Myoelectric control systems—a survey. *Biomedical Signal Processing and Control*, 2(4):275–294, 2007.

[21] Mohammad H Rahman, Cristobal Ochoa-Luna, Maarouf Saad, and Philippe Archambault. Emg based control of a robotic exoskeleton for shoulder and elbow motion assist. *J Aut Con Eng*, 3(4), 2015.

[22] Yinfeng Fang, Honghai Liu, Gongfa Li, and Xiangyang Zhu. A multichannel surface emg system for hand motion recognition. *International Journal of Humanoid Robotics*, 12(02):1550011, 2015.

[23] Lukai Liu, Pu Liu, Edward A Clancy, Erik Scheme, and Kevin B Englehart. Electromyogram whitening for improved classification accuracy in upper limb prosthesis control. *IEEE Transactions on Neural Systems and Rehabilitation Engineering*, 21(5):767–774, 2013.

[24] Ann M Simon, Levi J Hargrove, Blair A Lock, and Todd A Kuiken. A decision-based velocity ramp for minimizing the effect of misclassifications during real-time pattern recognition control. *IEEE Transactions on Biomedical Engineering*, 58(8):2360–2368, 2011.

[25] Mohammadreza Asghari Oskoei and Huosheng Hu. Support vector machine-based classification scheme for myoelectric control applied to upper limb. *IEEE Transactions on Biomedical Engineering*, 55(8):1956–1965, 2008.

[26] Zhaojie Ju, Gaoxiang Ouyang, Marzena Wilamowska-Korsak, and Honghai Liu. Surface emg based hand manipulation identification via nonlinear feature extraction and classification. *IEEE Sensors Journal*, 13(9):3302–3311, 2013.

[27] Xinpu Chen, Dingguo Zhang, and Xiangyang Zhu. Application of a self-enhancing classification method to electromyography pattern recognition for multifunctional prosthesis control. *Journal of neuroengineering and rehabilitation*, 10(1):44, 2013.

[28] Ning Jiang, Strahinja Dosen, Klaus-Robert Müller, and Dario Farina. Myoelectric control of artificial limbs—is there a need to change focus. *IEEE Signal Process. Mag*, 29(5):152–150, 2012.

[29] Dennis Tkach, He Huang, and Todd A Kuiken. Study of stability of time-domain features for electromyographic pattern recognition. *Journal of Neuroengineering and Rehabilitation*, 7(1):1, 2010.

[30] Yinfeng Fang, Nalinda Hettiarachchi, Dalin Zhou, and Honghai Liu. Multi-modal sensing techniques for interfacing hand prostheses: a review. *IEEE Sensors Journal*, 15(11):6065–6076, 2015.

[31] J Stefan Karlsson, Karin Roeleveld, Christer Grönlund, Andreas Holtermann, and Nils Östlund. Signal processing of the surface electromyogram to gain insight into neuromuscular physiology. *Philosophical Transactions of the Royal Society of London A: Mathematical, Physical and Engineering Sciences*, 367(1887):337–356, 2009.

[32] PEng Erik Scheme MSc and PEng Kevin Englehart PhD. Electromyogram pattern recognition for control of powered upper-limb prostheses: State of the art and challenges for clinical use. *Journal of Rehabilitation Research and Development*, 48(6):643, 2011.

[33] Jianwei Liu, Xinjun Sheng, Dingguo Zhang, Jiayuan He, and Xiangyang Zhu. Reduced daily recalibration of myoelectric prosthesis classifiers based on domain adaptation. *IEEE Journal of Biomedical and Health Informatics*, 20(1):166–176, 2016.

[34] Angkoon Phinyomark, Franck Quaine, Sylvie Charbonnier, Christine Serviere, Franck Tarpin-Bernard, and Yann Laurillau. Emg feature evaluation for improving myoelectric pattern recognition robustness. *Expert Systems with Applications*, 40(12):4832–4840, 2013.

[35] Todd A Kuiken, Laura A Miller, Kristi Turner, and Levi J Hargrove. A comparison of pattern recognition control and direct control of a multiple degree-of-freedom transradial prosthesis. *IEEE Journal of Translational Engineering in Health and Medicine*, 4:1–8, 2016.

[36] Melissa Mae White, Wenjuan Zhang, Anna T Winslow, Maryam Zahabi, Fan Zhang, He Huang, and David B Kaber. Usability comparison of conventional direct control versus pattern recognition control of transradial prostheses. *IEEE Transactions on Human-Machine Systems*, 47(6):1146–1157, 2017.

[37] Levi J Hargrove, Laura A Miller, Kristi Turner, and Todd A Kuiken. Myoelectric pattern recognition outperforms direct control for transhumeral amputees with targeted muscle reinnervation: A randomized clinical trial. *Scientific reports*, 7(1):13840, 2017.

[38] Jonathon W Sensinger, Blair A Lock, and Todd A Kuiken. Adaptive pattern recognition of myoelectric signals: exploration of conceptual framework and practical algorithms. *IEEE Transactions on Neural Systems and Rehabilitation Engineering*, 17(3):270–278, 2009.

[39] Ernest N Kamavuako, Kevin B Englehart, Winnie Jensen, and Dario Farina. Simultaneous and proportional force estimation in multiple degrees of freedom from intramuscular emg. *IEEE Transactions on Biomedical Engineering*, 59(7):1804–1807, 2012.

[40] Jianwei Liu, Xinjun Sheng, Dingguo Zhang, Ning Jiang, and Xiangyang Zhu. Towards zero retraining for myoelectric control based on common model component analysis. *IEEE Transactions on Neural Systems and Rehabilitation Engineering*, 24(4):444–454, 2016.

[41] Natasha Alves and Tom Chau. Uncovering patterns of forearm muscle activity using multi-channel mechanomyography. *Journal of electromyography and kinesiology*, 20(5):777–786, 2010.

[42] Xin Chen, Yong-Ping Zheng, Jing-Yi Guo, and Jun Shi. Sonomyography (smg) control for powered prosthetic hand: a study with normal subjects. *Ultrasound in medicine & biology*, 36(7):1076–1088, 2010.

[43] Ernest Nlandu Kamavuako, Dario Farina, Ken Yoshida, and Winnie Jensen. Relationship between grasping force and features of single-channel intramuscular emg signals. *Journal of neuroscience methods*, 185(1):143–150, 2009.

[44] David J Warren, Spencer Kellis, Jacob G Nieveen, Suzanne M Wendelken, Henrique Dantas, Tyler S Davis, Douglas T Hutchinson, Richard A Normann, Gregory A Clark, and V John Mathews. Recording and decoding for neural prostheses. *Proceedings of the IEEE*, 104(2):374–391, 2016.

[45] Todd A Kuiken, GA Dumanian, RD Lipschutz, LA Miller, and KA Stubblefield. The use of targeted muscle reinnervation for improved myoelectric prosthesis control in a bilateral shoulder disarticulation amputee. *Prosthetics and orthotics international*, 28(3):245–253, 2004.

[46] Carlo J De Luca. Physiology and mathematics of myoelectric signals. *IEEE Transactions on Biomedical Engineering*, (6):313–325, 1979.

[47] Emma F Hodson-Tole and James M Wakeling. Motor unit recruitment for dynamic tasks: current understanding and future directions. *Journal of Comparative Physiology B*, 179(1):57–66, 2009.

[48] Lauren H Smith, Todd A Kuiken, and Levi J Hargrove. Real-time simultaneous and proportional myoelectric control using intramuscular emg. *Journal of neural engineering*, 11(6):066013, 2014.

[49] Lauren H Smith, Todd A Kuiken, and Levi J Hargrove. Evaluation of linear regression simultaneous myoelectric control using intramuscular emg. *IEEE Transactions on Biomedical Engineering*, 63(4):737–746, 2016.

[50] Lauren H Smith and Levi J Hargrove. Comparison of surface and intramuscular emg pattern recognition for simultaneous wrist/hand motion classification. In *Engineering in Medicine and Biology Society (EMBC), 2013 35th Annual International Conference of the IEEE*, pages 4223–4226. IEEE, 2013.

[51] Alex Andrews, Evelyn Morin, and Linda McLean. Optimal electrode configurations for finger movement classification using emg. In *Engineering in Medicine and Biology Society, 2009. EMBC 2009. Annual International Conference of the IEEE*, pages 2987–2990. IEEE, 2009.

[52] Guanglin Li, Yanjuan Geng, Dandan Tao, and Ping Zhou. Performance of electromyography recorded using textile electrodes in classifying arm movements. In *Engineering in Medicine and Biology Society, EMBC, 2011 Annual International Conference of the IEEE*, pages 4243–4246. IEEE, 2011.

[53] Levi J Hargrove, Kevin Englehart, and Bernard Hudgins. A comparison of surface and intramuscular myoelectric signal classification. *IEEE Transactions on Biomedical Engineering*, 54(5):847–853, 2007.

[54] Dario Farina, Mauro Fosci, and Roberto Merletti. Motor unit recruitment strategies investigated by surface emg variables. *Journal of Applied Physiology*, 92(1):235–247, 2002.

[55] Dario Farina, Roberto Merletti, and Roger M Enoka. The extraction of neural strategies from the surface emg. *Journal of Applied Physiology*, 96(4):1486–1495, 2004.

[56] Aleš Holobar, Dario Farina, Marco Gazzoni, Roberto Merletti, and Damjan Zazula. Estimating motor unit discharge patterns from high-density surface electromyogram. *Clinical Neurophysiology*, 120(3):551–562, 2009.

[57] Dario Farina, Aleš Holobar, Roberto Merletti, and Roger M Enoka. Decoding the neural drive to muscles from the surface electromyogram. *Clinical neurophysiology*, 121(10):1616–1623, 2010.

[58] Dario Farina, Roberto Merletti, and Roger M Enoka. The extraction of neural strategies from the surface emg: an update. *Journal of Applied Physiology*, 117(11):1215–1230, 2014.

[59] Dario Farina, Ivan Vujaklija, Massimo Sartori, Tamás Kapelner, Francesco Negro, Ning Jiang, Konstantin Bergmeister, Arash Andalib, Jose Principe, and Oskar C Aszmann. Man/machine interface based on the discharge timings of spinal motor neurons after targeted muscle reinnervation. *Nature Biomedical Engineering*, 1(2):0025, 2017.

[60] Xiangxin Li, Oluwarotimi Williams Samuel, Xu Zhang, Hui Wang, Peng Fang, and Guanglin Li. A motion-classification strategy based on semg-eeg signal combination for upper-limb amputees. *Journal of NeuroEngineering and Rehabilitation*, 14(1):2, 2017.

[61] Youjia Huang and Honghai Liu. Performances of surface emg and ultrasound signals in recognizing finger motion. In *Human System Interactions (HSI), 2016 9th International Conference on*, pages 117–122. IEEE, 2016.

[62] Weichao Guo, Xinjun Sheng, Honghai Liu, and Xiangyang Zhu. Development of a multi-channel compact-size wireless hybrid semg/nirs sensor system for prosthetic manipulation. *IEEE Sensors Journal*, 16(2):447–456, 2016.

[63] Nalinda Hettiarachchi, Zhaojie Ju, and Honghai Liu. A new wearable ultrasound muscle activity sensing system for dexterous prosthetic control. In *Systems, Man, and Cybernetics (SMC), 2015 IEEE International Conference on*, pages 1415–1420. IEEE, 2015.

[64] Natasha Alves and Tom Chau. Vision-based segmentation of continuous mechanomyographic grasping sequences. *IEEE Transactions on Biomedical Engineering*, 55(2):765–773, 2008.

[65] Stefan Herrmann, Andreas Attenberger, and Klaus Buchenrieder. Prostheses control with combined near-infrared and myoelectric signals. In *International Conference on Computer Aided Systems Theory*, pages 601–608. Springer, 2011.

[66] Nan Li, Dapeng Yang, Li Jiang, Hong Liu, and Hegao Cai. Combined use of fsr sensor array and svm classifier for finger motion recognition based on pressure distribution map. *Journal of Bionic Engineering*, 9(1):39–47, 2012.

[67] J Carpaneto, A Cutrone, SILVIA Bossi, P Sergi, L Citi, J Rigosa, Paolo Maria Rossini, and S Micera. Activities on pns neural interfaces for the control of hand prostheses. In *Engineering in Medicine and Biology Society, EMBC, 2011 Annual International Conference of the IEEE*, pages 4637–4640. IEEE, 2011.

[68] Mario Tombini, Jacopo Rigosa, Filippo Zappasodi, Camillo Porcaro, Luca Citi, Jacopo Carpaneto, Paolo Maria Rossini, and Silvestro Micera. Combined analysis of cortical (eeg) and nerve stump signals improves robotic hand control. *Neurorehabilitation and neural repair*, 26(3):275–281, 2012.

[69] Silvestro Micera, Paolo M Rossini, Jacopo Rigosa, Luca Citi, Jacopo Carpaneto, Stanisa Raspopovic, Mario Tombini, Christian Cipriani, Giovanni Assenza, Maria C Carrozza, et al. Decoding of grasping information from neural signals recorded using peripheral intrafascicular interfaces. *Journal of neuroengineering and rehabilitation*, 8(1):53, 2011.

[70] Kiyotaka Fukumoto, Satoshi Muraki, Masayoshi Tsubai, and Osamu Fukuda. Calibration of cross-sectional images measured by an ultrasound-based muscle evaluation system. In *Engineering in Medicine and Biology Society, 2009. EMBC 2009. Annual International Conference of the IEEE*, pages 428–431. IEEE, 2009.

[71] Claudio Castellini, Georg Passig, and Emanuel Zarka. Using ultrasound images of the forearm to predict finger positions. *IEEE Transactions on Neural Systems and Rehabilitation Engineering*, 20(6):788–797, 2012.

[72] Yong-Ping Zheng, MMF Chan, Jun Shi, Xin Chen, and Qing-Hua Huang. Sonomyography: Monitoring morphological changes of forearm muscles in actions with the feasibility for the control of powered prosthesis. *Medical engineering & physics*, 28(5):405–415, 2006.

[73] Qing-Hua Huang, Yong-Ping Zheng, X Chena, JF He, and Jun Shi. A system for the synchronized recording of sonomyography, electromyography and joint angle. *The open biomedical engineering journal*, 1:77, 2007.

[74] Jun Shi, Shu-xian Hu, Zhi Liu, Jing-Yi Guo, Yong-jin Zhou, and Yong-ping Zheng. Recognition of finger flexion from ultrasound image with optical flow: A preliminary study. In *Biomedical Engineering and Computer Science (ICBECS), 2010 International Conference on*, pages 1–4. IEEE, 2010.

[75] Siddhartha Sikdar, Huzefa Rangwala, Emily B Eastlake, Ira A Hunt, Andrew J Nelson, Jayanth Devanathan, Andrew Shin, and Joseph J Pancrazio. Novel method for predicting dexterous individual finger movements by imaging muscle activity using a wearable ultrasonic system. *IEEE Transactions on Neural Systems and Rehabilitation Engineering*, 22(1):69–76, 2014.

[76] Xingchen Yang, Xueli Sun, Dalin Zhou, Yuefeng Li, and Honghai Liu. Towards wearable a-mode ultrasound sensing for real-time finger motion recognition. *IEEE Transactions on Neural Systems and Rehabilitation Engineering*, 26(6):1199–1208, 2018.

[77] Youjia Huang, Xingchen Yang, Yuefeng Li, Dalin Zhou, Honghai Liu, and Keshi He. Ultrasound-based sensing models for finger motion classification. *IEEE Journal of Biomedical and Health Informatics*, 2017.

[78] Erik Scheme, A Fougner, Øyvind Stavdahl, Adrian DC Chan, and Kevin Englehart. Examining the adverse effects of limb position on pattern recognition based myoelectric control. In *Engineering in Medicine and Biology Society (EMBC), 2010 Annual International Conference of the IEEE*, pages 6337–6340. IEEE, 2010.

[79] Christian Cipriani, Rossella Sassu, Marco Controzzi, and Maria Chiara Carrozza. Influence of the weight actions of the hand prosthesis on the performance of pattern recognition based myoelectric control: preliminary study. In *Engineering in Medicine and Biology Society, EMBC, 2011 Annual International Conference of the IEEE*, pages 1620–1623. IEEE, 2011.

[80] Anders Fougner, Erik Scheme, Adrian DC Chan, Kevin Englehart, and Øyvind Stavdahl. Resolving the limb position effect in myoelectric pattern recognition. *IEEE Transactions on Neural Systems and Rehabilitation Engineering*, 19(6):644–651, 2011.

[81] Arjan Gijsberts, Manfredo Atzori, Claudio Castellini, Henning Muller, and Barbara Caputo. Movement error rate for evaluation of machine learning methods for semg-based hand movement classification. *IEEE Trans. Neural Syst. Rehabil. Eng*, 22(4):735–744, 2014.

[82] J Silva, T Chau, and A Goldenberg. Mmg-based multisensor data fusion for prosthesis control. In *Engineering in Medicine and Biology Society, 2003. Proceedings of the 25th Annual International Conference of the IEEE*, volume 3, pages 2909–2912. IEEE, 2003.

[83] Alessander Danna-Dos Santos, Brach Poston, Mark Jesunathadas, Lisa R Bobich, Thomas M Hamm, and Marco Santello. Influence of fatigue on hand muscle coordination and emg-emg coherence during three-digit grasping. *Journal of neurophysiology*, 104(6):3576–3587, 2010.

[84] Akikazu Sakudo, Hirohiko Kuratsune, Takanori Kobayashi, Seiki Tajima, Yasuyoshi Watanabe, and Kazuyoshi Ikuta. Spectroscopic diagnosis of chronic fatigue syndrome by visible and near-infrared spectroscopy in serum samples. *Biochemical and biophysical research communications*, 345(4):1513–1516, 2006.

[85] Stefan Herrmann and Klaus Buchenrieder. Fusion of myoelectric and near-infrared signals for prostheses control. In *Proceedings of the 4th International Convention on Rehabilitation Engineering & Assistive Technology*, page 54. Singapore Therapeutic, Assistive & Rehabilitative Technologies (START) Centre, 2010.

[86] Luca Rossini and Paolo M Rossini. Combining eng and eeg integrated analysis for better sensitivity and specificity of neuroprosthesis operations. In *Engineering in Medicine and Biology Society (EMBC), 2010 Annual International Conference of the IEEE*, pages 134–137. IEEE, 2010.

[87] Dong Ni, Xin Chen, Wanguan Yi, Yong-Ping Zheng, Zhenyu Zhu, and Shing-Chow Chan. In vivo behavior of human muscle during isometric ramp contraction: A simultaneous emg, mmg and ultrasonography investigation. In *Signal Processing, Communication and Computing (ICSPCC), 2012 IEEE International Conference on*, pages 59–62. IEEE, 2012.

[88] Jorge Silva, Winfried Heim, and Tom Chau. Mmg-based classification of muscle activity for prosthesis control. In *Engineering in Medicine and Biology Society, 2004. IEMBS'04. 26th Annual International Conference of the IEEE*, volume 1, pages 968–971. IEEE, 2004.

[89] Yong Zeng, Zhengyi Yang, Wei Cao, and Chunming Xia. Hand-motion patterns recognition based on mechanomyographic signal analysis. In *BioMedical Information Engineering, 2009. FBIE 2009. International Conference on Future*, pages 21–24. IEEE, 2009.

[90] SI Yaniger. Force sensing resistors: A review of the technology. In *Electro International, 1991*, pages 666–668. IEEE, 1991.

[91] Kelvin HT Chu, Xianta Jiang, and Carlo Menon. Wearable step counting using a force myography-based ankle strap. *Journal of Rehabilitation and Assistive Technologies Engineering*, 4:2055668317746307, 2017.

[92] Vikram Ravindra and Claudio Castellini. A comparative analysis of three non-invasive human-machine interfaces for the disabled. *Frontiers in neurorobotics*, 8:24, 2014.

[93] Xianta Jiang, Lukas-Karim Merhi, Zhen Gang Xiao, and Carlo Menon. Exploration of force myography and surface electromyography in hand gesture classification. *Medical engineering & physics*, 41:63–73, 2017.

[94] ADCCKEA Fougner, Erik Scheme, Adrian DC Chan, Kevin Englehart, and Øyvind Stavdahl. A multi-modal approach for hand motion classification using surface emg and accelerometers. In *Engineering in Medicine and Biology Society, EMBC, 2011 Annual International Conference of the IEEE*, pages 4247–4250. IEEE, 2011.

[95] Skyler Ashton Dalley, Huseyin Atakan Varol, and Michael Goldfarb. A method for the control of multigrasp myoelectric prosthetic hands. *IEEE Transactions on Neural Systems and Rehabilitation Engineering*, 20(1):58–67, 2012.

[96] Sophie M Wurth and Levi J Hargrove. A real-time comparison between direct control, sequential pattern recognition control and simultaneous pattern recognition control using a fitts' law style assessment procedure. *Journal of neuroengineering and rehabilitation*, 11(1):91, 2014.

[97] Francesca Lunardini, Claudia Casellato, Andrea d'Avella, Terence D Sanger, and Alessandra Pedrocchi. Robustness and reliability of synergy-based myocontrol of a multiple degree of freedom robotic arm. *IEEE Transactions on Neural Systems and Rehabilitation Engineering*, 24(9):940–950, 2016.

[98] Johnny LG Nielsen, Steffen Holmgaard, Ning Jiang, Kevin B Englehart, Dario Farina, and Phil A Parker. Simultaneous and proportional force estimation for multifunction myoelectric prostheses using mirrored bilateral training. *IEEE Transactions on Biomedical Engineering*, 58(3):681–688, 2011.

[99] Silvia Muceli and Dario Farina. Simultaneous and proportional estimation of hand kinematics from emg during mirrored movements at multiple degrees-of-freedom. *IEEE transactions on neural systems and rehabilitation engineering*, 20(3):371–378, 2012.

[100] Shunchong Li, Jiayuan He, Xinjun Sheng, Honghai Liu, and Xiangyang Zhu. Synergy-driven myoelectric control for emg-based prosthetic manipulation: A case study. *International Journal of Humanoid Robotics*, 11(02):1450013, 2014.

[101] Claudio Castellini and Patrick van der Smagt. Evidence of muscle synergies during human grasping. *Biological cybernetics*, 107(2):233–245, 2013.

[102] Silvia Muceli, Ning Jiang, and Dario Farina. Extracting signals robust to electrode number and shift for online simultaneous and proportional myoelectric control by factorization algorithms. *IEEE Transactions on Neural Systems and Rehabilitation Engineering*, 22(3):623–633, 2014.

[103] Ning Jiang, Kevin B Englehart, and Philip A Parker. Extracting simultaneous and proportional neural control information for multiple-dof prostheses from the surface electromyographic signal. *IEEE Transactions on Biomedical Engineering*, 56(4):1070–1080, 2009.

[104] David Hofmann, Ning Jiang, Ivan Vujaklija, and Dario Farina. Bayesian filtering of surface emg for accurate simultaneous and proportional prosthetic control. *IEEE Transactions on Neural Systems and Rehabilitation Engineering*, 24(12):1333–1341, 2016.

[105] Linda Resnik, He Helen Huang, Anna Winslow, Dustin L Crouch, Fan Zhang, and Nancy Wolk. Evaluation of emg pattern recognition for upper limb prosthesis control: a case study in comparison with direct myoelectric control. *Journal of neuroengineering and rehabilitation*, 15(1):23, 2018.

[106] Shuxiang Guo, Muye Pang, Baofeng Gao, Hideyuki Hirata, and Hidenori Ishihara. Comparison of semg-based feature extraction and motion classification methods for upper-limb movement. *Sensors*, 15(4):9022–9038, 2015.

[107] Hubertus Rehbaum and Dario Farina. Adaptive common average filtering for myocontrol applications. *Medical & biological engineering & computing*, 53(2):179–186, 2015.

[108] Xu Zhang and Ping Zhou. Sample entropy analysis of surface emg for improved muscle activity onset detection against spurious background spikes. *Journal of Electromyography and Kinesiology*, 22(6):901–907, 2012.

[109] Dapeng Yang, Huajie Zhang, Yikun Gu, and Hong Liu. Accurate emg onset detection in pathological, weak and noisy myoelectric signals. *Biomedical Signal Processing and Control*, 33:306–315, 2017.

[110] Sebastian Amsüss, Peter M Goebel, Ning Jiang, Bernhard Graimann, Liliana Paredes, and Dario Farina. Self-correcting pattern recognition system of surface emg signals for upper limb prosthesis control. *IEEE Transactions on Biomedical Engineering*, 61(4):1167–1176, 2014.

[111] Erik J Scheme and Kevin B Englehart. Validation of a selective ensemble-based classification scheme for myoelectric control using a three-dimensional fitts' law test. *IEEE transactions on neural systems and rehabilitation engineering*, 21(4):616–623, 2013.

[112] Claudio Castellini, Angelo Emanuele Fiorilla, and Giulio Sandini. Multi-subject/daily-life activity emg-based control of mechanical hands. *Journal of neuroengineering and rehabilitation*, 6(1):41, 2009.

[113] Francesco Orabona, Claudio Castellini, Barbara Caputo, Angelo Emanuele Fiorilla, and Giulio Sandini. Model adaptation with least-squares svm for adaptive hand prosthetics. In *Robotics and Automation, 2009. ICRA'09. IEEE International Conference on*, pages 2897–2903. IEEE, 2009.

[114] Levi Hargrove, Kevin Englehart, and Bernard Hudgins. A training strategy to reduce classification degradation due to electrode displacements in pattern recognition based myoelectric control. *Biomedical signal processing and control*, 3(2):175–180, 2008.

[115] Thomas Lorrain, Ning Jiang, and Dario Farina. Influence of the training set on the accuracy of surface emg classification in dynamic contractions for the control of multifunction prostheses. *Journal of neuroengineering and rehabilitation*, 8(1):25, 2011.

[116] Paul Kaufmann, Kevin Englehart, and Marco Platzner. Fluctuating emg signals: Investigating long-term effects of pattern matching algorithms. In *Engineering in Medicine and Biology Society (EMBC), 2010 Annual International Conference of the IEEE*, pages 6357–6360. IEEE, 2010.

[117] Levi J Hargrove, Guanglin Li, Kevin B Englehart, and Bernard S Hudgins. Principal components analysis preprocessing for improved classification accuracies in pattern-recognition-based myoelectric control. *IEEE Transactions on Biomedical Engineering*, 56(5):1407–1414, 2009.

[118] Paul W Hodges and Bang H Bui. A comparison of computer-based methods for the determination of onset of muscle contraction using electromyography. *Electroencephalography and Clinical Neurophysiology/Electromyography and Motor Control*, 101(6):511–519, 1996.

[119] Andrea Merlo, Dario Farina, and Roberto Merletti. A fast and reliable technique for muscle activity detection from surface emg signals. *IEEE Transactions on Biomedical Engineering*, 50(3):316–323, 2003.

[120] Xiaoyan Li, Ping Zhou, and Alexander S Aruin. Teager-kaiser energy operation of surface emg improves muscle activity onset detection. *Annals of biomedical engineering*, 35(9):1532–1538, 2007.

[121] Lauren H Smith, Levi J Hargrove, Blair A Lock, and Todd A Kuiken. Determining the optimal window length for pattern recognition-based myoelectric control: balancing the competing effects of classification error and controller delay. *IEEE Transactions on Neural Systems and Rehabilitation Engineering*, 19(2):186–192, 2011.

[122] Todd R Farrell and Richard F Weir. The optimal controller delay for myoelectric prostheses. *IEEE Transactions on neural systems and rehabilitation engineering*, 15(1):111–118, 2007.

[123] Sebastian Amsuss, Liliana P Paredes, Nina Rudigkeit, Bernhard Graimann, Michael J Herrmann, and Dario Farina. Long term stability of surface emg pattern classification for prosthetic control. In *Engineering in Medicine and Biology Society (EMBC), 2013 35th Annual International Conference of the IEEE*, pages 3622–3625. IEEE, 2013.

[124] Karina de OA de Moura and Alexandre Balbinot. Virtual sensor of surface electromyography in a new extensive fault-tolerant classification system. *Sensors (Basel, Switzerland)*, 18(5), 2018.

[125] Ning Jiang, Silvia Muceli, Bernhard Graimann, and Dario Farina. Effect of arm position on the prediction of kinematics from emg in amputees. *Medical & biological engineering & computing*, 51(1-2):143–151, 2013.

[126] Mahyar Zardoshti-Kermani, Bruce C Wheeler, Kambiz Badie, and Reza M Hashemi. Emg feature evaluation for movement control of upper extremity prostheses. *IEEE Transactions on Rehabilitation Engineering*, 3(4):324–333, 1995.

[127] Carmen Vidaurre, A Schlogl, Rafael Cabeza, Reinhold Scherer, and Gert Pfurtscheller. A fully on-line adaptive bci. *IEEE Transactions on Biomedical Engineering*, 53(6):1214–1219, 2006.

[128] Haitham M Al-Angari, Gunter Kanitz, Sergio Tarantino, and Christian Cipriani. Distance and mutual information methods for emg feature and channel subset selection for classification of hand movements. *Biomedical Signal Processing and Control*, 27:24–31, 2016.

[129] Rami N Khushaba, Maen Takruri, Jaime Valls Miro, and Sarath Kodagoda. Towards limb position invariant myoelectric pattern recognition using time-dependent spectral features. *Neural Networks*, 55:42–58, 2014.

[130] Jiayuan He, Dingguo Zhang, Xinjun Sheng, Shunchong Li, and Xiangyang Zhu. Invariant surface emg feature against varying contraction level for myoelectric control based on muscle coordination. *IEEE journal of biomedical and health informatics*, 19(3):874–882, 2015.

[131] Ali H Al-Timemy, Rami N Khushaba, Guido Bugmann, and Javier Escudero. Improving the performance against force variation of emg controlled multifunctional upper-limb prostheses for transradial amputees. *IEEE Transactions on Neural Systems and Rehabilitation Engineering*, 24(6):650–661, 2016.

[132] Mohammadreza Asghari Oskoei and Huosheng Hu. Ga-based feature subset selection for myoelectric classification. In *2006 IEEE International Conference on Robotics and Biomimetics*, pages 1465–1470. IEEE, 2006.

[133] Rami N Khushaba and Adel Al-Jumaily. Channel and feature selection in multifunction myoelectric control. In *Engineering in Medicine and Biology Society, 2007. EMBS 2007. 29th Annual International Conference of the IEEE*, pages 5182–5185. IEEE, 2007.

[134] Ernest Nlandu Kamavuako, Jakob Celander Rosenvang, Ronnie Horup, Winnie Jensen, Dario Farina, and Kevin B Englehart. Surface versus untargeted intramuscular emg based classification of simultaneous and dynamically changing movements. *IEEE Transactions on neural systems and rehabilitation engineering*, 21(6):992–998, 2013.

[135] Aaron J Young, Levi J Hargrove, and Todd A Kuiken. The effects of electrode size and orientation on the sensitivity of myoelectric pattern recognition systems to electrode shift. *IEEE Transactions on Biomedical Engineering*, 58(9):2537–2544, 2011.

[136] Adrian DC Chan and Kevin B Englehart. Continuous myoelectric control for powered prostheses using hidden markov models. *IEEE Transactions on Biomedical Engineering*, 52(1):121–124, 2005.

[137] Yonghong Huang, Kevin B Englehart, Bernard Hudgins, and Adrian DC Chan. A gaussian mixture model based classification scheme for myoelectric control of powered upper limb prostheses. *IEEE Transactions on Biomedical Engineering*, 52(11):1801–1811, 2005.

[138] Levi J Hargrove, Erik J Scheme, Kevin B Englehart, and Bernard S Hudgins. Multiple binary classifications via linear discriminant analysis for improved controllability of a powered prosthesis. *IEEE Transactions on Neural Systems and Rehabilitation Engineering*, 18(1):49–57, 2010.

[139] Kaveh Momen, Sridhar Krishnan, and Tom Chau. Real-time classification of forearm electromyographic signals corresponding to user-selected intentional movements for multifunction prosthesis control. *IEEE Transactions on Neural Systems and Rehabilitation Engineering*, 15(4):535–542, 2007.

[140] Erik J Scheme, Bernard S Hudgins, and Kevin B Englehart. Confidence-based rejection for improved pattern recognition myoelectric control. *IEEE Transactions on Biomedical Engineering*, 60(6):1563–1570, 2013.

[141] Erik J Scheme, Kevin B Englehart, and Bernard S Hudgins. Selective classification for improved robustness of myoelectric control under nonideal conditions. *IEEE Transactions on Biomedical Engineering*, 58(6):1698–1705, 2011.

[142] Pradeep Shenoy, Kai J Miller, Beau Crawford, and Rajesh PN Rao. Online electromyographic control of a robotic prosthesis. *IEEE transactions on biomedical engineering*, 55(3):1128–1135, 2008.

[143] Ning Jiang, Thomas Lorrain, and Dario Farina. A state-based, proportional myoelectric control method: online validation and comparison with the clinical state-of-the-art. *Journal of neuroengineering and rehabilitation*, 11(1):110, 2014.

[144] Rami N Khushaba, Sarath Kodagoda, Maen Takruri, and Gamini Dissanayake. Toward improved control of prosthetic fingers using surface electromyogram (emg) signals. *Expert Systems with Applications*, 39(12):10731–10738, 2012.

[145] Ki-Hee Park and Seong-Whan Lee. Movement intention decoding based on deep learning for multiuser myoelectric interfaces. In *Brain-Computer Interface (BCI), 2016 4th International Winter Conference on*, pages 1–2. IEEE, 2016.

[146] Hyeon-min Shim and Sangmin Lee. Multi-channel electromyography pattern classification using deep belief networks for enhanced user experience. *Journal of Central South University*, 22(5):1801–1808, 2015.

[147] Rita Laezza. Deep neural networks for myoelectric pattern recognition.

[148] Weidong Geng, Yu Du, Wenguang Jin, Wentao Wei, Yu Hu, and Jiajun Li. Gesture recognition by instantaneous surface emg images. *Scientific reports*, 6:36571, 2016.

[149] Yu Du, Wenguang Jin, Wentao Wei, Yu Hu, and Weidong Geng. Surface emg-based inter-session gesture recognition enhanced by deep domain adaptation. *Sensors*, 17(3):458, 2017.

[150] Ulysse Côté-Allard, Cheikh Latyr Fall, Alexandre Campeau-Lecours, Clément Gosselin, François Laviolette, and Benoit Gosselin. Transfer learning for semg hand gestures recognition using convolutional neural networks. In *Systems, Man, and Cybernetics (SMC), 2017 IEEE International Conference on*, pages 1663–1668. IEEE, 2017.

[151] Adam Hartwell, Visakan Kadirkamanathan, and Sean R Anderson. Compact deep neural networks for computationally efficient gesture classification from electromyography signals. *arXiv preprint arXiv:1806.08641*, 2018.

[152] Xiaolong Zhai, Beth Jelfs, Rosa HM Chan, and Chung Tin. Self-recalibrating surface emg pattern recognition for neuroprosthesis control based on convolutional neural network. *Frontiers in neuroscience*, 11:379, 2017.

[153] Ulysse Côté Allard, François Nougarou, Cheikh Latyr Fall, Philippe Giguère, Clément Gosselin, François Laviolette, and Benoit Gosselin. A convolutional neural network for robotic arm guidance using semg based frequency-features. In *Intelligent Robots and Systems (IROS), 2016 IEEE/RSJ International Conference on*, pages 2464–2470. IEEE, 2016.

[154] Muhammad Zia ur Rehman, Asim Waris, Syed Omer Gilani, Mads Jochumsen, Imran Khan Niazi, Mohsin Jamil, Dario Farina, and Ernest Nlandu Kamavuako. Multiday emg-based classification of hand motions with deep learning techniques. *Sensors*, 18:2497, 2018.

[155] Manfredo Atzori, Arjan Gijsberts, Claudio Castellini, Barbara Caputo, Anne-Gabrielle Mittaz Hager, Simone Elsig, Giorgio Giatsidis, Franco Bassetto, and Henning Müller. Electromyography data for non-invasive naturally-controlled robotic hand prostheses. *Scientific data*, 1:140053, 2014.

[156] Christoph Amma, Thomas Krings, Jonas Böer, and Tanja Schultz. Advancing muscle-computer interfaces with high-density electromyography. In *Proceedings of the 33rd Annual ACM Conference on Human Factors in Computing Systems*, pages 929–938. ACM, 2015.

[157] Max Ortiz-Catalan, Rickard Brånemark, and Bo Håkansson. Biopatrec: A modular research platform for the control of artificial limbs based on pattern recognition algorithms. *Source code for biology and medicine*, 8(1):11, 2013.

[158] Novi Patricia, Tatiana Tommasit, and Barbara Caputo. Multi-source adaptive learning for fast control of prosthetics hand. In *Pattern Recognition (ICPR), 2014 22nd International Conference on*, pages 2769–2774. IEEE, 2014.

[159] Max Ortiz-Catalan, Faezeh Rouhani, Rickard Brånemark, and Bo Håkansson. Offline accuracy: a potentially misleading metric in myoelectric pattern recognition for prosthetic control. In *Engineering in Medicine and Biology Society (EMBC), 2015 37th Annual International Conference of the IEEE*, pages 1140–1143. IEEE, 2015.

[160] Max Ortiz-Catalan, Bo Håkansson, and Rickard Brånemark. Real-time and simultaneous control of artificial limbs based on pattern recognition algorithms. *IEEE Transactions on Neural Systems and Rehabilitation Engineering*, 22(4):756–764, 2014.

[161] Liselotte M Hermansson, Anne G Fisher, Birgitta Bernspång, and Ann-Christin Eliasson. Assessment of capacity for myoelectric control: a new rasch-built measure of prosthetic hand control. *Journal of rehabilitation medicine*, 37(3):166–71, 2005.

[162] Jiayuan He, Dingguo Zhang, Ning Jiang, Xinjun Sheng, Dario Farina, and Xiangyang Zhu. User adaptation in long-term, open-loop myoelectric training: implications for emg pattern recognition in prosthesis control. *Journal of neural engineering*, 12(4):046005, 2015.

[163] Marina M-C Vidovic, Han-Jeong Hwang, Sebastian Amsüss, Janne M Hahne, Dario Farina, and Klaus-Robert Müller. Improving the robustness of myoelectric pattern recognition for upper limb prostheses by covariate shift adaptation. *IEEE Transactions on Neural Systems and Rehabilitation Engineering*, 24(9):961–970, 2016.

[164] Rami N Khushaba, Ali Al-Timemy, and Sarath Kodagoda. Influence of multiple dynamic factors on the performance of myoelectric pattern recognition. In *Engineering in Medicine and Biology Society (EMBC), 2015 37th Annual International Conference of the IEEE*, pages 1679–1682. IEEE, 2015.

[165] Yinfeng Fang, Dalin Zhou, Kairu Li, and Honghai Liu. Interface prostheses with classifier-feedback-based user training. *IEEE transactions on biomedical engineering*, 64(11):2575–2583, 2017.

[166] Michael A Powell and Nitish V Thakor. A training strategy for learning pattern recognition control for myoelectric prostheses. *Journal of prosthetics and orthotics: JPO*, 25(1):30, 2013.

[167] Ronald A Fisher. The statistical utilization of multiple measurements. *Annals of eugenics*, 8(4):376–386, 1938.

[168] Manli Zhu and Aleix M Martinez. Subclass discriminant analysis. *IEEE Transactions on Pattern Analysis and Machine Intelligence*, 28(8):1274–1286, 2006.

[169] Alex Krizhevsky, Ilya Sutskever, and Geoffrey E Hinton. Imagenet classification with deep convolutional neural networks. In *Advances in neural information processing systems*, pages 1097–1105, 2012.

[170] Nitish Srivastava, Geoffrey Hinton, Alex Krizhevsky, Ilya Sutskever, and Ruslan Salakhutdinov. Dropout: a simple way to prevent neural networks from overfitting. *The Journal of Machine Learning Research*, 15(1):1929–1958, 2014.

[171] Sergey Ioffe and Christian Szegedy. Batch normalization: Accelerating deep network training by reducing internal covariate shift. *arXiv preprint arXiv:1502.03167*, 2015.

[172] Dumitru Erhan, Yoshua Bengio, Aaron Courville, Pierre-Antoine Manzagol, Pascal Vincent, and Samy Bengio. Why does unsupervised pre-training help deep learning? *Journal of Machine Learning Research*, 11(Feb):625–660, 2010.

[173] Dumitru Erhan, Pierre-Antoine Manzagol, Yoshua Bengio, Samy Bengio, and Pascal Vincent. The difficulty of training deep architectures and the effect of unsupervised pre-training. In *Artificial Intelligence and Statistics*, pages 153–160, 2009.

[174] Antonietta Stango, Francesco Negro, and Dario Farina. Spatial correlation of high density emg signals provides features robust to electrode number and shift in pattern recognition for myocontrol. *IEEE Transactions on Neural Systems and Rehabilitation Engineering*, 23(2):189–198, 2015.

[175] Mislav Jordanić, Mónica Rojas-Martínez, Miguel Angel Mañanas, Joan Francesc Alonso, and Hamid Reza Marateb. A novel spatial feature for the identification of motor tasks using high-density electromyography. *Sensors*, 17(7):1597, 2017.

[176] Angkoon Phinyomark, Pornchai Phukpattaranont, and Chusak Limsakul. Feature reduction and selection for emg signal classification. *Expert Systems with Applications*, 39(8):7420–7431, 2012.

[177] Ernest Nlandu Kamavuako, Erik Justin Scheme, and Kevin Brian Englehart. Determination of optimum threshold values for emg time domain features; a multi-dataset investigation. *Journal of neural engineering*, 13(4):046011, 2016.

[178] Ali H Al-Timemy, Guido Bugmann, Javier Escudero, and Nicholas Outram. Classification of finger movements for the dexterous hand prosthesis control with surface electromyography. *IEEE Journal of Biomedical and Health Informatics*, 17(3):608–618, 2013.

[179] Adenike A Adewuyi, Levi J Hargrove, and Todd A Kuiken. Evaluating emg feature and classifier selection for application to partial-hand prosthesis control. *Frontiers in neurorobotics*, 10:15, 2016.

[180] Angkoon Phinyomark, Rami N Khushaba, and Erik Scheme. Feature extraction and selection for myoelectric control based on wearable emg sensors. *Sensors*, 18(5):1615, 2018.

[181] János Botzheim, Cristiano Cabrita, László T Kóczy, and AE Ruano. Fuzzy rule extraction by bacterial memetic algorithms. *International Journal of Intelligent Systems*, 24(3):312–339, 2009.

[182] PW Hodges, LHM Pengel, RD Herbert, and SC Gandevia. Measurement of muscle contraction with ultrasound imaging. *Muscle & nerve*, 27(6):682–692, 2003.

[183] Heather Daley, Kevin Englehart, Levi Hargrove, and Usha Kuruganti. High density electromyography data of normally limbed and transradial amputee subjects for multifunction prosthetic control. *Journal of Electromyography and Kinesiology*, 22(3):478–484, 2012.

[184] Nvdia. A little genius goes a long way. http://www.nvidia.com/object/embedded-systems-dev-kits-modules.html, 2017.

[185] CEVA. Ceva-xm6: Fifth-generation computer vision and deep learning embedded platform. https://www.ceva-dsp.com/product/ceva-xm6/, 2017.

[186] Mark Sandler, Andrew Howard, Menglong Zhu, Andrey Zhmoginov, and Liang-Chieh Chen. Inverted residuals and linear bottlenecks: Mobile networks for classification, detection and segmentation. *arXiv preprint arXiv:1801.04381*, 2018.

[187] Joseph Redmon and Ali Farhadi. Yolov3: An incremental improvement. *arXiv preprint arXiv:1804.02767*, 2018.

[188] Claudio Castellini and Patrick van der Smagt. Surface emg in advanced hand prosthetics. *Biological cybernetics*, 100(1):35–47, 2009.

[189] Kairu Li, Yinfeng Fang, Yu Zhou, and Honghai Liu. Non-invasive stimulation-based tactile sensation for upper-extremity prosthesis: a review. *IEEE Sensors Journal*, 17(9):2625–2635, 2017.

Appendix A

Dissemination

Relevant publications for the award of the degree include:

Journal articles:

Fang Y, Hettiarachchi N, **Zhou D**, Liu H. Multi-modal sensing techniques for interfacing hand prostheses: a review. IEEE Sensors Journal. 2015 Nov;15(11):6065-76.

Fang Y, **Zhou D**, Li K, Liu H. Interface prostheses with classifier-feedback based user training. IEEE Transactions on Biomedical Engineering. 2017 Nov;64(11):2575-83.

Yang X, Sun X, **Zhou D**, Li Y, Liu H. Towards wearable A-mode ultrasound sensing for real-time finger motion recognition. IEEE Transactions on Neural Systems and Rehabilitation Engineering. 2018 Jun;26(6):1199-208.

Huang Y, Yang X, Li Y, **Zhou D**, Liu H, He K. Ultrasound-based sensing models for finger motion classification. IEEE Journal of Biomedical and Health Informatics. 2018 Sep;22(5):1395-405.

Book chapters:

Zhou D, Fang Y, Ju Z, Liu H. Multi-length windowed feature selection for surface EMG based hand motion recognition. InInternational Conference on Intelligent Robotics and Applications 2018 Aug 9 (pp. 264-274). Springer, Cham.

Conference papers:

Huang W, Chan PP, **Zhou D**, Fang Y, Liu H, Yeung DS. Multiple classifier system with sensitivity based dynamic weighting fusion for hand gesture recognition. In Wavelet Analysis and Pattern Recognition (ICWAPR), 2016 International Conference on 2016 Jul 10 (pp. 31-36). IEEE.

Zhou D, Fang Y, Botzheim J, Kubota N, Liu H. Bacterial memetic algorithm based feature selection for surface EMG based hand motion recognition in long-term use. In Computational Intelligence (SSCI), 2016 IEEE Symposium Series on 2016 Dec 6 (pp. 1-7). IEEE.

Li QX, Chan PP, **Zhou D**, Fang Y, Liu H. Improving robustness against electrode shift of sEMG based hand gesture recognition using online semi-supervised learning. In 15th International Conference on Machine Learning and Cybernetics: ICMLC 2016 Jul 10 (Vol. 1, pp. 344-349). IEEE.

Fang Y, **Zhou D**, Li K, Ju Z, Liu H. A force-driven granular model for EMG based grasp recognition. InSystems, Man, and Cybernetics (SMC), 2017 IEEE International Conference on 2017 Oct 5 (pp. 2939-2944). IEEE.

FORM UPR16

Research Ethics Review Checklist

Please include this completed form as an appendix to your thesis (see the Postgraduate Research Student Handbook for more information

Postgraduate Research Student (PGRS) Information				**Student ID:**	753778
PGRS Name:	Dalin Zhou				
Department:	School of Computing	**First Supervisor:**	Honghai Liu		
Start Date: (or progression date for Prof Doc students)	**1 October 2014**				
Study Mode and Route:	Part-time ☒	MPhil ☐	MD ☐		
	Full-time ☐	PhD ☒	Professional Doctorate ☐		

Title of Thesis:	Vision-based Human Activity Analysis
Thesis Word Count: (excluding ancillary data)	33571

If you are unsure about any of the following, please contact the local representative on your Faculty Ethics Committee for advice. Please note that it is your responsibility to follow the University's Ethics Policy and any relevant University, academic or professional guidelines in the conduct of your study

Although the Ethics Committee may have given your study a favourable opinion, the final responsibility for the ethical conduct of this work lies with the researcher(s).

UKRIO Finished Research Checklist:
(If you would like to know more about the checklist, please see your Faculty or Departmental Ethics Committee rep or see the online version of the full checklist at: http://www.ukrio.org/what-we-do/code-of-practice-for-research/)

a)	Have all of your research and findings been reported accurately, honestly and within a reasonable time frame?	YES ☒ NO ☐
b)	Have all contributions to knowledge been acknowledged?	YES ☒ NO ☐
c)	Have you complied with all agreements relating to intellectual property, publication and authorship?	YES ☒ NO ☐
d)	Has your research data been retained in a secure and accessible form and will it remain so for the required duration?	YES ☒ NO ☐
e)	Does your research comply with all legal, ethical, and contractual requirements?	YES ☒ NO ☐

Candidate Statement:

I have considered the ethical dimensions of the above named research project, and have successfully obtained the necessary ethical approval(s)

Ethical review number(s) from Faculty Ethics Committee (or from NRES/SCREC):	TECH 2018 - B.L- 03

If you have *not* submitted your work for ethical review, and/or you have answered 'No' to one or more of questions a) to e), please explain below why this is so:

Signed *(PGRS)*:	Dalin Zhou	**Date:** 31/08/2018